

University of Memphis

University of Memphis Digital Commons

Electronic Theses and Dissertations

1-1-2020

APPLICATION OF SINGLE BOARD COMPUTERS AND SENSORS TO AUTOMATE ANALYTICAL METHODS AND MINIATURIZE THE ANALYTICAL DEVICES

NAGA PRASANNA DHANUNJAY BOPPANA

Follow this and additional works at: <https://digitalcommons.memphis.edu/etd>

Recommended Citation

BOPPANA, NAGA PRASANNA DHANUNJAY, "APPLICATION OF SINGLE BOARD COMPUTERS AND SENSORS TO AUTOMATE ANALYTICAL METHODS AND MINIATURIZE THE ANALYTICAL DEVICES" (2020). *Electronic Theses and Dissertations*. 2885.
<https://digitalcommons.memphis.edu/etd/2885>

This Dissertation is brought to you for free and open access by University of Memphis Digital Commons. It has been accepted for inclusion in Electronic Theses and Dissertations by an authorized administrator of University of Memphis Digital Commons. For more information, please contact khggerty@memphis.edu.

APPLICATION OF SINGLE BOARD COMPUTERS AND SENSORS TO
AUTOMATE ANALYTICAL METHODS AND MINIATURIZE THE
ANALYTICAL DEVICES

by

NAGA PRASANNA DHANUNJAY BOPPANA

A Dissertation

Submitted in Partial Fulfillment of the

Requirements for the Degree of

Doctor of Philosophy

Major: Analytical Chemistry

The University of Memphis

May 2020

Dedicated to:

My parents, teachers and friends who supported me through the journey of my doctoral
program

&

Five Armors of Life: Earth, Water, Fire, Air and Soil

ACKNOWLEDGEMENTS

I am grateful to my two great advisors Dr. Paul S. Simone Jr and Dr. Gary L. Emmert for their incredible support and guidance not only for successfully finishing my research but also shaping me as a researcher and person that I am today. I would like to thank each of the remaining committee members Dr. Xiaohua Huang, Dr. Nathan J. DeYonker and Dr. Michael A. Brown for their assistance and valuable contributions to this dissertation.

This material is based upon work support by the National Science Foundation under grant No.1556127. I gratefully acknowledge the support of The University of Memphis Department of Chemistry, Foundation Instruments Inc. I also like to thank all the employees at the Lebanon Water Treatment Plant and the Woodruff Water Treatment Plant.

I would like to thank all my past and current members of Mobile Analytical Monitoring and Modeling Laboratory (MAMML) who supported and taught me several aspects of research and life. I would like to thank Dr. Robyn A.Snow, a great friend and colleague who always inspired me and supported through my journey in the MAMML group. I would like to thank Dr. Michael A. Brown, a great mentor and colleague for his continuous support and teachings. I am proud to be a member of the MAMML group and I look ahead for great research emerging from our group. Finally, I thank my parents, my younger brother N.V.Vijay Krishna Boppana (Ph.D candidate), teachers and friends for their unconditional love and encouragement.

ABSTRACT

Naga Prasanna Dhanunjay Boppana.Ph.D. The University of Memphis. May 2020.
Application of Single Board Computers and Sensors to Automate Analytical Methods and Miniaturize the Analytical Devices. Major Professors: Paul S. Simone Jr. Ph.D., Gary L. Emmert. Ph.D.

In this dissertation, a low cost liquid delivery system and an automated titration system have been developed using a Raspberry Pi single board computer, 3D printing, and commercial-off-the-shelf components. In addition, an on-line single point internal calibration method has been developed for haloacetic acid rapid-response (HAA-RR) system, a commercial analyzer for analysis of nine haloacetic acids (HAA9) in drinking water.

The low cost liquid delivery system, the EZ-AutoPipet, was developed to deliver microliter volumes accurately and reproducibly. The EZ-AutoPipet produced excellent results regardless of analyst experience and performed better than traditional and commercial dosing devices at lower volumes. Several validation studies have been performed to establish the accuracy and precision of liquid delivery. The hardness and alkalinity titrations were performed using the EZ-AutoPipet to verify the feasibility of using it as automated buret.

The automated titration system was adapted from the EZ-AutoPipet and further developed into the EZ-AutoTitrator. It is a semi-automated system capable of performing potentiometric (pH-based) and spectrochemical titrations, pH and temperature measurements. The standard titration methods for alkalinity (pH titration) and total hardness (spectrochemical titration) have been adapted to the EZ-AutoTitrator. The alkalinity and hardness methods were validated and tested at two different water treatment plants. The EZ-AutoTitrator had good accuracy and precision for both titration methods. The preliminary testing of iodometric titration for determination of free available chlorine (FAC) in bleach samples has been performed.

An on-line single point internal calibration for the HAA-RR system was developed and tested. The internal calibration addressed issues with external calibration by injecting the internal standard (2-Bromobutanoic acid) and haloacetic acid sample sequentially using a ten-port injection valve and two vial autosampler. The HAA-RR system was completely automated and can analyze the drinking water samples for a week without operator interaction. This work eliminated the errors associated with sample preparation and manual addition of the internal standard. The robustness studies showed that the internal calibration compensates for changes in response due to changes in system.

Table of Contents

List of Tables	xi
List of Figures	xiii
List of Symbols and Abbreviations	xvii
CHAPTER 1: INTRODUCTION	1
Research at the Nexus of Commercialization and Analytical Chemistry	1
Single Board Computing	2
Raspberry Pi in Analytical Chemistry	3
Machine Learning in Analytical Chemistry	6
3D Printing	7
Types of 3D Printing	8
3D Printing in Analytical Chemistry	9
Outline of the Present Research	10
CHAPTER 2: DEVELOPMENT OF A LOW COST LIQUID DELIVERY SYSTEM USING RASPBERRY-PI AND 3D-PRINTING	12
Introduction	12
History and Evolution of Pipet	12
Necessity for Development of the Automated Liquid Delivery System	12
Experimental	13
Development of EZ-AutoPipet	13
<i>Raspberry Pi Single Board Computer</i>	14
<i>Python Programing Language</i>	14
<i>3D Printing Syringe Pump Components</i>	16
<i>Stepper Motor Based Liquid Delivery System</i>	17
<i>Plunger Position Monitoring System</i>	19

Chemicals, Reagents and Standards	20
Results and Discussion	21
Calibration of the Stepper Motor for Liquid Delivery	21
Position Sensor Calibration	22
Operation of the EZ-AutoPipet	24
Validation of Liquid Delivery	26
Accuracy and Precision of Liquid Delivery with 1.0 and 0.1 mL Syringes	31
Re-evaluation of Accuracy and Precision for Low Volume Deliveries	32
Method Detection Limit, Accuracy and Precision of Trihalomethanes Rapid Response System (THM-RR)	33
EZ-AutoPipet as a Digital Buret for Titrimetric Analysis	36
<i>Determination of Total Hardness</i>	36
<i>Determination of Total Alkalinity</i>	37
Conclusion	39
CHAPTER 3: DEVELOPMENT OF LOW-COST AUTOMATED TITRATION SYSTEM FOR POTENTIOMETRIC AND SPECTROCHEMICAL END-POINT DETECTION	40
Introduction	40
Necessity for Automation	40
Total Alkalinity of Water	41
Total Hardness of Water	43
FAC Concentrations in Sodium Hypochlorite Solutions	44
Experimental	46
Development of EZ-AutoTitrator	46
<i>Titrant Dosing System</i>	46
<i>Potentiometric Detector</i>	46
<i>Spectrochemical Detector</i>	47

<i>Fabrication of Spectrochemical Detector</i>	48
<i>Control, Signal Processing, Communication, and Output</i>	49
Operation of the EZ-AutoTitrator	50
<i>pH based Titrations by AutoTitrator</i>	50
<i>Spectrochemical Titrations by EZ-AutoTitrator</i>	52
Development of the Color Prediction Model	53
Chemicals, Reagents and Standards	57
Procedure for Total Alkalinity Using the EZ-AutoTitrator	58
Procedure for Total Hardness Using the EZ-AutoTitrator	60
Procedure for FAC Using the EZ-AutoTitrator	60
Validation of EZ-AutoTitrator Analyses	61
Real World testing of EZ-AutoTitrator	61
Results and Discussion	62
Validation Results for the Automated Alkalinity Titrations	62
Comparison of the EZ-Autotitrator and Manual Titration Methods for Determination of Alkalinity at Lebanon TN, WTP	65
Comparison of the EZ-AutoTitrator and Manual titration Methods for Determination of Alkalinity at Woodruff-Roebuck SC, WTP	68
Validation of the Hardness Titrimetric Analysis	71
Comparison of the EZ-AutoTitrator Method and Manual Titration for Hardness at the Lebanon TN, WTP	74
Comparison of the EZ-AutoTitrator and Manual Titration Methods for Determination of Total hardness at Woodruff SC, WTP	76
Results of Full Scale Titrations for Standardization of Strong Acids and Bases and pK_a Determination of Unknown Acids	78
Preliminary Spectrochemical Titrations of FAC in Sodium Hypochlorite Solutions	81
Comparison of the Specifications of the EZ-AutoTitrator to a Commercially Available Autotitrator	82

Conclusions	85
CHAPTER 4: ON-LINE ADDITION OF INTERNAL STANDARD (2-BBA) FOR CONTINUOUS CALIBRATION OF HALOACETIC ACID RAPID-RESPONSE SYSTEM (HAA-RR)	86
Introduction	86
Overview of Haloacetic Acid Rapid Response (HAA-RR)	88
Overview of External Calibration for On-Line Monitoring of HAA9 Species	89
Overview of Single Point Internal Standard Calibration for On-line Monitoring of HAA9 Species	90
Significance and Goals of Research	91
Experimental	92
Modified HAA-RR Sample Injection System for On-Line Internal Standard	92
Chemicals, Reagents and Standards	94
Results and Discussion	95
Stability of Internal Standard (2-BBA)	95
Preliminary Testing of the Modified Injection System	96
Robustness of HAA-RR using Single Point Internal Standard Calibration	97
<i>LED Intensity Robustness Study</i>	98
<i>Nicotinamide Robustness Study</i>	103
<i>KOH Reagent Robustness Study</i>	107
<i>Post Column Reagent Mixture Flow Rate</i>	112
<i>Effect of Flow Rate on Analytical Signal</i>	112
<i>Effect of Reagent Flow Rate on Retention Times</i>	117
Single Point Internal Standard Calibration Performance at Different Concentrations of HAA9	118
Spiked Recovery Studies in Memphis Tap Water	122
Comparison of MDL, Accuracy and Precision from current research to previous research	123

Conclusions	126
CHAPTER 5: CONCLUSIONS AND RECOMMENDATIONS FOR FUTURE RESEARCH	127
Microliter Volume Liquid Delivery System - EZ-AutoPipet	127
Future Work	128
The Automated Titration System – EZ-AutoTitrator	128
Future Work	129
On-line Single Point Internal Calibration – HAA-RR	130
Future Work	131
References	132
Appendix	140

List of Tables

Table	Page
1 Register address and bit structure used to set motor driver parameters ¹⁰¹ .	18
2 Slopes, Intercepts and R^2 values of calibration curves for three different size syringes.	22
3 Results from testing of position sensing system over two consecutive days with a 5 mL syringe.	24
4 Validation results for EZ-AutoPipet.	28
5 Accuracy and Precision of EZ-AutoPipet using 1.0 mL and 0.1 mL syringes to deliver the low microlitre volumes.	31
6 Results of liquid deliveries using 0.1 mL syringe using better balance and controlled environment.	32
7 Detailed MDL, Accuracy and Precision of THM-RR using EZ-AutoPipet and Mohr pipet.	35
8 Comparison of Hardness from EZ-AutoPipet, Dosimat and Manual titration using buret.	37
9 Comparison of Alkalinity from EZ-AutoPipet, Dosimat and Manual titration using buret.	38
10 Lower limit of dispensing volumes for 5, 1, and 0.1 mL syringes.	39
11 Broad classification of potable water based on the level of hardness.	43
12 Confusion matrix showing actual vs predicted values	54
13 Summary of various metrics for four different models tested for predicting red and blue color in hardness titrations.	56
14 Summary of various metrics for four different models tested for predicting straw color and clear solution in FAC titrations.	56
15 Validation results of EZ-AutoTitrator method for Alkalinity.	63
16 Summary of results of Alkalinity from EZ-AutoTitrator at different concentrations.	64
17 Comparison of alkalinity results from EZ-AutoTitrator and manual titrations.	65
18 Summary of alkalinity testing in raw and finished water at Lebanon, TN WTP.	67
19 Summary of alkalinity testing in raw, floc-3 and finished water at woodruff, SC WTP.	70

20	Validation results of EZ-AutoTitrator method for Hardness.	71
21	Measured total hardness from EZ-AutoTitrator at different concentrations.	73
22	Comparison of total hardness between the EZ-AutoTitrator and manual hardness titrations.	73
23	Summary of hardness testing at Lebnon,TN WTP.	75
24	Summary of hardness testing at Woodruff, SC WTP.	77
25	Results of acid-base titrations from EZ-AutoTitrator, VIT-90 and Manual Titrations.	79
26	Molar mass of polyprotic acids determined using EZ-AutoTitrator.	79
27	pK_a of weak polyprotic acids determined by EZ-AutoTitrator using half-equivalence method.	80
28	Comparison of FAC results from EZ-AutoTitrator and VIT-90. End-point detection of EZ-AutoTitrator is by color change while VIT-90 based on potentiometry.	81
29	Detailed comparison of EZ-AutoTitrator with Hannah instruments titration system.	83
30	Summary of HAA-RR results using external and single point internal calibration at three different LED intensities.	100
31	Summary of HAA-RR results using external and single point internal calibration at three different NCA concentrations.	104
32	Summary of HAA-RR results using external and single point internal calibration at four different KOH concentrations.	109
33	Summary of HAA-RR results from external and internal calibration at four different reagent flow rates.	114
34	Summary of retention and relative retention times of HAA9 with changing reagent flow rates.	118
35	The % Recoveries calculated for individual HAA species using single point internal standard (SIS) and External calibration (Ext.).	121
36	Spiked recoveries from external and single point internal calibration in Memphis tap water.	123
37	Detailed comparison of USEPA MDL, Accuracy and Precision from present work to previous work from 2011 ⁹⁸ and 2019 ¹⁰ . PCR-IC 2011 work uses syringe pump for on-line internal standard addition whereas in present work a ten port two position injection valve was used for on-line internal standard addition.	125

List of Figures

Figure	Page
1 The figure depicting how this research is operating at the intersection of analytical chemistry, single board computing, and additive manufacturing.	1
2 Graphical user interface developed for EZ-Autopipet. (A) shows the manual page where user can perform dilution calculation and (B) shows the THM-RR page where user can dispense multiple volumes with a touch of a button.	15
3 Photo of completed 3D printed stepper motor based. syringe pump	16
4 Characteristics of digital square pulses used to drive the stepper motor. T is the time period of square wave. Since Raspberry Pi generates 3.3 V high logic, amplitude (A) is +3.3 V. Rising edge is the transition from Low logic (0 V) to high logic (3.3V).	17
5 Resistance on output channel of soft-pot changes with distance from base	19
6 Calibration of stepper motor using three different size syringes. Plot with blue diamond markers is for 5mL, red square markers is for 1 mL and green triangle markers represent 0.1 mL syringe.	21
7 Calibration plot for position sensor. Voltage output readings from linear potentiometer (soft-pot) are plotted against known plunger positions of 5 mL syringe.	23
8 Flow chart showing the important steps in the operation of EZ-AutoPipet.	25
9 Comparison of calibration of THM-RR using Mohr pipet (Manual) and EZ-AutoPipet. Red continuous line shows calibration curve using EZ-AutoPipet and blue dotted line shows calibration using Manual pipetting (Mohr pipet). Calibration plots for A. chloroform B. dichlorobromomethane C. dibromochloromethane D. bromoform.	35
10 Fractional composition diagram of carbonic acid, bicarbonate ion, and carbonate ion. This plot shows the fraction of each species of carbonic acid ($pK_{a1} = 6.4$ and $pK_{a2} = 10.3$) at various pH. Below 4.4, carbonic acid is the dominant form and carbonate ion species dominates above pH 12. At the pH of drinking water ~ 7.5 , the bicarbonate ion is the primary species present.	42
11 Plot of normalized response versus wavelength for an AS7262 spectral sensor that detects visible wavelengths with peak sensitivities at 450 nm, 500 nm, 550 nm, 570 nm, 600 nm and 650 nm. Each channel has a bandwidth of 40 nm full width at half maxima (FWHM)	47
12 Top down view of the 3D-printed spectrochemical cell holder with a magnetic stirrer underneath.	48
13 Graphical user interface (GUI) for the titrator. Left side of the image shows the titrator page and right side of the image shows the result log page.	49

14	A decision tree that outlines the functioning of EZ-AutoTitrator for performing potentiometric pH titrations.	51
15	Flow chart outlines the detection of color change by EZ-AutoTitrator at the end-point. For hardness, color changes from reddish pink to pinkish violet whereas in FAC titrations, color changes from dark yellow to clear.	52
16	An example titration curve showing last few points and linear interpolation to calculate the exact acid volume. pH1 and pH2 are pH values that bracket pH 4.3 and V1 and V2 are added acid volumes at pH1 and pH2 respectively. Vx is the volume at pH 4.3 estimated by linear Interpolation.	59
17	Alkalinity measured in (A) raw and (B) finished water by the EZ-AutoTitrator and manual titrations at Lebanon TN water treatment plant. In the red line with triangle markers is the alkalinity measured manually whereas the blue line with square markers shows the measurements from EZ-AutoTitrator.	66
18	Bland-Altman plots for alkalinity comparisons in (A) raw and (B) finished water at Lebanon TN, WTP.	66
19	Alkalinity measured in raw (A), floc-3 (B) and finished water (C) by EZ-AutoTitrator and manual titrations at woodruff SC, water treatment plant. In the red line with triangle markers is the alkalinity measured manually whereas the blue line with square markers shows the measurements from EZ-AutoTitrator.	69
20	Bland-Altman plots for comparison of alkalinity from EZ-AutoTitrator and manual titrations at Woodruff, SC water treatment plant in raw (A), floc-3 (B) and finished water (C).	70
21	Total hardness measured in raw (A) and finished water (B) by EZ-AutoTitrator and manual titrations at Lebanon, TN water treatment plant. In the red line with triangle markers is the hardness measured manually whereas the blue line with square markers shows the measurements from EZ-AutoTitrator.	74
22	Bland-Altman plots for comparison of hardness from EZ-AutoTitrator and manual titrations at Lebanon, TN water treatment plant in raw (A) and finished water (B).	75
23	Total hardness measured in raw (A), floc-3 (B) and finished water (C) using EZ-AutoTitrator and manual titrations at Woodruff, SC water treatment plant. In the red line with triangle markers is the hardness measured manually whereas the blue line with square markers shows the measurements from EZ-AutoTitrator.	77
24	Bland-Altman plots for comparison of hardness from EZ-AutoTitrator and manual titrations at Woodruff, SC water treatment plant in raw (A), floc-3 (B), and finished water (C).	78
25	Block Diagram of HAA-RR. E1 and E2 are 200mM KOH and Reagent water eluent respectively. R1 and R2 are 2M KOH and 3.2M NCA post column	

	reagents respectively. GP1 and GP2 are high pressure gradient pumps. V_{is} is the 6-port injection valve. K1 is 40 m KOT and K2 is 1 m KOT.	89
26	On-line Internal standard injection system. Position A injects the sample on to the column and allows loading of the IS (20 μ L loop). Position B injects IS on to the column and allows loading of sample (2 mL loop).	93
27	Stability of 2-BBA in reagent water at 2°C. The central line is the average of day 1 and day 2 responses. The upper and lower dotted lines represent the 3% deviation window	95
28	Stability of 2-BBA in reagent water at room temperature. Over the week, the response of 2-BBA decreased	96
29	Comparison between blank chromatogram and chromatogram with only internal standard injection. The red line represents the blank run and the black line represents a run with internal standard (2-BBA) injection and injected reagent water as a sample.	96
30	Comparison between chromatogram with both IS and standard HAA9 injection (Red chromatogram) and only IS injection (black chromatogram).	97
31	The % Recovery of MCAA was calculated using external calibration and single point internal standard calibration at three different source LED intensities. The blue, striped bars represent concentration from external calibration and white bars represent the concentration from single point internal standard calibration. The error bars show the % RSD from three replicates.	99
32	The % Recovery of MCAA calculated using external calibration (blue, striped bars) and single point internal standard calibration (white bars) at three different NCA concentration. The error bars shows the % RSD from three replicates. SOC represents the standard operating concentration of NCA.	103
33	The % Recovery of MCAA was calculated using external calibration and single point internal standard calibration at four different KOH concentration. The striped bars represent concentration from external calibration and clear bars represent the concentration from single point internal standard calibration. The error bars shows the % RSD from three replicates. SOC represents standard operating concentration for KOH.	107
34	The % Recovery of MCAA calculated using external calibration and single point internal standard calibration at four different reagent mixture flow rate. The HAA-RR was calibrated by External calibration at 0.4 mL/min. The striped bars represent concentration from external calibration and clear bars represent the concentration from single point internal standard calibration. The error bars shows the % RSD from three replicates. SOF represents standard operation flow rate.	113
35	Bar graph shows the % Recoveries of MCAA at various concentrations. The striped Bars shows the concentration from external and clear bars shows	

	concentrations from internal standard calculations. The concentrations were calculated using peak heights and error bars shows the % RSD from quadruplicate analyses.	119
36	The Picture of EZ-AutoPipet.	127
37	The Picture of EZ-AutoTitrator.	129
38	The Picture of HAA-RR system.	130
39	The schematic of EZ-AutoTitrator.	141
40	The schematic of EZ-AutoPipet.	141
41	The electrical schematic of EZ-AutoTitrator/EZ-AutoPipet.	142

List of Symbols and Abbreviations

2-BBA	2-Bromobutanoic acid
ADC	Analog to digital converter
ANOVA	Analysis of variance
~	Approximately
HCO_3^-	Bicarbonate
BO_3^{3-}	Borate
BCAA	Bromochloroacetic acid
BDCAA	Bromodichloroacetic acid
CHCl_2Br	Bromodichloromethane
CHBr_3	Bromoform
Cd	Cadmium
CaCO_3	Calcium carbonate
Ca(OH)_2	Calcium hydroxide
CE	Capillary electrophoresis
CO_3^{2-}	Carbonate
°C	Celsius
Cl^-	Chloride
Cl_2	Chlorine
CHCl_3	Chloroform
Cr	Chromium
CSV	Comma separated value
COTS	Commercial-off-the-shelf
CMOS	Complementary metal oxide silicon
CAD	Computer aided design
CNC	Computer numerical control
Cu	Copper
DBAA	Dibromoacetic acid
DBCAA	Dibromochloroacetic acid
CHClBr_2	Dibromochloromethane
DCAA	Dichloroacetic acid
DPC	Diphenylcarbazine

DC	Direct current
ECD	Electron capture detector
E1	Eluent 1: 200 mM KOH
E2	Eluent 2: Reagent water
EDTA	Ethylene diamine tetra acetic acid
Ext	External calibration
FAC	Free available chlorine
FDM	Fused deposition modeling
GC	Gas chromatography
GPIO	General purpose input output
GP	Gradient pump
g	Gram
GUI	Graphical user interface
>	Greater than
HAA	Haloacetic acid
HAA-RR	Haloacetic acid Rapid Response
HDMI	High definition multimedia interface
HPLC	High performance liquid chromatography
OH ⁻	Hydroxide
HOCl	Hypochlorous acid
IR	Infrared
V _{is}	Injection valve
I2C	Inter-integrated communication
ID	Internal diameter
IS	Internal standard
IOT	Internet of Things
IP	Internet protocol
I ⁻	Iodide
IC	Ion chromatography
KNN	K-nearest neighbor
KOTS	Knitted open tubular coils
LOM	Laminated object manufacturing
Pb	Lead

<	Less than
LED	Light emitting diode
LDA	Linear discriminant analysis
LC	Liquid Chromatography
L	Liter
ML	Machine learning
Mn	Manganese
MS	Mass spectrometry
MCL	Maximum contaminant level
MDL	Method detection limit
MTBE	methyl tertiary butyl ether
K_m	Michaelis-Menten constant
$\mu\text{g/L}$	Microgram per liter
μL	Microliter
mg/L	Milligram per liter
mL	Milliliter
mm	Millimeter
mM	millimolar
mins	Minutes
MAMML	Mobile analytical and modeling laboratory
M	Molar
MBAA	Monobromoacetic acid
MCAA	Monochloroacetic acid
Ni	Nickel
NCA	Nicotinamide
R2	Nicotinamide (3.07 M)
NMR	Nuclear magnetic resonance
OS	Operating system
/	Per
%	Percent
PC	Personal computer
PO_4^{3-}	Phosphate
\pm	Plus or minus

PTFE	Polytetrafluoroethylene
PCR	Post column reaction
KOH	Potassium hydroxide
R1	Potassium hydroxide (2.0 M)
PWM	Pulse width modulation
RH	Relative humidity
RRF	Relative Response factor
RRT	Relative retention time
RSD	Relative standard deviation
RF	Response factor
RT _x	Retention time of a compound
RT _s	Retention time of reference
SLS	Selective laser sintering
SPI	Serial peripheral interface
SIS	Single point internal standard calibration
Na ₂ CO ₃	Sodium carbonate
NaOCl	Sodium hypochlorite
SPE	Solid phase extraction
SS	Stainless steel
SLA	Stereolithography
SOC	Standard operation concentration
SOF	Standard operation flow
SBD-RPS	Styrene Divinylbenzene - Reversed Phase Sulfonate
SVM	Support vector machine
S ₄ O ₆ ²⁻	Tetrathionate
S ₂ O ₃ ²⁻	Thiosulfate
TOC	Total organic carbon
TBAA	Tribromoacetic acid
TCAA	Trichloroacetic acid
THM-RR	Trihalomethane Rapid Response
THM	Trihalomethanes
I ₃ ⁻	Triiodide
USEPA	United States Environmental Protection Agency

USGS	United States geological survey
UART	Universal asynchronous receive and transmit
USB	Universal serial bus
UI	User interface
VGA	Video graphics array
VAC	Voltage alternate current
V	Volts
WTP	Water treatment plant
Zn	Zinc

CHAPTER 1

INTRODUCTION

Research at the Nexus of Commercialization and Analytical Chemistry

The research described herein uses novel technologies such as single board computers (Raspberry Pi) and 3D printing (additive manufacturing) to develop cost effective analytical instrumentation. The scope of this research is depicted in Figure 1 showing how the work here is enhanced with the use of Raspberry Pi and additive manufacturing to develop new products that will be spun out of the research laboratory and subsequently commercialized. The shaded region in Figure 1 explains the core idea of this research where the flexibility of the Raspberry Pi system and 3D printing (additive manufacturing) has transformed the capabilities in the research lab, enabling rapid development of automated analytical methods. The combination of those three fields led to the development of EZ-AutoPipet, EZ-AutoTitrator, and the Haloacetic Acids Rapid Response (HAA-RR) instruments.

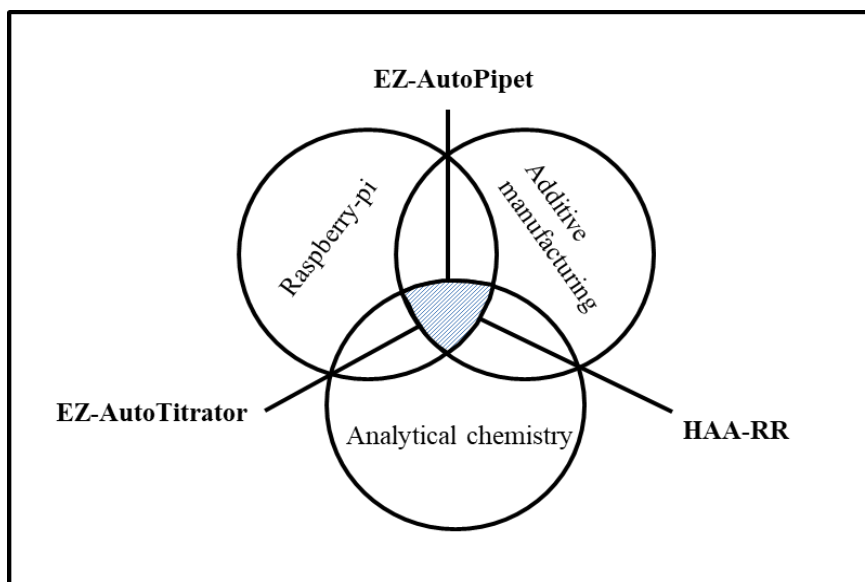


Figure 1. The figure depicting how this research is operating at the intersection of analytical chemistry, single board computing, and additive manufacturing.

Single Board Computing

Personal computers have transformed scientific research prominently over the past decades. Computers have been assisting students and researchers in a number of ways and at speeds not possible by human beings. The obvious is the increase in performing calculation. Less obvious, is the ability to perform routine tasks many times without error and with high precision. More recently, there has been an exponential increase in the amount of data that can be stored locally, allowing for collection and analysis of large data sets. Early computers were large with relatively small amounts of computing power and were not readily accessible. In 1965, an American engineer and co-founder of Intel Corporation, Gordon Moore predicted that the number of transistors per integrated circuit doubles every two years which is known as Moore's law^{1,2}. Moore's prediction helped semiconductor industry to set goals and roadmaps which lead to the development of modern day devices such as computers, smartphones, and tablets like those on popular science fiction shows³. Moore's prediction in fact implies that as the size of the integrated circuit decreases, the size of the computers decreases, computing speed increase while cost and energy usage of the computers decreases. The development of single board computers is an implication of Moore's law. There are several single board computers available in the market; however, the Raspberry Pi has become dominant in the past five years^{4,5} due to its standardization of form factor and the open-source resources developed for it. The Raspberry Pi is a small credit card sized yet powerful computer that costs around \$35. The origin of Pi dated back to 2006 where young engineers and professors at The University of Cambridge teamed up to bring the concept of single board palm held computers to reality. Originally, the Raspberry Pi was developed with an intention to provide relatively inexpensive computing device for education (where is succeeded) but now it found applications in many disciplines of science and technology. The Raspberry Pi Foundation provides Linux based fully featured operating system called

Raspbian. There are several other operating systems such as Ubuntu, RISC OS and Windows 10 Internet of Things (IoT) Core etc. that are supported on Pi. The Raspberry Pi community promotes python and scratch as the core programming languages though Pi supports many other programming languages such as C, C++, Java etc.

Raspberry Pi in Analytical Chemistry

With the advent of single board computers and open source software libraries for data acquisition and data processing, analytical instrumentation is less of a 'Black Box'. Many undergraduate courses have been designed up on using single board computers to enable students build their own analytical devices and better understand the operating principles. The Raspberry Pi and open source software have also been used to develop low-cost analytical instrumentation that is comparable with commercially available devices.

The EDEL group at London imperial college designed an undergraduate course⁶ to allow students to develop and optimize the analytical instrumentation such as a visible spectrophotometer using a Raspberry Pi and python programming language. Samuel et. al developed a low cost strip chart recorder for chromatographic detectors using Raspberry Pi⁷. This recorder can acquire, filter and processes the chromatographic data and showed that the developed system performs equally with a commercially available data acquisition system. Katherine et. al used a Raspberry Pi in conjunction with a digital camera for colorimetric analysis⁸. For this work, a Raspberry Pi was programmed to capture images of paper based enzymatic assays every minute using a camera and subsequently perform a color analysis. The change in color intensities calculated from image analysis was used to determine the Michaelis-Menten enzyme constants V_{\max} and K_M . Kumar et al. used a Raspberry Pi, IoT libraries, and commercial-off-the-shelf (COTS) components for real time monitoring of water quality parameters such as turbidity, pH, conductivity and dissolved oxygen⁹.

Recently, the Mobile Analytical Monitoring and Modeling Laboratory (MAMML) at the University of Memphis developed a low-cost, binary gradient pump by modifying a commercially available high pressure liquid chromatography (LC) pumps for delivering eluents and post column reagents in Haloacetic Acids Rapid Response (HAA-RR) system¹⁰. In this work, a multichannel liquid proportioning valve was programmed and controlled using a Raspberry Pi General Purpose Input Output (GPIO) pins along with python programming to generate a binary mobile phase gradient.

The Raspberry Pi and its readily accessible GPIO pins in conjunction with python programming and open source libraries have a nearly limitless set of applications. The GPIO pins and open-source libraries allow an application to connect to the physical world and interact with it. The python programming language is an open source platform that uses relatively simple to read and write syntax¹¹. Since it is an open source platform and community developed, there is an ever-growing catalogue of libraries that are nearly turn-key usable. These libraries make the process of software application development faster and simpler even with complex programs involving artificial intelligence (machine learning). This is especially true for new analytical chemists who may not have significant expertise in programming or IO processes.

Machine learning (ML) is a prominent domain in artificial intelligence and has been a subject of interest in many fields of science and technology. The term Machine Learning was first coined by Arthur Samuel in 1959, an American pioneer in computer gaming and artificial intelligence. Machine learning uses statistical models to provide computers the ability to automatically learn and improve from the past experience without being explicitly programmed¹². There are several applications of machine learning in our daily routine. Netflix viewing suggestions is one good example of machine learning application. When the user accesses the Netflix service, the recommendation system provides suggestions based on

past experience. The viewing history, information about titles, rating given for titles, time of the day user watch a title and how long a user watches etc. are used as inputs for the recommendation algorithm to provide personalized suggestions¹³. Email classification is another classical example of machine learning. The incoming emails will be sorted into groups based several factors such as email fields (To, From, Cc and Message-ID), domain or internet protocol (IP) address from which email is generated, key words and their frequency¹⁴ etc. The examples presented here are just a couple of the growing number of applications of machine learning.

Machine learning algorithms are classified broadly into two categories: supervised and unsupervised^{15,16}. Supervised learning uses the input data (Features) and its known responses (Labels/Target) to train the model and predicts the response from the unknown instance. The known responses are identified by an outside agent, typically a person who might be a laboratory technician or a programmer. Supervised learning uses classification algorithms and regression techniques to develop predictive models. Classification models use discrete responses and classify the input into categories. The most widely used classification algorithms include logistic regression, K-nearest neighbors (KNN), support vector machine (SVM), linear discriminant analysis (LDA), and decision tree. Regression models predict a continuous response and there are several regression models but typically the most used models include linear, logistic, and polynomial regression.

Unsupervised learning on the other hand does not have labeled data (features). These algorithms recognize the patterns or the naturally occurring trends within the data and sort the data into groups or clusters where objects within the cluster have similar properties. This is identified as clustering. Unsupervised models are less accurate and trustworthy when compared to supervised models. In other words, they are more of a “Black Box” when it

comes to how the developed model arrives at a given decision. The exact route to any particular answer may not be clear.

Machine Learning in Analytical Chemistry

A large number of ML algorithms have been implemented since 1990 in analytical chemistry to compare and classify the nuclear magnetic resonance^{17,18} (NMR), mass spectra^{19–21}, infrared (IR) spectra^{18,22,23} and several other spectra of compounds. Some studies showed ML has been successfully used for predicting the excitation spectra of the compounds based on electronic structure of the compounds²⁴. Machine learning has been applied to chromatography to discover knowledge from chromatographic data. Several ML tools have been implemented to acquire the knowledge from published chromatographic data to recommend chiral stationary phases for enantiomeric separations in high performance liquid chromatography (HPLC)²⁵. Rowe et. al used neural networks to classify the chromatographic peak shapes. They compared the performance of developed algorithm with a human expert for classifying 396 individual peaks. The authors reported 85% accuracy for both; however, the neural network took only 8.5 secs to finish the task whereas expert took 8 hours (over three thousand times faster)²⁶. Ting-poi et. al combined artificial intelligence with chromatographic principles to develop automated HPLC method development tool called LabExpert. The authors showed that the developed software recommended analytical conditions similar to empirically determined parameters by highly experienced chromatographic scientists. The LabExpert tool determined separation conditions such as flow rate, elution profile (Isocratic or Gradient), temperature, equilibration time for mixture of four test compounds within 13 hours of unattended environment²⁷.

Machine learning has become prominent today to an extent where the tools and libraries are readily available. The field of chemistry will see a surge in application of artificial intelligence in the near future and have greater impact on decision making and data

analysis of chemical experiments. Such efforts are already underway and have provided a way to prioritize research efforts at the laboratory bench^{28,29}. The research presented in Chapters 3 applied ML to field of analytical chemistry for the development and operation of the EZ-AutoTitrator.

3D Printing

Additive Manufacturing, also called 3D printing or solid-freeform technology, is one of the greatest advancements in manufacturing methods in the 20th century. Traditional manufacturing processes include subtractive manufacturing and formative manufacturing. Subtractive manufacturing includes machining, milling, and CNC versions of both. Formative manufacturing is typically processed like injection molding, die casting and stamping. Both additive manufacturing and traditional manufacturing have their own advantages and disadvantages. It is unlikely that 3D printing will replace traditional manufacturing in the near future. However, it surpasses the traditional methods in certain aspects of manufacturing. 3D printing creates an object by adding material layer by layer and this process produces little to waste. Whereas, a subtractive manufacturing process removes material to create an object which generates large amounts of waste. The primary advantage of 3D printing over traditional methods is “Rapid Prototyping” where a plastic part can be created in 2 – 3 hours to ensure proper fit of a part prior to more expensive manufacturing methods in both materials and labor time. In contract, traditional manufacturing can take days to weeks even with highly skilled labor for prototype development. Another advantage is complex geometries which are impossible to create using traditional methods can be readily designed and then printed by 3D printing technologies.

The limitations of 3D printing are typically seen in build volume, structural integrity and production volumes and this is where traditional methods generally surpass 3D printing. Most 3D printers have small build chamber and thus parts larger in size than chamber needs

to be divided into sections and assembled after printing which increases the production time. Consumer-grade and prototyping-grade 3D-printed, plastic parts are not as strong as parts made from traditional manufacturing processes. For example, delamination is a major problem with fused deposition modelling (FDM) printers. Parts printed using stereolithography and laminate object manufacturing are brittle. However, there is large selection of materials which works, and 3D printed parts made using laser welding largely side-step many of these issues in exchange for expense. Ultimately, 3D printing is useful for prototyping and is cost effective for producing parts in small quantities or with a fast turnaround. However, traditional methods become more cost effective and take less time when mass production of parts is required.

Types of 3D Printing

The main 3D printing techniques are fused desposition modeling (FDM), stereolithography (SLA), inkjet printing, selective laser sintering (SLS) and laminate object manufacturing (LOM). FDM printers work by depositing melted plastic filament layer by layer to create an object. FDM printers are inexpensive and widely accessible. The downsides of FDM printing are lower resolution and delamination of layers³⁰⁻³². An SLA printer has material in powder or liquid form and a laser selectively cures or bounds layer by layer to create an object. SLA printer yields low resolution and have wide range of resins including resins that are biocompatible. SLA printers are relatively expensive and cost of printing is also relatively higher when compared to other types³⁰⁻³². In inkjet printers, the powder material will be leveled onto a stage with roller and then an inkjet head dispenses liquid binder onto the powder to form layer of an object. Although, the print process is fast and inexpensive, the printed object has rough surface quality and has poor mechanical strength. SLS printer has similar operation to that of inkjet printers, except the powder material is sintered by a guided laser to form object³⁰⁻³². In LOM printing, a sheet of material (Paper,

plastic, metal) is loaded onto a stage and a laser or a razor traces a 2D layer of object. The excess material is removed, and second layer of material covers the previous layer and a laser or razor traces the second layer of the object. This process continues until the object is finished. These printers are relatively inexpensive. The LOM printers are limited by slow build times, low resolution and delamination³⁰⁻³².

3D Printing in Analytical Chemistry

Recently, 3D printing technology has become more common due to lower costs and a concurrent wider availability of computer aided design (CAD) software. Increased access to these technologies has led to researchers adapting to solve more specialized problems in their individual fields.

Calderilla et. al developed a 3D printed device for the fully automated disk-based solid-phase extraction (SPE) of Cr (VI) from water samples. The authors used 1, 5-diphenylcarbazide (DPC) in acidic medium to complex the Cr (VI) and the subsequent retention of the complex in a Styrene Divinylbenzene - Reversed Phase Sulfonate (SBD-RPS) disk contained within the 3D printed device. The 3D printed device is comprised of connectors, mixers needed for flow analysis³³. The Cheng group reported a 3D printed extraction chamber using polyacrylate polymers to manufacture a solid phase extraction preconcentrator for the selective extraction of trace elements (Mn, Ni, Zn, Cu, Cd, and Pb) from sea water³⁴. Fee et. al used a multijet 3D printer to print various packed column bed geometries. The authors developed octahedral beads packed in a simple cubic pattern, monoliths with hexagonal channels in parallel and herringbone design. The authors concluded from their preliminary tests, that 3D printing can be a potential method for production of porous media columns³⁵. Sandron et. al in 2012 developed metal liquid chromatography (LC) columns using SLS printers and demonstrated functional 3D printed chromatography columns. They developed two types of printed columns: one stainless steel

(SS) column packed with reverse phased silica (octadecyl silica) and the other one is a methacrylate polymer monolith packed in a titanium coil³⁶.

A simple, low cost, LED based fluorescence detector was reported in 2014 by Prikryl and Foret. The detector housings are printed using a FDM printer. The developed detector operated in epifluorescence mode used in conjunction with capillary electrophoresis³⁷ (CE). Recently, the MAMML group at The University of Memphis has developed low-cost, filter-based fluorescence detector that works specifically for nicotinamide chemistry in haloacetic acid analysis. The 3D printed detector has shown equivalent results to that of a commercially available detector and was developed for on-line analysis¹⁰.

Outline of the Present Research

In the research presented here, two new devices were developed and validated: the EZ-AutoPipet and the EZ-AutoTitrator. In addition, the HAA Rapid Response (HAA-RR) system was improved through the addition of automated, on-line standard addition. The development of EZ-AutoPipet, a low-cost liquid delivery system using Raspberry Pi and 3D printing technology will be presented in Chapter 2. The major objective of this work is to develop a liquid delivery system that can deliver microliter volumes accurately and precisely with a touch of a button. The developed EZ-AutoPipet will help analysts who do not have formal analytical training to deliver volumes accurately and reproducibly for preparing standards and solutions. This chapter also presents the various validation studies used to establish the accuracy and precision of the liquid delivery and also shows the ability of the EZ-AutoPipet to perform titrations.

In Chapter 3, the development of an automated titration system called the EZ-AutoTitrator capable of performing potentiometric and spectrochemical titrations is presented. The EZ-AutoTitrator was developed by adapting the liquid delivery system (EZ-

AutoPipet). This chapter presents the alkalinity, total hardness and free available chlorine (FAC) titration methods for the EZ-AutoTitrator adapted from standard methods. The development of color predicting machine learning models for hardness and FAC titration end point color detection will be discussed. This chapter also presents various validation comparisons for establishing accuracy and precision of alkalinity and hardness titrations. Finally, results from real world testing of the EZ-AutoTitrator at Lebanon, TN and Woodruff, SC water treatment plants (WTPs) will be presented.

Finally, Chapter 4 describes the on-line addition of internal standard for a continuous calibration method for the HAA-RR. This chapter describes some of the issues with current (external) calibration method used and how single point internal calibration method addresses the issues with external calibration. This chapter shows how a ten port two position injection valve was adapted for on-line addition of internal standard. Furthermore, this chapter presents various robustness studies to show how internal standard compensates for haloacetic acids response due to changes in the system such as LED intensity of fluorescence detector, reagent concentration and reagent flow rates.

CHAPTER 2

DEVELOPMENT OF A LOW COST LIQUID DELIVERY SYSTEM USING RASPBERRY-PI AND 3D-PRINTING

Introduction

History and Evolution of Pipet

The pipet is a laboratory staple and several kinds of pipets are often seen in analytical laboratories including volumetric pipets, mohr pipets, serological pipets, micropipets, and piston displacement pipets. The history of the pipet dates back to the 18th century. In 1818 Francois Descroizilles, a French chemist invented ‘Alcalimetre’, the precursor of modern-day pipet³⁸. Later the Francois design was modified by Louis Gay-Lussac in 1824 and coined the term ‘Pipet’³⁹. In 1957, Heinrich Schnitger at The University of Marburg developed the first piston-stroke pipet – Precursor for modern-day air-displacement pipet⁴⁰. Later, Eppendorf a medical supplies company acquired the rights from Schnitger and commercialized them as ‘Eppendorf’ pipets. The early Eppendorf pipets were fixed volume and suitable for variable volume dispensing. In 1972, Warren Gilson and Henry Lardy patented an adjustable micropipet capable of delivering variable volumes^{40,41}. Then the first stepper motor based electronic pipet was patented by Rainin in 1984⁴². Eli and Sutter have recently developed the world’s smallest pipet which can generate drops of molten gold-germanium alloy with a volume of a few zepto-liters⁴³. Pipetting technology has been advanced greatly in the past two decades to deliver up to nano-liter volumes accurately and precisely.

Necessity for Development of the Automated Liquid Delivery System

Liquid handling and standard preparation in analytical methods are crucial for producing accurate and reproducible results. Pipetting is one of the most common steps in liquid handling and a good pipetting technique is required for minimization of variability in test results. Manual pipetting is one of the largest sources of error in instrumental analysis⁴⁴.

⁴⁵. This is particularly true when dealing with ultra-low volume (micro and nano-liter) range and if the analyst has minimal expertise in dealing with such low-volumes. Consider a case where analysts such as drinking water treatment plant (WTP) operators who may not have formal analytical training are running daily routine analytical tests. Differences in the pipetting technique between analysts could be a major source of variability in test results. Moreover, some recent studies show long term repetitive use of a pipet can lead to an increased risk of developing muscle and tendon related conditions such as Tendonitis, Carpal Tunnel Syndrome, Epicondylitis, etc^{46,47}. There are commercially available dispensers, such as the Hamilton Microlab 600 that retails for \$7,500, but they are not affordable by small-scale, analytical laboratories. In this case, the focus of this research is in the WTP analytical laboratory.

To address the issue of precision and accuracy in pipetting, automation of the technique with a “push button” approach might be an appropriate solution. Moreover, automation of the pipetting technique can reduce the effort, time in making standard solutions and eliminate analyst to analyst variability. The major goal of this work is to develop the EZ-AutoPipet, a low-cost liquid delivery system that can dispense microliter volumes accurately and reproducibly using Raspberry Pi and 3D printing technology.

Experimental

Development of EZ-AutoPipet

The EZ-AutoPipet is an automated liquid delivery system that is comprised of five essential components: (1) Raspberry Pi single board computer; (2) python programming; (3) 3D-printed parts; (4) stepper motor based liquid delivery system; and (5) plunger positioning system.

Raspberry Pi Single Board Computer

The Raspberry Pi is a credit-card sized single-board computer used to control and communicate with the external hardware such as stepper drivers, and position sensor. In this work, a Raspberry Pi 3 Model 3+ is used (Raspberry Pi Foundation, UK) with a 7-inch capacitive touch display (Raspberry Pi Foundation, UK) to facilitate user interaction with the EZ-AutoPipet application. Raspberry Pi have a fully-featured operating system, Raspbian (Jessie), which facilitates programing and control of the various hardware interfaces. For this research, the most useful feature of the Raspberry Pi is the availability of 40 general purpose input output (GPIO) pins⁴⁸. These pins include three types of serial communication pins⁴⁸ such as Universal Asynchronous Read and Transmit (UART), Inter-Integrated Circuit (I2C) and Serial Peripheral Interface (SPI). The positional sensor communicates with the Raspberry Pi through I2C and the stepper driver uses SPI. Apart from communication pins, there are two 5 V and two 3.3 V voltage pins and several ground pins on board. The remaining GPIO pins can be configured as either output or inputs. The output pins can be configured as either 3.3 V or 0 V to trigger external devices and input pins can read either 3.3 V or 0 V typically to identify the status of a peripheral device⁴⁹.

Python Programing Language

Python programming has gained enormous popularity over the past decade due to the following reasons^{11,50}: (1) the simplicity of syntax simplifies programming and understanding; (2) availability of numerous open-source libraries which aids in the rapid development of applications; (3) and python is a cross-platform language. Thus, an application developed on one system can be run on other systems with little or no modifications.

The EZ-AutoPipet application has been developed using two open source libraries, RPi.GPIO and Tkinter. The Rpi.GPIO module⁵¹ (Python Software Foundation, Fredericksburg, VA, USA) facilitates access to the GPIO pins on the Raspberry Pi for control and communication with external hardware. The Tkinter module⁵² (Python Software Foundation, Fredericksburg, VA, USA) is a standard python graphical user interface (GUI)

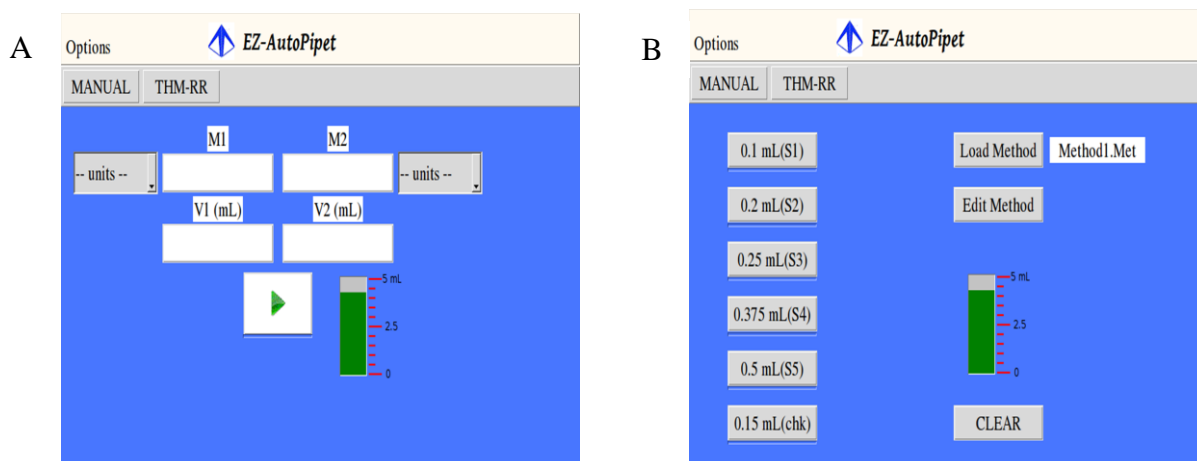


Figure 2. Graphical user interface developed for EZ-Autopipet. (A) shows the manual page where user can perform dilution calculation and (B) shows the THM-RR page where user can dispense multiple volumes with a touch of a button.

package was used to create the GUI as shown in Figure 2. The GUI has two pages one for manually calculating the volumes (Figure 2A) using basic dilution equation ($C_1V_1 = C_2V_2$) and another page for dispensing multiple predefined volumes (Figure 2B). In the basic dilution equation, C_1 is the concentration of the first solution, C_2 is the concentration of the second solution, V_1 is the volume of the aliquot of first solution used, and V_2 is the final volume of second solution prepared. New, predefined intended volumes can be saved to a method file and can be loaded onto the EZ-AutoPipet to customize standards delivery and preparation. This allows the user to save time as well as avoid making mistakes in calculating volumes. The options menu at the top left hand corner (Figure 2A&B) has options for the user to refill or empty the syringe from any position of the syringe plunger. The priming

option accounts for the dead volume of the system. The green bar in the application indicates the plunger position, therefore showing the liquid level in the syringe.

3D Printing Syringe Pump Components

Additive manufacturing, also called 3D printing, is used for rapid prototyping and manufacture with minimal waste of material⁵³. 3D printed parts as support structures along with standard mechanical hardware have been used to construct a syringe pump, shown in Figure 3. TurboCAD 2016 (IMSI/Design, Novato, CA, USA), a computer-aided design (CAD) software package, was used to design the parts and files were saved in stereolithography format files (.STL). Then .STL files were uploaded to Formlabs Preform software (Formlabs Inc., Somerville, MA USA) and models were printed by commercially available Form 2 Stereolithography Apparatus (SLA) printer (Formlabs, Somerville, MA, USA). After printing was completed, the models were then soaked in isopropyl alcohol to remove excess resin for 40 minutes and dried under normal laboratory conditions for 2-3 hours. Supports were detached from the models and parts were assembled to finish the syringe pump.

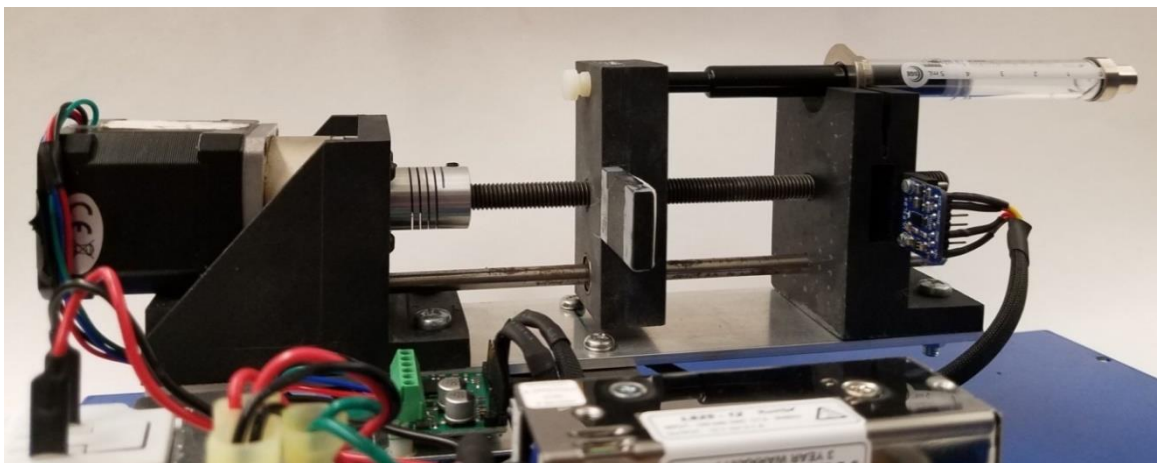


Figure 3. Photo of completed 3D printed stepper motor based.

Stepper Motor Based Liquid Delivery System

The developed liquid delivery system was a stepper motor-based syringe pump which accurately delivers liquid as low as microliter volumes depending on the nominal volume of the syringe. Stepper motors are brushless motors whose rotation is controlled by a digital square wave^{54,55} as shown in Figure 4. The degree of rotation of the stepper motor is proportional to the number of pulses sent to stepper motor via stepper driver^{54,55}. For example, a stepper motor with 1.8° step resolution requires 100 steps to rotate 180° accurately in full-step mode. Since the digital pulses can be accurately and precisely controlled with the Raspberry Pi, the degree of rotation of the motor can also be accurately controlled. The time period (T) of the square wave governs the speed of the motor and thus the rate of volume delivery. Digital pulses required to drive the stepper motor were generated by alternatively driving a GPIO pin on the Raspberry Pi connected to step pin on the stepper driver between active Low (0V) and active High (+3.3V) with a pulse width of 0.001sec. In present work, NEMA-17 1:5 gear ratio bipolar stepper motor (Stepper On-line, China) and

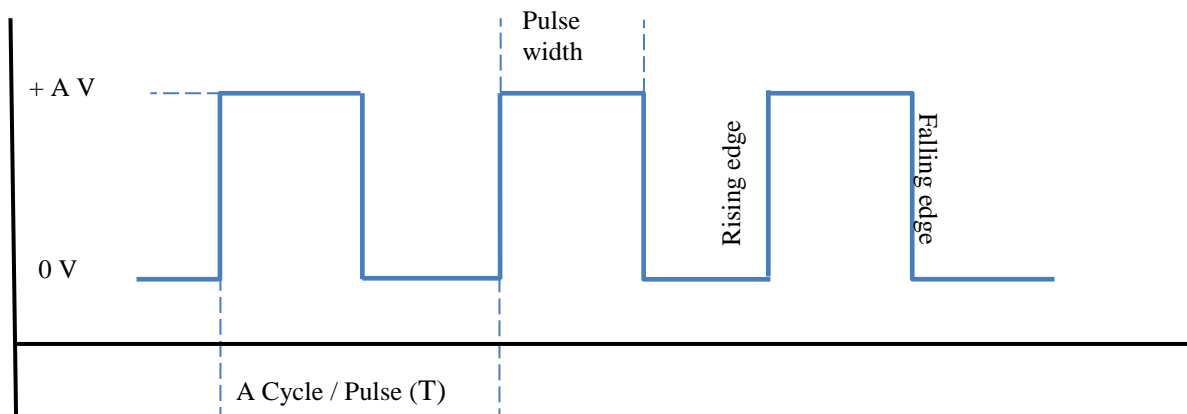


Figure 4. Characteristics of digital square pulses used to drive the stepper motor. T is the time period of square wave. Since Raspberry Pi generates 3.3 V high logic, amplitude (A) is +3.3 V. Rising edge is the transition from Low logic (0 V) to high logic (3.3V).

AMIS-30543 (Pololu, Las Vegas, NV, USA) micro stepping bipolar stepper motor driver were used. The stepper driver accepts the digital pulses from the Raspberry Pi and converts those into a sequence of high amplitude signals to drive the motor. Using this approach, the

stepper driver controls the current flow to the stepper motor, direction, and speed of rotation in revolutions per minute (rpm).

Table 1. Register address and bit structure used to set motor driver parameters¹⁰¹.

Parameter	Register Address	Bit Structure	
Enable Motor	0x03	0b10000000	
Motor Coil Current (0.35A)	0x01	0b10000010	
Direction	0x02	clockwise	0b01000000
		counterclockwise	0b11000000
Step mode (Half-step)	0x01	0b10000010	

The AMIS-30543 stepper driver was initialized and configured by writing 8-bit binary sequences to four control registers in the AMIS-30543 through Serial Peripheral Communication (SPI) interface (Table 1). These 8-bit binary sequences control parameters such as motor current, step-size, and direction of rotation. The first bit in the bit sequence writing to register at 0x03 enables(1) or disables(0) the motor outputs. The direction of rotation was controlled by direction bit (the first bit in 0x02 register bit sequence) in combination with the logic level on the input direction pin on the driver. The first three bits in 0x01 register bit sequence were used to select step mode and the remaining five bits were used to select the motor current.

Plunger Position Monitoring System

The plunger position monitoring system is critical for safe operation of the syringe pump by providing an exact position of the plunger at any point in time. This ensures the plunger is within the physical limits of the syringe barrel. In addition, the position monitoring system provides feedback to determine the volume required to refill or empty the syringe and if the desired volume was dispensed or not. In other words, the position system knows where the plunger is at all times and provides feedback to the Raspberry Pi for calculations and physical aspects of operation. A 10 cm linear potentiometer (soft-pot) (Spectrasymbol, Salt Lake City, UT, USA) is coupled with an ADS115 16-bit analog to digital converter (ADC) (Adafruit, New York, NY, USA) was used to obtain the plunger position. The piece that drives the plunger has a wiper (a spring-loaded nut) at the bottom.

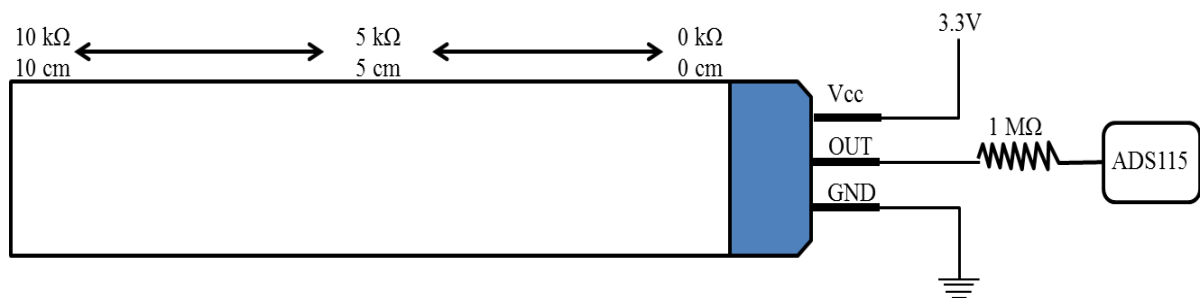


Figure 5. Resistance on output channel of soft-pot changes with distance from base (0 cm). The voltage drop across 1 MΩ is read by ADS115.

The wiper presses the soft-pot constantly and when the plunger driving piece moves, the electrical resistance on the output channel of the soft-pot changes as a function of distance from the base at which it is pressed on and the voltage drop across 1 MΩ resistor is determined using the ADC (Figure 5). A 1 MΩ resistor was used to achieve a linear electrical response with the change in plunger position. The millivolt response from ADS115 can be converted to a position (in volume) using a calibration curve.

Chemicals, Reagents and Standards

All the reagents and standards were prepared using reagent grade water with a resistivity of at least 18.2 M Ω -cm and total organic carbon (TOC) of 10 μ g/L or less produced by a Barnstead E-Pure water purification system (ThermoFischer Scientific, Waltham, MA, USA). All the chemicals were reagent grade or ACS certified grade except the calmagite which was indicator grade. Calmagite and sodium carbonate were purchased from Acros Organics (New Jersey, USA). All other chemicals and reagents were purchased from Fisher Scientific.

Calibration and validation tests were performed using reagent grade water. The hardness stock standard was 1016 mg/L CaCO₃ and prepared by adding 0.5008 g of calcium carbonate dried at 120°C for 2 hrs into 500 mL beaker containing 250 mL reagent water. A 50% dilution of concentrated hydrochloric acid (HCl) was added slowly until all the calcium carbonate was dissolved. The solution was heated to expel all the CO₂ and the pH was adjusted to ~5 with a 50% dilution of concentrated ammonia solution (NH₃). Finally, the solution was diluted to a final volume of 500.00 mL using reagent water in a volumetric flask. An alkalinity stock standard of 1021 mg/L as CaCO₃ was prepared by diluting 0.5390 g of sodium carbonate dried at 120°C for 2hrs to 500.00 mL reagent water. The standard alkalinity and hardness solutions were prepared by diluting the stock solutions appropriately. A 0.02 N HCl solution was prepared by volumetrically diluting concentrated acid with reagent water and standardized with sodium carbonate (Na₂CO₃) solution⁵⁶. A 0.01 M ethylenediaminetetraacetic acid (EDTA) solution was prepared by dissolving an appropriate amount of EDTA disodium salt dihydrate into reagent water and standardized with a standard calcium solution⁵⁷. Calmagite indicator solution (0.1% W/V) was prepared by diluting 0.1 g of solid calmagite in 100.00 mL of reagent water. An ammonia buffer (pH 10.3) was

prepared by dissolving 1.179 g EDTA disodium salt dihydrate and 0.780 g magnesium sulfate heptahydrate in 100.00 mL of reagent water. Then, 16.9 g ammonium chloride (NH_4Cl) and 143 mL of concentrated ammonium hydroxide (NH_4OH) was added to the solution above and diluted to 250.00 mL with reagent water.

Results and Discussion

Calibration of the Stepper Motor for Liquid Delivery

The stepper motor must be calibrated to dispense a particular volume because the Raspberry Pi and stepper driver at the outset as they do not “know” how much to turn the motor to deliver a particular volume. The stepper motor was calibrated by sending a known number of digital pulses to stepper motor. The average mass of reagent water dispensed was measured to 0.1 mg by an analytical balance (Model SI-114, Denver Instruments, Bohemia, NY, USA) and the volume dispensed was calculated using the density of water at the temperature of the solution. A five-point calibration curve was constructed by plotting the actual dispensed volume as a function of numbers of pulses using three different size syringes: 0.1, 1, 5 mL (Figure 6).

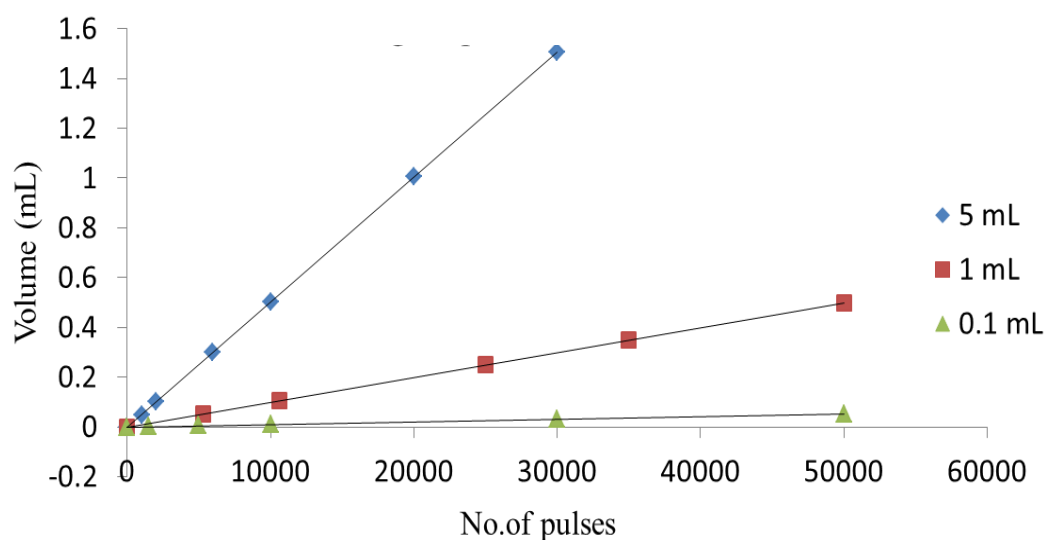


Figure 6. Calibration of stepper motor using three different size syringes. Plot with blue diamond markers is for 5mL, red square markers is for 1 mL and green triangle markers represent 0.1 mL syringe.

Table 2. Slopes, Intercepts and R^2 values of calibration curves for three different size syringes.

Syringe Volume	R^2	Slope	Volume/pulse	Intercept
5 mL	0.999	5×10^{-5}	50 nL	-0.0008
1 mL	0.999	1×10^{-5}	10 nL	-0.0005
0.1 mL	0.999	1×10^{-6}	1 nL	-0.0003

The number of pulses required to dispense a particular volume is calculated from the linear regression line equation and sent to the stepper driver to rotate the motor an appropriate amount. Table 2 presents the coefficient of determination (R^2), slopes and intercepts of the calibration plots for three syringe sizes. All three plots have R^2 values close to 1 showing good linearity. The slope values are the volume dispensed in mL per pulse as shown in Table 2. The slopes for 5, 1- and 0.1-mL syringes are in the ratio of 5:1:0.1 respectively which suggests that the plunger travels the same linear distance independent of syringe size for particular number of pulses and the volume delivered is solely dependent on syringe diameter in this case. Theoretically, the syringe pump can deliver volumes in the range of nanoliters. In practice, this may not be true and requires a different measurement approach to verify.

Position Sensor Calibration

The soft-pot has been calibrated to read the exact position of the syringe plunger. Using a 5 mL syringe, the plunger was moved to a known position and output voltage from soft-pot was measured by ADS115. Then ADC values (voltage reading) were plotted as a function of plunger position in milliliters. The calibration plot shown in Figure 7 has good linearity with an R^2 value of 0.999.

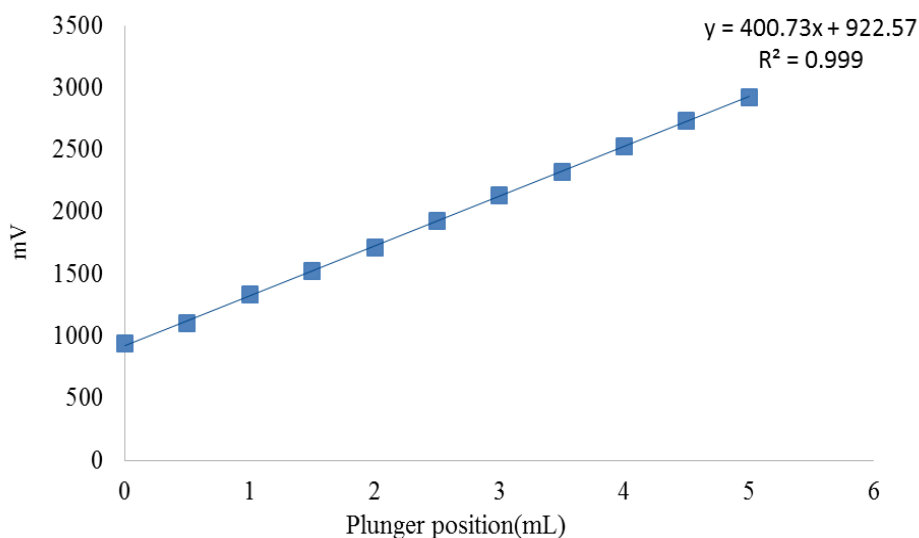


Figure 7. Calibration plot for position sensor. Voltage output readings from linear potentiometer (soft-pot) are plotted against known plunger positions of 5 mL syringe.

The accuracy of the position sensing system was tested by moving the plunger to a known position and then calculating the required steps to deliver a known volume. The syringe plunger was manually set at the 5 mL mark carefully and digital pulses required for moving the plunger to a particular position were calculated from the calibration plot for the 5 mL syringe (Figure 6). Then the plunger position from the sensing system was calculated from the calibration plot shown in Figure 7. The same experiment was repeated two consecutive days to check the reproducibility of the system. Table 3 summarizes the results from testing of the position sensing system and absolute error was calculated as “Calculated – Actual volume”. The absolute error ranges from + 0.00 to 0.04 mL (0 to 40 μ L) and calculated volumes did not change significantly over two days indicating decent reproducibility and stability of calibration.

Table 3. Results from testing of position sensing system over two consecutive days with a 5 mL syringe.

Day-1			Day-2	
Actual Volume (mL)	Calculated (mL)	Absolute Error (mL)	Calculated (mL)	Absolute Error (mL)
0.9	0.91	+ 0.01	0.91	+ 0.01
1.6	1.62	+ 0.02	1.62	+ 0.02
2	2.00	+ 0.00	2.00	+ 0.00
5	5.04	+ 0.04	5.03	+ 0.03

Operation of the EZ-AutoPipet

After the system is powered on, an analyst has two choices for EZ-AutoPipet operation: load a method that contain pre-determined volume delivery for a standard method; or use the manual tab to determine volume delivery for a given standard, final concentration and final volume. Figure 8 outlines the operational steps of EZ-AutoPipet to deliver a selected (or calculated) volume. When a particular method is loaded, dispensing volumes will be assigned to the on-screen buttons. When a button is pressed, the corresponding volume will be converted to the number of digital pulses required to dispense that volume using the calibration curve (Figure 6). The position of the plunger is then acquired from the position sensing system. Based on the position, the system calculates the amount of liquid available in the syringe. If the liquid available is enough, then the Raspberry Pi generates the digital pulses and drives the motor. A checkmark will appear next to the button after dispensing and EZ-AutoPipet will be ready for the next delivery. If the available volume is not enough, system prompts the user to refill. When the user selects refill, system will change the direction of the motor rotation and calculates the volume and digital pulses required to refill. Once refilled the system changes direction to prime the line and is ready for liquid

dispensing. These same processes apply to the manual page except the desired volume is calculated from dilution calculation.

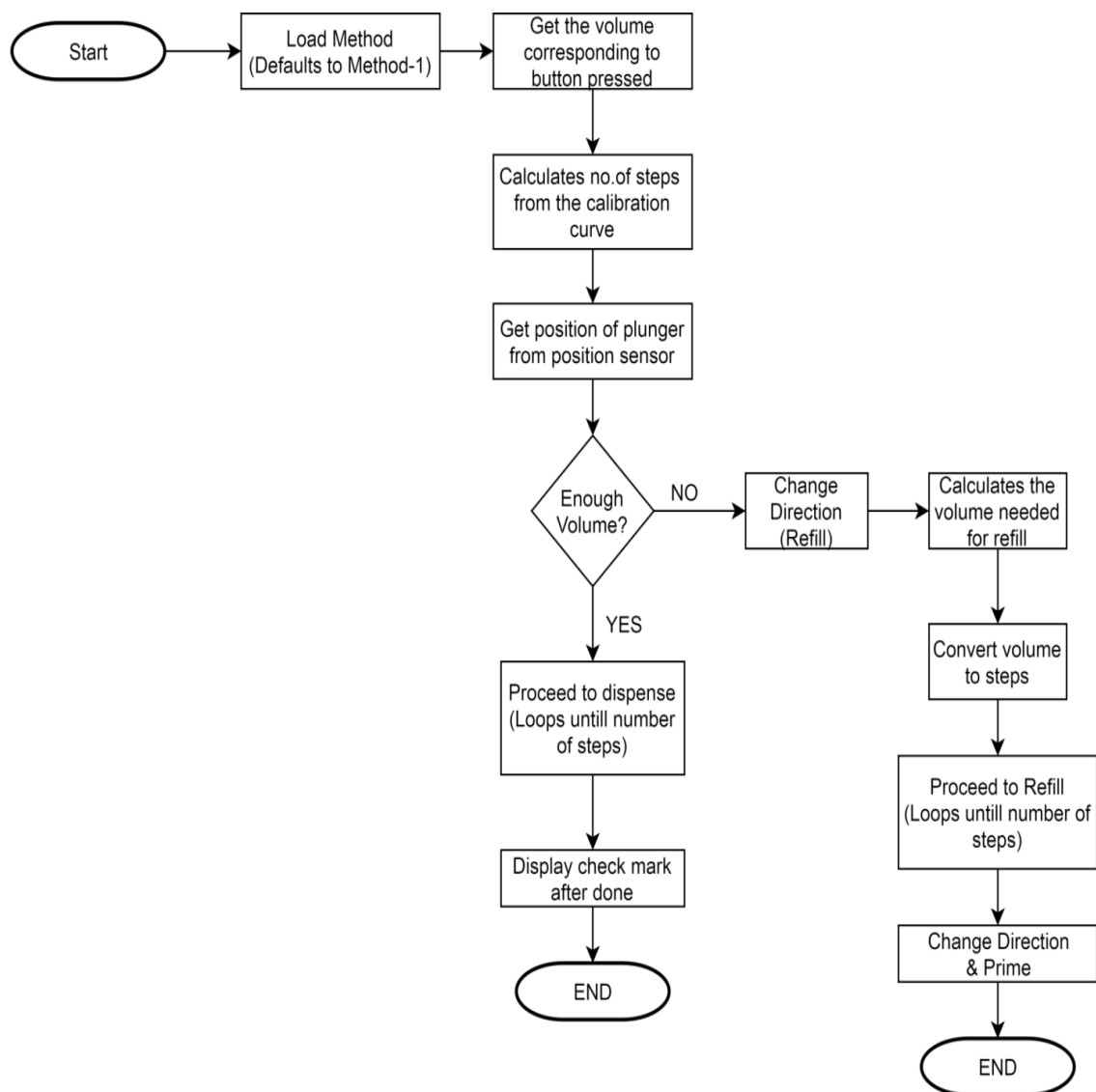


Figure 8. Flow chart showing the important steps in the operation of EZ-AutoPipet.

Validation of Liquid Delivery

The EZ-AutoPipet was evaluated on an intra-instrumental, inter-instrumental, inter-day, and intra-day, accuracy, and precisions using a 5 mL syringe delivering 0.1 mL, 0.5 mL and 1 mL volumes. For each volume, reagent water was dispensed seven times and the mass dispensed each time was determined using an analytical balance with resolution of 0.1 mg. The average mass dispensed is converted to volume using temperature compensated density of water. Accuracy was calculated as mean percent recovery^{58,59} as shown in Equation (1). Precision was calculated as the percent relative standard deviation of seven replicates^{58,59} using Equation (2).

$$\text{Accuracy} = \frac{\text{Mean Calculated Volume}}{\text{Nominal Volume}} \times 100\% \quad (1)$$

$$\text{Precision} = \frac{\text{Standard deviation of calculated delivered volume}}{\text{Mean Calculated Volume}} \times 100\% \quad (2)$$

An Analysis of Variance (ANOVA) test was performed to identify the differences between the means within a study. If the p-value of the analysis is less than 0.05 (significance level), the null hypothesis can be rejected⁶⁰. This means that the calculated means of the volume are statistically different and indicated as ‘YES’ in Table 4. Otherwise, the means are statistically **not** different and indicated as ‘NO’. Three EZ-AutoPipets at three different volumes were compared to evaluate intra-instrumental accuracy and precision (Table 4). The mean percent recovery of all three pipets for all three volumes ranges from 98.9 to 102.1% with precision ranging from 0.6 to 3.0%. The ANOVA test for individual volumes has a p-value greater than 0.05 indicating the means are statistically not different. The intra-instrumental study demonstrated the precision and robustness of the electronics (particularly stepper motor and drivers) and the EZ-AutoPipet assembly. More importantly, the intra-instrumental study established that a single calibration curve (Figure 6) can be used

comfortably on multiple systems without having to calibrate each pipet separately and instead a quality assurance check can be conducted to ensure proper performance.

In a second set of comparisons, an EZ-AutoPipet was compared to a commercially available dispenser - Dosimat (Metrohm, Riverview, FL, USA) and a graduated, 1 mL mohr pipet. This study was performed by a student with little experience using all the three delivery systems which is a similar situation expected in a water treatment plant (WTP). The student delivered three different volumes with the three instruments and then determined the volume delivered by mass and temperature corrected density conversion. For the 0.1 mL delivery, the EZ-AutoPipet has a better accuracy and precision when compared to the other two. Manual pipetting has an accuracy of 148.3% for 0.1 mL volume. At higher volumes (0.5 and 1 mL), the Dosimat has comparable accuracy and precision to the EZ-AutoPipet but manual pipetting has mean percent recoveries that are higher, ranging from 109 – 119 %. The means from three different pipetting techniques at all test volumes are significantly different. During the studies, the EZ-AutoPipet proved to be free from operation error and produced acceptable results irrespective of analyst expertise.

Table 4. Validation results for EZ-AutoPipet.

						Means Statistically different? (P < 0.05)
Intra-instrumental		EZ-AutoPipet-1	EZ-AutoPipet-2		EZ-AutoPipet-3	
Actual Volumes	Calculated (mL)	Accuracy	Calculated (mL)	Accuracy	Calculated (mL)	Accuracy
0.1 mL	0.1020 ± 0.002 ₄	102.1 ± 2.4%	0.0994 ± 0.002 ₆	99.4 ± 2.6%	0.0989 ± 0.003 ₀	98.9 ± 3.0%
0.5 mL	0.4995 ± 0.005 ₀	99.9 ± 1.0%	0.4980 ± 0.004 ₅	99.6 ± 0.6%	0.4970 ± 0.004 ₅	99.4 ± 0.9%
1 mL	0.9915 ± 0.021 ₈	99.1 ± 2.2%	0.9990 ± 0.007 ₀	99.9 ± 0.7%	0.9936 ± 0.006 ₀	99.3 ± 0.6%
Inter-instrumental		EZ-AutoPipet	Dosimat		Mohr pipet	
0.1 mL	0.0994 ± 0.002 ₆	99.4 ± 2.6%	0.1412 ± 0.003 ₇	141.2 ± 3.7%	0.1483 ± 0.003 ₂	148.3 ± 3.2%
0.5 mL	0.4978 ± 0.004 ₆	99.6 ± 0.9%	0.5321 ± 0.010 ₆	106.4 ± 2.0%	0.5953 ± 0.010 ₄	119.1 ± 1.7%
1 mL	0.9985 ± 0.006 ₆	99.9 ± 0.7%	1.0294 ± 0.009 ₇	102.9 ± 0.9%	1.0976 ± 0.018 ₇	109.3 ± 1.7%

Table 4. Continued.

Inter-day	Day-1			Day-2			Day-3			Are Means Statistically Different?
	Actual Volumes	Calculated (mL)	Accuracy	Calculated (mL)	Accuracy	Calculated (mL)	Calculated (mL)	Accuracy	Accuracy	
	0.1 mL	0.1021 ± 0.002 ₄	102.1 ± 2.4%	0.1011 ± 0.001 ₇	101.1 ± 1.7%	0.0999 ± 0.001 ₈		99.9 ± 1.8%		NO
	0.5 mL	0.4993 ± 0.005 ₀	99.9 ± 1.0%	0.5005 ± 0.003 ₄	100.1 ± 0.7%	0.4977 ± 0.005 ₂		99.5 ± 1.0%		NO
	1 mL	0.9913 ± 0.021 ₅	99.1 ± 2.2%	1.0024 ± 0.004 ₅	100.2 ± 0.4%	0.9954 ± 0.007 ₉		99.5 ± 0.8%		NO
Intra-day			Iteration-1		Iteration-2			Iteration-3		
	0.1 mL	0.1011 ± 0.001 ₇	101.1 ± 1.7%	0.0985 ± 0.002 ₄	98.5 ± 2.4%	0.1004 ± 0.001 ₂		100.4 ± 1.2%		NO
	0.5 mL	0.5005 ± 0.003 ₄	100.1 ± 0.7%	0.4995 ± 0.003 ₇	99.9 ± 0.7%	1.004 ± 0.001 ₂		99.3 ± 1.6%		NO
	1 mL	1.0024 ± 0.004 ₅	100.2 ± 0.4%	1.0017 ± 0.005 ₆	100.2 ± 0.6%	0.9956 ± 0.011 ₇		99.5 ± 1.2%		NO

An intra-day study was conducted by using a single EZ-AutoPipet to deliver 0.1 mL, 0.5 mL, and 5 mL volumes using a 5 mL syringe for seven replicates at three different times in a day (Table 4). The accuracy ranges from 98.5 to 100.2% with precision ranging from 0.4 to 2.4% for all three volumes over the time period of a single day. For each test volume, the mean calculated volumes from different times were statistically equivalent. The same EZ-AutoPipet was then used in an inter-day study using the same volumes and approach has been tested over three consecutive days and the mean calculated volumes from different days at each tested volume agree and the accuracy ranges from 99.1 to 102.1% with precision ranging from 0.4 to 2.4%. Again, the mean calculated volume delivered for each volume for the inter-day study was statistically equivalent (Table 4). The inter and intra-day studies indicate the stability of the stepper motor calibration and that the accuracy of the EZ-AutoPipet does not change over time regardless of dispensing volume. For the combined replicates on all experiments for the intra-day and inter-day measurements, the average accuracies and precisions for 0.1, 0.5 and 1 mL are $100.3 \pm 2.2\%$ (0.1003 ± 0.0022 mL), $99.7 \pm 0.9\%$ (0.4986 ± 0.0045 mL) and $99.7 \pm 1.0\%$ (0.9973 ± 0.0049 mL) respectively. The 0.1 mL deliveries have a precision of ~2 % and are worse than the 0.5 mL and 1 mL precision values. It is likely that a delivered volume of 0.1 mL is nearing the limit of acceptable error for a 5 mL syringe. Thus, smaller volumes require smaller syringes.

To put these results in context, a Class A, 5 mL volumetric pipet has a reported absolute error of ± 0.01 mL (0.2 %RSD)⁶¹ for a 5 mL volume delivery. The reported error for a Class A, 5 mL, graduated Mohr pipet ± 0.02 mL (0.4 %RSD). The EZ-AutoPipet can deliver a volume of 1 mL in a 5 mL syringe with a %RSD of 1.0% without the need for specialized skills and training. This is a significant advantage for WTP operators that likely do not have the specialized training yet need the ability to prepare accurate standards for calibration of instrumentation.

Accuracy and Precision of Liquid Delivery with 1.0- and 0.1-mL Syringes

An EZ-AutoPipet was used to test the accuracy and precision of liquid delivery at the low microliters range using a 1 mL and 0.1 mL syringe (Table 5). In these studies, an EZ-AutoPipet with a 1 mL glass syringe was used to deliver seven replicates of 100 μ L with an accuracy of 100.9% and a precision of 1.2%. A volume of 50 μ L was delivered over seven replicates to an accuracy of 101.4% with a precision of 1.7%. A similar study using 0.1 mL syringe and seven replicates at each volume was conducted for 5 μ L and 1 μ L. For 5 μ L, the EZ-AutoPipet dispensed with an accuracy of 100.9% and a precision of 3%. For 1 μ L, the accuracy was 123.8 % with a precision of 14.8 %. That typical mass of water measured for the 5 μ L and 1 μ L studies were \sim 5 mg and \sim 1 mg, respectively. When measured on an analytical balance, the balance itself has a standard deviation of \pm 0.1 mg (0.1 μ L)⁶² which contributes to 10 % of the standard deviation observed in the measurements. Alternative methods to measure such low volumes need to be investigated as well as better control over the environment is required to improve the accuracy.

Table 5. Accuracy and Precision of EZ-AutoPipet using 1.0 mL and 0.1 mL syringes to deliver the low microlitre volumes.

1 mL syringe	Calculated (mL)	Accuracy
0.05 mL (50 μ L)	0.0507 ± 0.0009	$101.4 \pm 1.7\%$
0.1 mL (100 μ L)	$0.1009 \pm 0.001_2$	$100.9 \pm 1.2\%$
0.1 mL syringe		
0.001 mL (1 μ L)	0.0012 ± 0.0002	$123.8 \pm 14.8\%$
0.005 mL (5 μ L)	$0.00504 \pm 0.0001_5$	$100.9 \pm 3\%$

Re-evaluation of Accuracy and Precision for Low Volume Deliveries

Liquid deliveries between 1 μL and 5 μL were re-examined using a 0.1 mL syringe with a high precision, five decimal (0.01 mg) balance (Sartorius R180D, Gottingen, Germany). The high precision balance was used to measure the mass of water dispensed in a closed room to minimize the air circulation and evaporative losses. Table 6 presents the EZ-AutoPipet accuracy and precision to deliver 1 μL , 1.5 μL , 2 μL and 5 μL volumes. A two-fold improvement in precision and a 20 % improvement in accuracy have been observed for 1 μL delivery when compared to previous results (Table 5). Even though the accuracies of all the tested volumes were close to 100%, precision for deliveries below 2 μL were greater than 3.0% and 2 μL and above volume deliveries has precision below 3.0%. Thus, the practical dispensing limit of a 0.1 mL syringe with the most acceptable precision is ~ 0.005 mL.

Table 6. Results of liquid deliveries using 0.1 mL syringe using better balance and controlled environment.

Nominal Volume	Delivered volume (mL)	Accuracy & Precision
0.001 mL (1 μL)	0.00097 ± 0.00006	$97.6 \pm 6.7\%$
0.0015 mL (1.5 μL)	0.00149 ± 0.00007	$99.3 \pm 4.5\%$
0.002 mL (2 μL)	0.00203 ± 0.00005	$101.6 \pm 2.7\%$
0.005 mL (5 μL)	0.00496 ± 0.00006	$99.2 \pm 1.3\%$

Method Detection Limit, Accuracy and Precision of Trihalomethanes Rapid Response System (THM-RR)

The THM-RR is a fully-automated, gas chromatography-based analyzer for on-line analysis and reporting of the concentrations of four regulated trihalomethanes (THMs) and has been previously described in detail. However, in a typical analysis by the THM-RR, the THMs in drinking water are extracted into the gas phase by a patented capillary membrane sampling device and analyzed by gas chromatograph with electron capture detector (GC-ECD). The four regulated THMs are chloroform (CHCl_3), bromodichloromethane (CHCl_2Br), dibromochloromethane (CHClBr_2) and bromoform (CHBr_3) in drinking water. The concentration of these four THMs is regulated in drinking water at a maximum contaminant level of 0.080 mg/L (80 $\mu\text{g/L}$)^{63,64}.

In this work, an EZ-AutoPipet and a Mohr pipet were used to prepare calibration and check standards to compare the MDL, accuracy, and precision of THM-RR from each pipetting technique. A set of calibration standards were prepared by using EZ-AutoPipet and another set was prepared by manual pipetting (Mohr Pipet). Then, five-point calibration plots over the range of $\sim 1 - 30 \mu\text{g/L}$ for individual THM species were constructed by plotting peak area versus concentration of each species. A check standard concentration of 3.2 $\mu\text{g/L}$ of each THM species was prepared seven times separately by EZ-AutoPipet and Mohr pipet. The check standards were subsequently analyzed to determine method detection limit (MDL), accuracy and precision of THM-RR for each species. MDL was calculated by multiplying standard deviation of the check standard concentration by the t-value for seven replicates at a 98% confidence level which is $3.143^{58,59,65}$ (3).

$$\text{MDL} = \text{Standard deviation} \times t - \text{value}_{n-1, 98\% \text{ confidence level}} \quad (3)$$

Accuracy was calculated as mean percent recovery of the check standards^{20,21} as in equation (4) and precision as a percent relative standard deviation (%RSD) of the check standards^{20,21} as in equation (5).

$$\text{Accuracy} = \frac{\text{Mean Calculated Concentration}}{\text{Actual Concentration}} \times 100 \% \quad (4)$$

$$\text{Precision} = \frac{\text{Standard deviation}}{\text{Mean Calculated Concentration}} \times 100 \% \quad (5)$$

The response of THM-RR to calibration standards prepared from EZ-AutoPipet and manual pipetting were nearly identical with a similar quadratically fit regression line for each THM species as shown in Figure 9. The R^2 values for all four compounds were 0.999 using EZ-AutoPipet whereas using manual pipetting yielded R^2 values ranging from 0.997 to 0.999. Accuracy values of the check standards ranged from 95 to 149% using EZ-AutoPipet while manual pipetting has accuracy ranging from 94 to 141%. Precision for the THM species ranged from 11 to 19 % and 13 to 21% using EZ-AutoPipet and manual pipetting, respectively. Overall, THM-RR yielded similar MDL, accuracy and precision for the four THM species as shown in Table 7 using EZ-AutoPipet as well as manual pipetting. Just as importantly, the preparation of the standards and check standards was accomplished by simply pressing a button on the touchscreen of the EZ-AutoPipet and delivering into a volumetric flask. When compared to the process of manual pipetting, the EZ-AutoPipet is markedly simpler and less prone to human error.

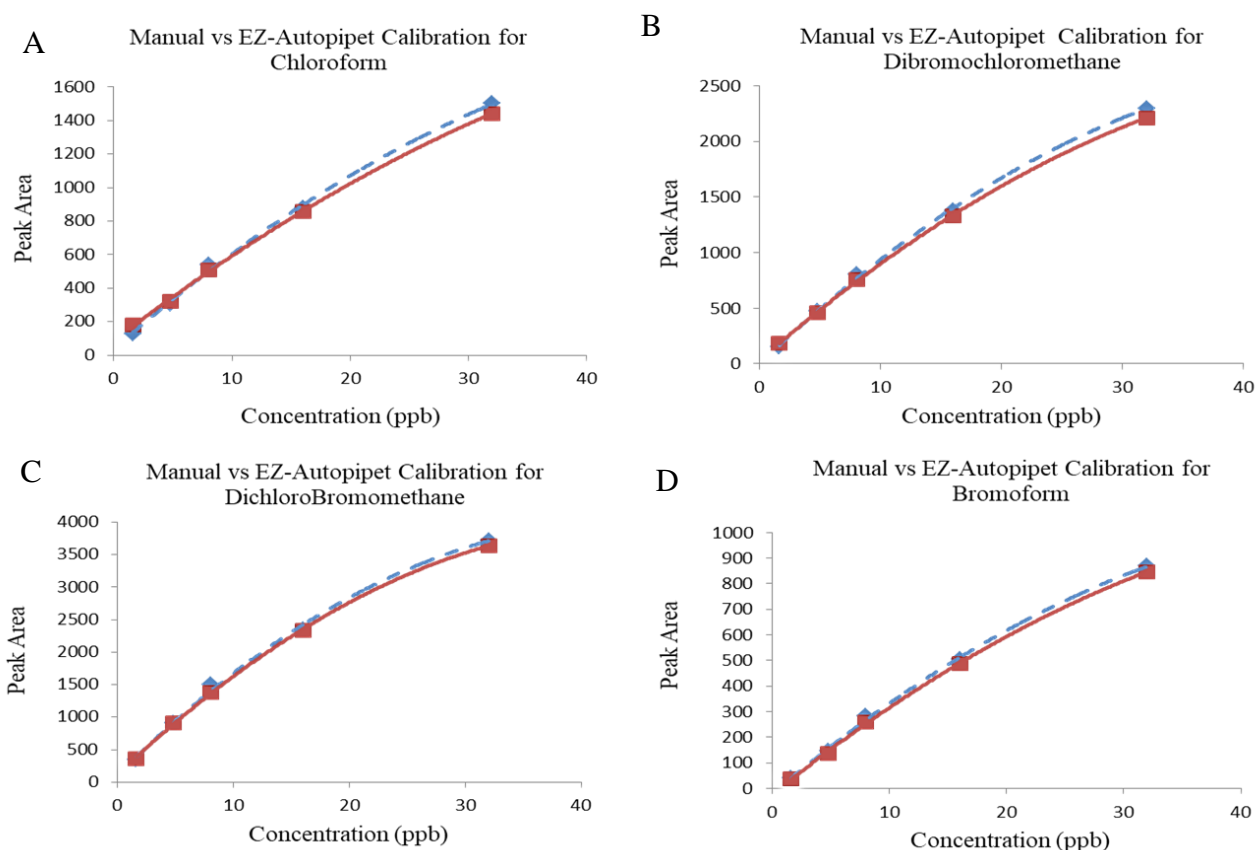


Figure 9. Comparison of calibration of THM-RR using Mohr pipet (Manual) and EZ-AutoPipet. Red continuous line shows calibration curve using EZ-AutoPipet and blue dotted line shows calibration using Manual pipetting (Mohr pipet). Calibration plots for A. chloroform B. dichlorobromomethane C. dibromochloromethane D. bromoform.

Table 7. Detailed MDL, Accuracy and Precision of THM-RR using EZ-AutoPipet and Mohr pipet.

Species	R^2		MDL (ppb)		Accuracy (Mean % Recovery)		Precision (% RSD)	
	EZ-Autopipet	Mohr	EZ-Autopipet	Mohr	EZ-Autopipet	Mohr	EZ-Autopipet	Mohr
CHCl ₃	0.999	0.997	1.0	1.3	95	94	11	13
CHCl ₂ Br	0.999	0.997	1.5	1.4	113	110	13	13
CHClBr ₂	0.999	0.999	1.7	1.9	125	122	14	16
CHBr ₃	0.999	0.999	3.0	2.8	149	141	19	21

EZ-AutoPipet as a Digital Buret for Titrimetric Analysis

The EZ-AutoPipet has been demonstrated to deliver liquid volumes at the microliters volume range both accurately and reproducibly. Given that titrations rely upon accurate and reproducible liquid delivery, an attempt has been made to use the EZ-AutoPipet as a digital buret. In this case, endpoint detection is not automated, but instead done traditionally using human eye to determine when the endpoint of the titration has been reached. Alkalinity and hardness titrations were performed using EZ-AutoPipet and compared with Dosimat and a 50 mL buret. Standard alkalinity and hardness solutions were titrated seven times using the three titrant delivery methods.

Determination of Total Hardness

The hardness titration was conducted as an EDTA titration using the calmagite indicator. A 15 mL of water sample was transferred using a 15 mL volumetric pipet into a 30 mL beaker followed by addition of three drops of calmagite indicator and three drops of ammonia buffer (pH 10.3). The sample was titrated with a standardized EDTA solution until the analyte solution turns to pinkish-blue color and the volume delivered is recorded as the endpoint. The Hardness of the sample is calculated⁵⁷ as shown in Equation (6)

$$\text{Hardness, } \frac{\text{mg}}{\text{L}} \text{ CaCO}_3 = \frac{V_y \times M \times 100,000}{\text{sample volume}} \quad (6)$$

Where V_y is the volume in mL of standardized EDTA used to titrate the sample and M is the molarity of the standardized EDTA. 100,000 mg/mol is a factor to convert the sum of moles per liter of calcium and magnesium to mg/L CaCO_3 . Table 8 shows the results of Hardness titrations from the three titrant delivery methods. The accuracy of hardness titrations from EZ-AutoPipet and manual buret titrations was 115.4 and 115.1 % respectively and Dosimat yielded a mean percent recovery (131.6%) higher than that of the other two methods.

Dosimat has slightly higher precision (± 0.3 mg/L) when compared to EZ-AutoPipet (± 0.6 mg/L) and manual titrations (± 1.5 mg/L). The Analysis of Variance (ANOVA) at 0.05 significance level shows that means from three methods are different which could be due to high mean hardness value from the Dosimat.

Table 8. Comparison of Hardness from EZ-AutoPipet, Dosimat and Manual titration using buret.

(n=7)	Nominal Hardness value (mg/L)	Calculated Hardness value (mg/L)	Accuracy & Precision	Means Statistically Different? (P < 0.05)
EZ-AutoPipet (5 mL syringe)	50.8	58.6 ± 0.6	$115.4 \pm 1.0\%$	
Dosimat (10 mL Buret)	50.8	66.8 ± 0.3	$131.6 \pm 0.4\%$	YES
Manual (50 mL Buret)	50.8	58.5 ± 1.5	$115.1 \pm 2.5\%$	

Determination of Total Alkalinity

The alkalinity titration was conducted as a potentiometric titration. A 15 mL of water sample was transferred using a 15 mL volumetric pipet into a 30 mL beaker. Then the sample was titrated to a pH of 4.3 using standardized 0.02 N Hydrochloric acid (HCl). The alkalinity of the sample is calculated⁵⁶ as shown in Equation (7)

$$\text{Alkalinity, } \frac{\text{mg}}{\text{L}} \text{CaCO}_3 = \frac{V_x \times N \times 50,000}{\text{sample volume}} \quad (7)$$

Where V_x is the volume of standardized acid in mL used to titrate the sample and N is the normality of the standardized acid. 50,000 is a factor with units of mg/equivalents to convert equivalents per liter of carbonate ion to mg/L CaCO_3 .

The results of alkalinity titrations from three titrant delivery methods are presented in Table 9. Accuracy of alkalinity titrations from EZ-AutoPipet and manual buret titrations was 110.0 and 107.6 % respectively whereas Dosimat yielded a mean percent recovery (142.0%) higher than that of the other two methods. EZ-AutoPipet has good precision (± 0.4 mg/L) when compared to Dosimat (± 2.4 mg/L) and manual titrations (± 7.8 mg/L). ANOVA shows that the means from three methods are different which could be due to high mean Alkalinity value from Dosimat.

Table 9. Comparison of Alkalinity from EZ-AutoPipet, Dosimat and Manual titration using buret.

(n=7)	Nominal Alkalinity value (mg/L)	Calculated Alkalinity value (mg/L)	Accuracy & Precision	Means Statistically Different? (P < 0.05)
EZ-AutoPipet (5 mL syringe)	51.0	56.1 ± 0.4	$110.0 \pm 0.6\%$	
Dosimat (10 mL Buret)	51.0	72.4 ± 2.4	$142.0 \pm 3.3\%$	YES
Manual (50 mL Buret)	51.0	54.9 ± 7.8	$107.6 \pm 14.3\%$	

Overall, the EZ-AutoPipet yielded good accuracy and precision for both hardness and alkalinity titrations and has great potential to be used as a digital buret to produce accurate and precise titration results. As with the dispensing of volume for the preparation of standards, using the EZ-AutoPipet as a digital buret simplifies the titration process and allows the analyst to focus on endpoint determination

Conclusion

A low-cost liquid delivery system (EZ-AutoPipet) was developed and tested successfully. A single channel system was constructed for under \$550 in components and a dual channel system was constructed for under \$750. Various validation tests show EZ-AutoPipet delivers liquids with high accuracy and precision which potentially reduces errors in standard preparations. The EZ-AutoPipet also produced excellent results regardless of analyst expertise which eliminates analyst to analyst variability in solution preparation thereby reducing the variability in test results. The THM-RR UI page (Figure 2B) can be adapted easily to perform different methods. Additionally, a Peltier cooling system has been implemented to improve the stability of thermally labile compounds. The lower limit of dispensing volume for different size syringes is selected such that % RSD is no more than 3.0% which is presented in Table 10 showing lower limits for 5, 1 and 0.1 mL syringes. The

Table 10. Lower limit of dispensing volumes for 5, 1, and 0.1 mL syringes.

Syringe Size	Lower Limit
5 mL	$100.0 \pm 2.2 \mu\text{L}$
1 mL	$50.0 \pm 0.9 \mu\text{L}$
0.1 mL	$2.00 \pm 0.05 \mu\text{L}$

EZ-AutoPipet produced good accuracy and precision for alkalinity and hardness titrations showing that it can be used not only as a pipet but also as a digital buret. The EZ-AutoPipet technology has been successfully adapted to develop a low-cost automated titration system – EZ-AutoTitrator which will be presented in the next chapter.

CHAPTER 3

DEVELOPMENT OF LOW-COST AUTOMATED TITRATION SYSTEM FOR POTENTIOMETRIC AND SPECTROCHEMICAL END-POINT DETECTION

Introduction

In a drinking water treatment plant (WTP), alkalinity, hardness, and iodometric titrations are conducted daily. These analyses determine water quality parameters that inform how a superintendent will adjust the addition of treatment chemicals for that shift and that day. These three parameters are typically determined using potentiometric or spectrochemical titration techniques that require pH probes or visual determination of the endpoint using an indicator dye, respectively. Liquid handling and endpoint determination for titrimetric analytical methods are crucial for producing accurate and reproducible results. In alkalinity, hardness, and iodometric titrations, determination of the end point is one of the key factors in reproducibility between analysts. In short, different analysts visually detect different end points of the titrations. In a drinking WTP, this can be a significant source of variability and thus cost the superintendent more in operating funds (i.e. chemical costs). In addition, titrations constitute large proportions of analytical procedures in quality control laboratories across a range of industries.

Necessity for Automation

Automation of scientific measurements has been reported since the late 18th century⁶⁶. Over the past three decades, demand for automation of laboratory methods has increased due to an increased number of samples, increased complexity of the chemical analysis methods, and a high demand for accuracy and precision regardless of personnel^{66,67}.

An automated titration system has several advantages over manual titrations. Manual titrations require skilled analysts and time to perform the analysis. In contrast, an autotitrator

does not need personnel with any prior experience and just a click of a button performs the titration for the analyst. Further advantages include: the analyst does not have to stay at the workstation to perform the titration and can focus on other tasks while a titration is performed by the titrator. An autotitrator reduces the subjective variability of endpoint determination which ultimately improves the accuracy and precision of the test results⁶⁸. Finally, these systems can also reduce reagent usage and limit human exposure to chemicals because there is no need for manual filling and dispensing of the titrant.

The primary goals of this research are to

1. Develop an automated titration system that can perform potentiometric and spectrochemical titrations and be able to monitor pH and temperature.
2. Develop titrimetric analysis methods for total alkalinity (potentiometric), hardness in water (spectrochemical) and free available chlorine (FAC) in bleach solutions (spectrochemical).

Total Alkalinity of Water

Total alkalinity refers to the ability of water to resist changes in pH⁵⁶. Generally, drinking water treatment plants report total alkalinity as milligrams per liter calcium carbonate (mg/L CaCO₃). In drinking water, it is mainly due to the presence of carbonates (CO₃²⁻), bicarbonates (HCO₃⁻) and hydroxides (OH⁻)⁵⁶. Silicates, phosphates (PO₄³⁻), borates (BO₃³⁻) and organic bases which are present in relatively smaller amounts are insignificant contribution towards alkalinity⁶⁹. The alkalinity of water does not have any adverse health effects but has implications on water treatment parameters/dosing with respect to turbidity and softening requirements. Turbidity is frequently removed from drinking water by coagulation and flocculation. This process releases hydrogen ions (H⁺) into the water especially when inorganic coagulants such as alum or ferric chloride is used⁷⁰. Alkalinity

concentrations must be present in excess of that neutralized by the hydrogen ion released for effective and complete coagulation to occur⁷¹. Hard waters are frequently softened by precipitation methods. The alkalinity of the water must be known in order to calculate the lime ($\text{Ca}(\text{OH})_2$) and soda ash (Na_2CO_3) requirements for precipitation softening⁷².

Alkalinity is typically determined by titrating a water sample to pH 4.3, since carbonates and bicarbonates are the primary components of alkalinity⁵⁶. In the titration, the addition of hydrochloric acid as the titrant protonates the carbonates and bicarbonates and forms carbonic acid as shown in Figure 10. In this case, the endpoint of pH 4.3 is determined potentiometrically, though it can also be determined spectrochemically using indicators.

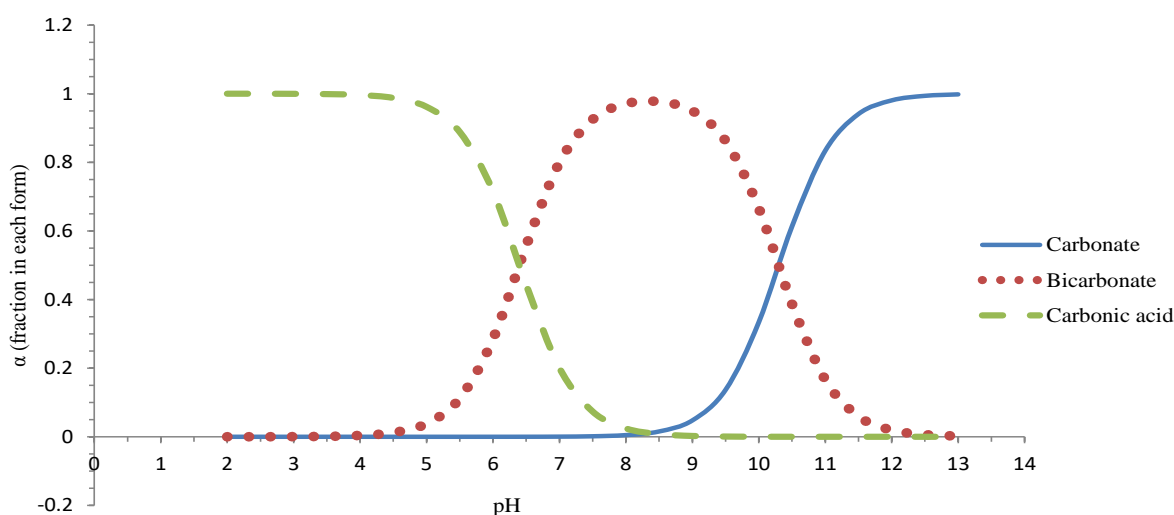


Figure 10. Fractional composition diagram of carbonic acid, bicarbonate ion, and carbonate ion. This plot shows the fraction of each species of carbonic acid ($\text{pKa}_1 = 6.4$ and $\text{pKa}_2 = 10.3$) at various pH. Below 4.4, carbonic acid is the dominant form and carbonate ion species dominates above pH 12. At the pH of drinking water ~ 7.5 , the bicarbonate ion is the primary species present.

Total Hardness of Water

In drinking water, hardness is mainly due to the presence of calcium and magnesium salts and is reported as mg/L CaCO_3 ⁷³. There are two types of hardness in water based on the counter ions of calcium and magnesium present, temporary hardness and permanent hardness. Temporary hardness is caused by the presence of the carbonate and bicarbonate salts of calcium and magnesium⁷⁴. Permanent hardness occurs when the sulfate and chloride salts of calcium and magnesium are the primary species present⁷⁴. Temporary hardness can be removed simply by heating the water to precipitate the carbonate salts from solution. Permanent hardness is generally difficult to remove through heating and typically requires an ion exchange process or water softener to alleviate. Table 11 shows the classification of water hardness adapted from United States Geological Survey (USGS)⁷³.

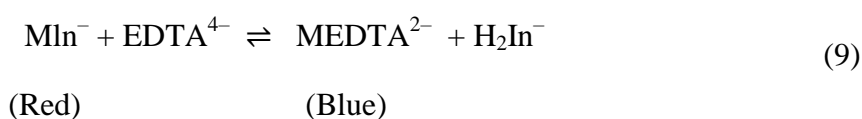
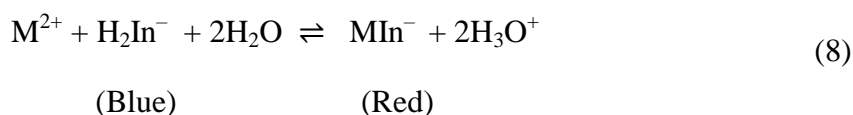
Table 11. Broad classification of potable water based on the level of hardness.

Classification	mg of CaCO_3 /L
Soft	0-60
Moderately hard	61-120
Hard	121-180
Very hard	>180

The hardness of water is primarily responsible for the formation of scales (usually calcium carbonates) which causes variety of problems in the distribution system, homes, and businesses. Scale formation inside the distribution supply pipes decreases the pipe carrying capacity and increases energy demand due to increased pumping costs. Moving parts of pumps, valves, and water meters are also subject to scale formation which increases maintenance costs due to parts and labor. In homes and businesses, hard water has higher

rates of scale formation in water heaters, boilers and hot water lines which increases the water heating costs.

Hardness in water is typically determined by buffering a sample to pH 10.3 followed by addition of calmagite indicator and titration with ethylene diamine tetraacetic acid (EDTA)⁵⁷. The endpoint is signaled by the calmagite indicator when it's color changes from a reddish-pink to a bluish-violet color. At the beginning of the titration and prior to addition of EDTA, the calcium and magnesium ions in the sample bind to the calmagite indicator producing reddish-pink as shown in equation (8). EDTA is a stronger complexing agent than indicator and as titration proceeds, EDTA displaces the metal ions from the indicator as shown in equation (2) allowing indicator to turn bluish-violet at the endpoint. The color transition from reddish pink to bluish-violet of calmagite seen in an EDTA titration makes it difficult to reproducibly determine the endpoint, unlike the transition of colorless to faint pink as seen in an acid-base titration with phenolphthalein.



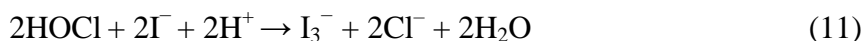
FAC Concentrations in Sodium Hypochlorite Solutions

Disinfection of drinking water by chlorine is the most widely used approach in the United States and is a cost-effective method. Generally, chlorine is added to water either as gaseous chlorine, aqueous sodium hypochlorite, or as solid calcium hypochlorite⁶⁴. The aqueous solution of sodium hypochlorite is commonly called bleach. Regardless of the chemical species used to dose chlorine, equilibrium exists between hypochlorous acid and hypochlorite ion at the pH range used in drinking water (Equation (10)). The pK_a of this

equilibrium is 7.5 and thus the equilibrium concentrations in drinking water of hypochlorous acid and hypochlorite ion are nearly equal.



The sum concentration of molecular chlorine, hypochlorous acid and hypochlorite ion in any solution is commonly referred as Free Available Chlorine (FAC). The Powell process is the most common method for bleach production and is done by bubbling chlorine gas through a solution of sodium hydroxide⁷⁵. This produces a sodium hypochlorite solution with pH values that are high (greater than 11) and thus the chlorine species in bleach is nearly all in the form of hypochlorite ion. Typically, bleach solutions produced with the Powell process contain 5-15 % of hypochlorite ion by weight. The concentration of FAC in bleach is usually determined with an iodometric titration. The iodometric titration is accomplished by adding excess sodium iodide to an acidified sample of bleach and titrating with standardized sodium thiosulfate. The excess iodide (I^-) ion is oxidized to triiodide (I_3^-) ion as shown in Equation (11) producing reddish-yellow color. As the titration proceeds, sodium thiosulfate is added to the solution as the titrant and the triiodide ion oxidizes thiosulfate ($\text{S}_2\text{O}_3^{2-}$) ion to the tetrathionate ($\text{S}_4\text{O}_6^{2-}$) ion⁷⁶ (Equation (12)).



The endpoint can be detected in multiple ways either direct visual detection (straw color to clear as the triiodide ion is consumed), a starch indicator that turns dark blue in the presence of triiodide ion, or by using potentiometry indicating the conversion of triiodide ion to iodide ion. In this work, the endpoint of the triiodide ion will be detected spectrochemically without the presence of a starch indicator.

Experimental

Development of EZ-AutoTitrator

The essential components of the developed EZ-AutoTitrator are: (1) a titrant dosing system, (2) a potentiometric detector, (3) a spectrochemical detector, (4) control, communication, and signal processing, and (5) output of end results.

Titrant Dosing System

The titrant dosing system was based on a stepper motor syringe pump as in EZ-AutoPipet work which accurately delivers the titrant. A 5 mL syringe is used in the syringe pump and is capable of delivering 100 μ L of titrant with 2% precision. The construction, development and operation of the developed syringe pump are described in detail in chapter 2.

Potentiometric Detector

The potentiometric detector was developed using an Atlas scientific EZO pH board (Atlas scientific LLC, Long Island City, NY, USA) and a combination pH probe. The EZO pH board was used to calibrate and read the signal of the pH probe. The EZO board was equipped with a PIC 18 microcontroller which converts the analog signal (mV) of the pH probe to pH and communicates with the Raspberry Pi through Inter-Integrated communication (I²C) protocol. The pH board has a precision of ± 0.002 pH units and a minimum response time of 1 sec.

Spectrochemical Detector

The spectrochemical detector is constructed from a white LED and a diode array sensor. The white LED is a Luxeon 3014 white 5700K LED (L130-5780HE1400001, LUMILEDS, San Jose, CA USA) which was equipped on the board to illuminate the sample for increasing the sensitivity of color discrimination. The spectral sensor was an AMS AS7262 (AMS AG, Austria) with six optical channels for color detection. Each channel has an interference filter deposited on the complementary metal-oxide semiconductor (CMOS) silicon and the spectral response of the sensor is shown in Figure 11. The analytical signal is a photocurrent produced from the individual channels which is digitized using an integrated 16-bit analog to digital converter. The analytical signal is recorded for processing by a Raspberry Pi.

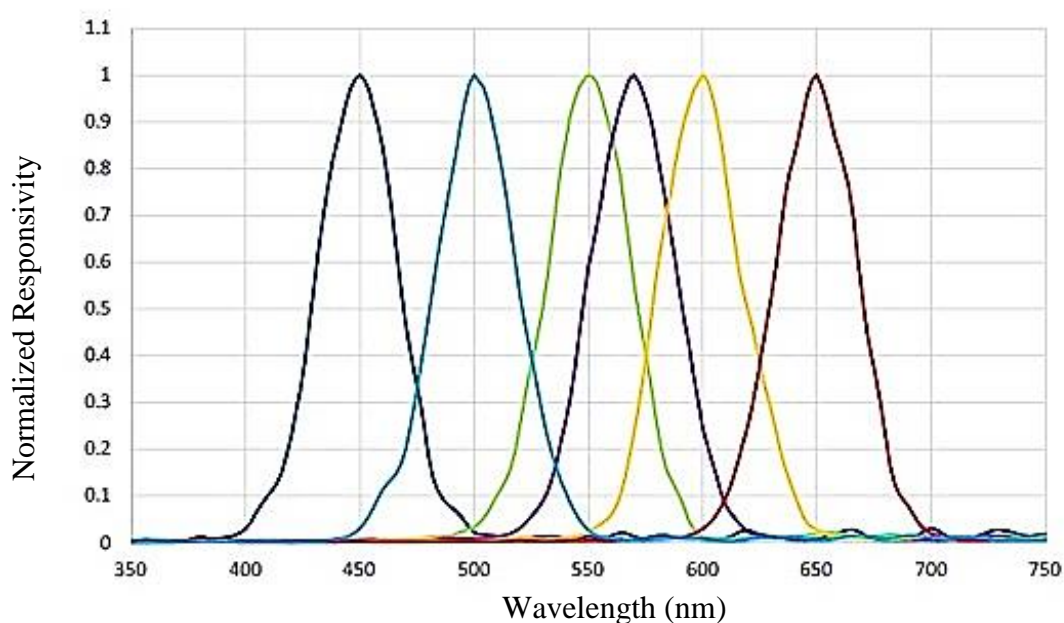


Figure 11. Plot of normalized response versus wavelength for an AS7262 spectral sensor that detects visible wavelengths with peak sensitivities at 450 nm, 500 nm, 550 nm, 570 nm, 600 nm and 650 nm. Each channel has a bandwidth of 40 nm full width at half maxima (FWHM).

Fabrication of Spectrochemical Detector

A cell holder that accommodates a 30 mL glass beaker, the white LED and the spectral sensor was 3D printed using a Form 2 printer (Formlabs, Somerville, MA, USA) (Figure 12). The hollow cylindrical part (B) as shown in Figure 12 holds the 30 mL beaker and AS7262 spectral sensor was screwed to the square wall (A) behind the hollow cylinder. AS7262 was enclosed in a 3D printed cover to shield it from water spills as well as minimize the interference from external light. Two apertures were included: one for allowing the light from LED to illuminate the sample and one to allow the reflected light from the sample to be

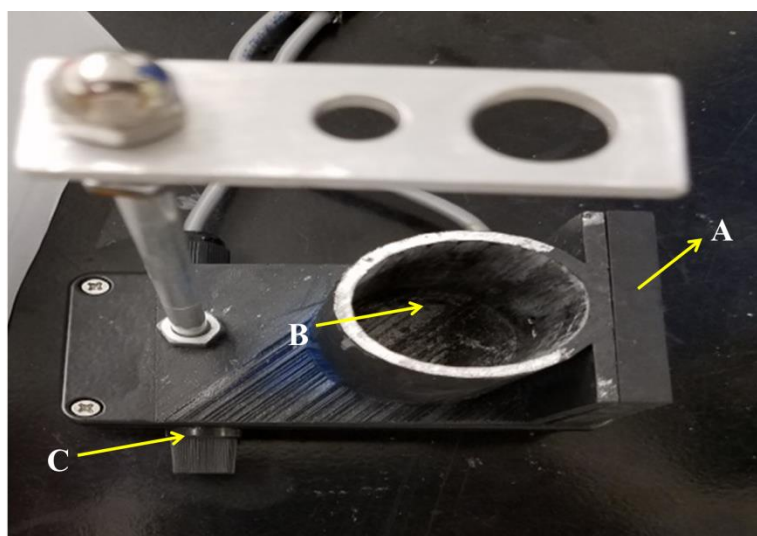


Figure 12. Top down view of the 3D-printed spectrochemical cell holder with a magnetic stirrer underneath.

detected by the spectral sensor. The whole detector assembly was attached to the top plate of a metal rectangular box. A 3D-printed vane holds two small neodymium magnets at each edge was attached to a 12V DC motor shaft. The DC-motor setup was positioned in the metal box exactly under the hollow cylinder (B). The stirring speed was controlled using a pulse width modulation (PWM) controller board (C).

Control, Signal Processing, Communication, and Output

A Raspberry Pi Model 3 B+ (Raspberry Pi Foundation, UK), an inexpensive credit-card sized, single-board computer, was used for control, signal processing, communication with the external hardware such as stepper drivers and detectors in conjunction with the python programming language. A Graphical User Interface (GUI) for the EZ-AutoTitrator was developed using Tkinter, a standard GUI package. The developed GUI has two pages as shown in Figure 13.

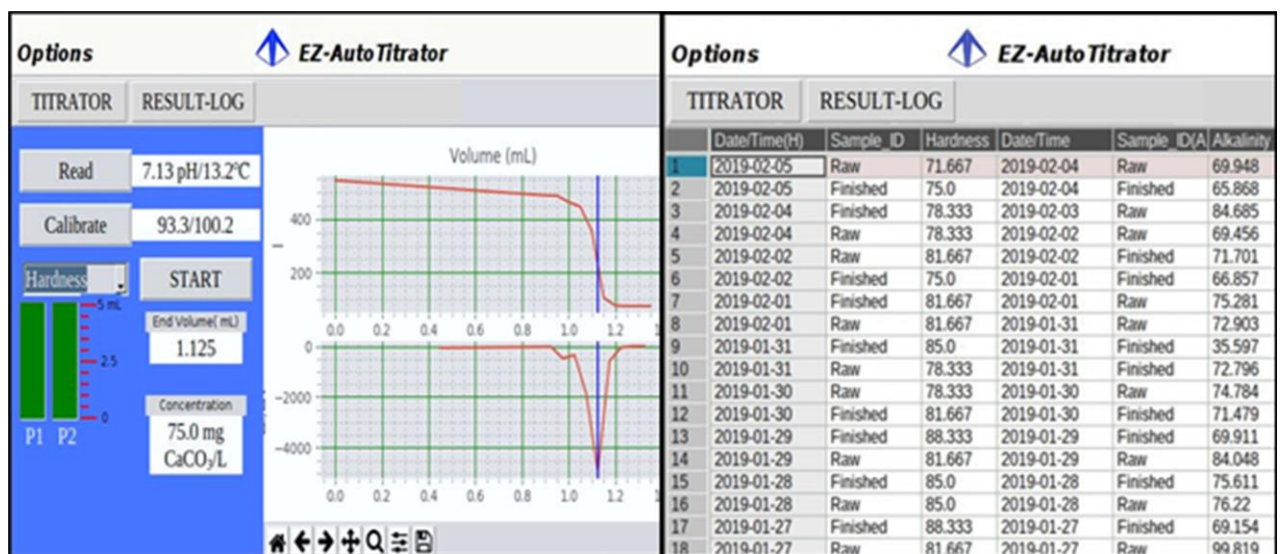


Figure 13. Graphical user interface (GUI) for the titrator. Left side of the image shows the titrator page and right side of the image shows the result log page.

The Titrator page has options to read pH, temperature and select the type of titration to perform. It also displays the Real-time pH or Intensity vs. Volume and corresponding first derivative plot and results of the titration. The Titrator page allows the user to change titration parameters such as the titrant concentration, sample volume, end-pH and predose volume, etc. The results log page saves the alkalinity and hardness results with a timestamp. A 7-inch capacitive touch display (Raspberry Pi Foundation, UK) was used to provide user interaction with the GUI and display the results.

The EZ-AutoTitrator is capable of performing potentiometric and spectrochemical titrations. Based on how the equivalence point is determined, potentiometric titrations are categorized into two classes: (1) titration to a pre-determined equivalence point and (2) full scale pH titrations. The total alkalinity titration is done to a pre-determined equivalence point where sample is titrated to a pH of 4.3. Full scale pH titrations are typically done when determining the pK_a of an unknown acid (or base) compound or if there are multiple endpoints suspected based on the chemical species present.

Operation of the EZ-AutoTitrator

pH based Titrations by AutoTitrator

A schematic of the decision tree for a potentiometric pH titration is presented in Figure 14. To begin a potentiometric titration, the analyst selects a pH based titration method in the drop-down menu shown in Figure 13. The EZ-AutoTitrator reads the initial pH of the sample to a variable in the software. If the titration is to a fixed equivalence-point then the end-pH (pH where titration will be stopped) is set to the user input value. For instance, end-pH in alkalinity titrations is 4.3. Whereas in the full-scale titration, end-pH is set to either 2 or 12 depending on analyte. The titrator then compares the initial pH of the sample to end-pH. If the initial pH is equal to end-pH, the titration will be stopped without adding any titrant and be ready for the next titration. Otherwise, the titrator adds a relatively large amount of titrant called a predose to speed up the titration. The pH stabilization factor is calculated as the rate of change in pH and the titrator will wait until the stabilization factor is less than or equal to 0.0025 which was determined experimentally and can be modified if necessary.

When the pH stabilizes, if the current pH is not equal to end-pH, the titrator adds relatively smaller quantities of titrant until the sample pH reaches to the end-pH. The smallest titrant delivery possible is set to 0.0500 mL. Finally, the EZ-AutoTitrator calculates the endpoint volume either by determining the highest or lowest point in the first derivative curve

in case of a full scale titration or using linear interpolation for titrations that end at predetermined pH values.

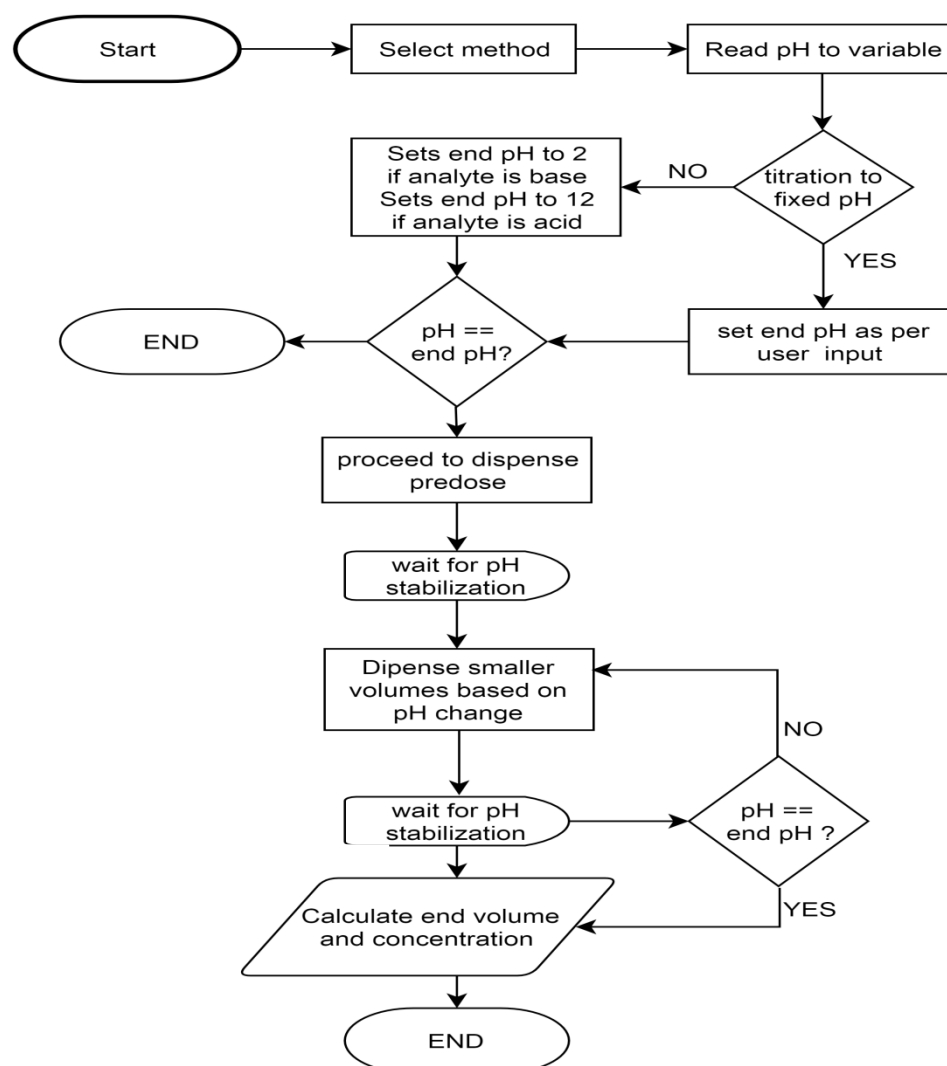


Figure 14. A decision tree that outlines the functioning of EZ-AutoTitrator for performing potentiometric pH titrations.

Spectrochemical Titrations by EZ-AutoTitrator

When spectrochemical methods such as hardness or FAC have been selected from the drop-down in Figure 13, this begins the decision tree shown in Figure 15. First, the appropriate optical channel in AS7262 is selected to read data continuously based on the selected titration. In the case of hardness, the 650 nm channel is used as it best overlaps with the calmagite indicator and the intensity of reflected light from the sample is measured. In the FAC iodometric titration, the 450 nm channel is used and intensity of absorbed light at that wavelength is measured. The titrator predicts the color of the sample using a machine

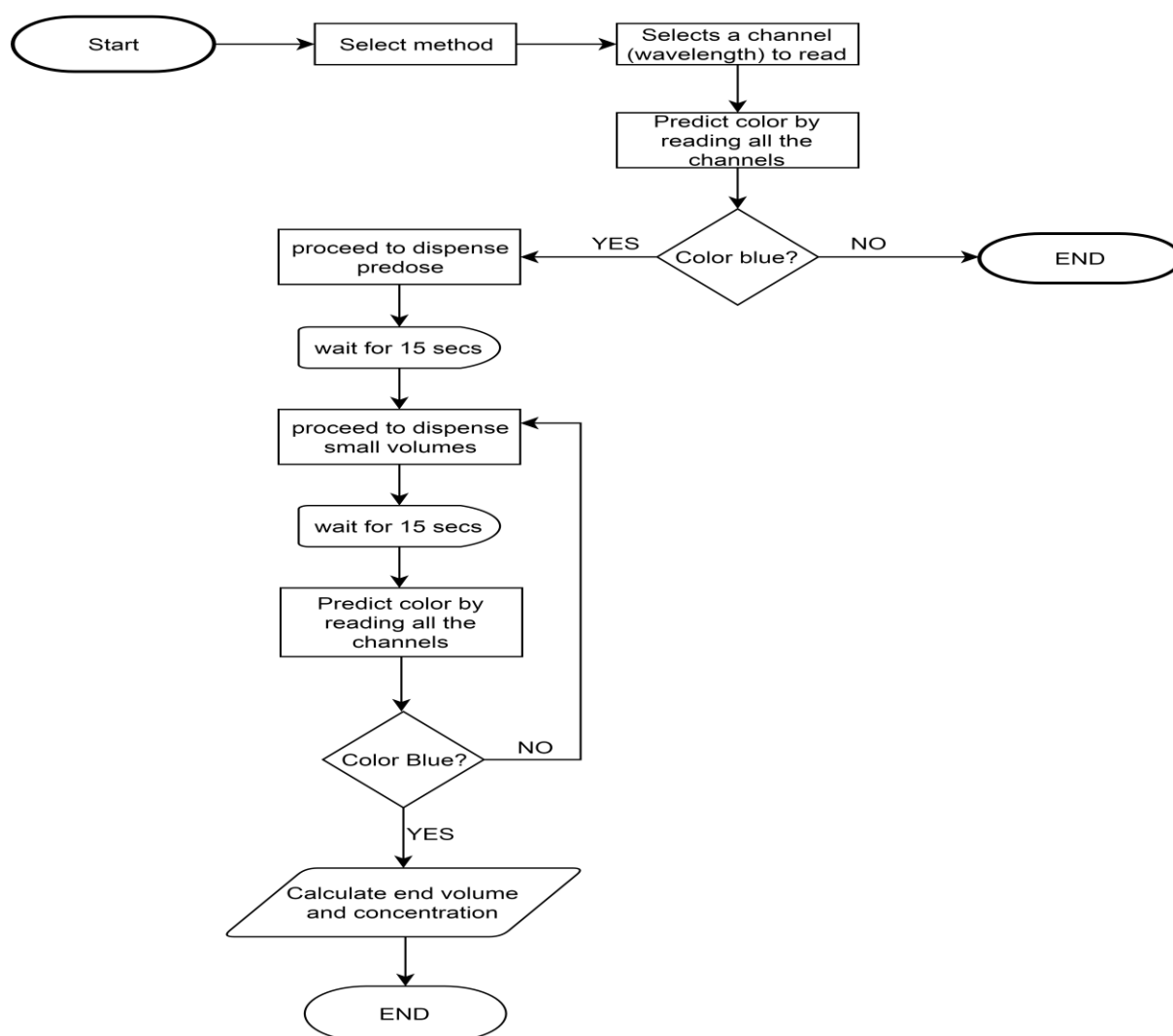


Figure 15. Flow chart outlines the detection of color change by EZ-AutoTitrator at the end-point. For hardness, color changes from reddish pink to pinkish violet whereas in FAC titrations, color changes from dark yellow to clear.

learning model discussed in the next section. If the color of the sample is not the endpoint color then the titrator adds a set predose similar to that discussed in pH titration and waits for 15 secs to allow titrant to mix with the sample as shown in Figure 14. The EZ-AutoTitrator then measures the light intensity from selected channel and predicts the color of the sample again. If the color is not the endpoint color, the EZ-AutoTitrator adds smaller doses of titrant and this process will be repeated until there is a color change as determined by the machine learning model. At the end of the titration, the endpoint volume is calculated based on first derivative plot generated from volume vs intensity of light from selected optical channel.

Development of the Color Prediction Model

Unlike most pH titrations, spectrochemical titrations do not have a specific “color” value where a titration can be stopped unless titrator can perceive the color of the sample and end the titration after desired color change has been achieved. The primary goal of this aspect of the research was to develop a color prediction model that can distinguish the starting and end-point color by using a simple machine learning algorithm. Scikit-Learn is a powerful yet simple to use open source machine learning python library that incorporates classification, regression and clustering algorithms which have been used for machine learning and modeling. Here, the classification aspects were used to develop the model for endpoint determination using color determination via the AS7262 spectral sensor.

Generally, the greater the variability in the training data to build a model results in better performance of the model during analysis⁷⁷. Several analyte samples were prepared by combining different amounts of analyte and reagents to generate the initial color. Subsequently, all samples were analyzed individually to obtain analytical signal data from the six optical channels of the spectral sensor (AS7262). The samples were then titrated until the desired color change was achieved and the analytical signal was recorded from the spectral sensor.

The data from these initial experiments was entered into a spreadsheet, Microsoft Excel in this case. The data was entered such that the analytical signal from the six channels were put into the first six columns and the corresponding color was entered into the seventh (last) column and saved as comma separated values (.CSV) format. The numerical values in the first six columns are called features (Predictor variables) and used to predict the target variable. The information in the last column contains labels (Target variables) that need to be predicted using features. Four different classification models were tested for the color prediction model and were Linear Discriminant Analysis (LDA), Logistic Regression (LR), K-Nearest Neighbors (KNN) and Decision Tree Classifier (DT). The collected data was imported to the python machine learning program and randomly divided the data set into training data and test data in the ratio of 80/20, a standard approach in machine learning. Each binary classification model was then trained on the training data set and the test data set was used to evaluate and select the best performing model out of four tested models. The model was selected based on metrics such as accuracy, precision, recall, and F1-score which were calculated from a confusion matrix as shown in Table 12.

Table 12. Confusion matrix showing actual vs predicted values.

	Predicted Negative	Predicted Positive
Actual Negative	No.of True Negative	No. of False Positive
Actual Positive	No. of False Negative	No.of True Positive

Accuracy is defined as a ratio of the sum of true positives and true negatives divided by total number of samples^{78,79}. Accuracy is good metric when cost associated with false negatives and false positives are equal and have symmetric data set (equal number of negative and positive outcomes).

$$\text{Accuracy} = \frac{\text{True Positives} + \text{True Negatives}}{\text{Total number of samples}} \quad (13)$$

Precision is the fraction of true positives compared to the total predicted positives^{78,79} (true and false) and calculated using Equation (14). If the occurrence of false positives is too high, and thus not acceptable, then the model must be optimized to have higher precision.

$$\text{Precision} = \frac{\text{True Positive}}{\text{True Positives} + \text{False Positives}} \quad (14)$$

The recall parameter is the fraction of true positives identified correctly compared to the total number of true positives and false negatives^{78,79} and calculated using Equation (15). If the cost of false negatives is high, then the model should be optimized for higher recall.

$$\text{Recall} = \frac{\text{True Positive}}{\text{True Positives} + \text{False Negatives}} \quad (15)$$

F1-score is the harmonic mean of precision and recall^{78,79} and calculated as in Equation (16). A good F1-score means predicted outcomes have low frequency of both false positives and false negatives.

$$\text{F1 - score} = \frac{2 \times \text{Precision} \times \text{Recall}}{\text{Precision} + \text{Recall}} \quad (16)$$

As there are two target variables (red and blue), each target variable has its own set of metrics. The weighted average for each metric was calculated as shown in Equation (17). Where n1 and n2 are the number of red and blue samples tested respectively. m1 and m2 represent the metric (accuracy, precision, recall, and F1) for red and blue samples.

$$\text{Weighted Average} = \frac{n1 \times m1 + n2 \times m2}{2} \quad (17)$$

The weighted averages of accuracy, precision, recall, and F1-score for four models tested were shown in Table 13. In each case, the values can range between 0 to 1, with a value of 1 as a good result. Based on these evaluation parameters, the KNN model performed the best with accuracy, precision, recall, and F1 score all equal to 1 and outperformed the

Table 13. Summary of various metrics for four different models tested for predicting red and blue color in hardness titrations.

Metric				
Model	Accuracy	Precision	Recall	F1-score
KNN	1.0	1.0	1.0	1.0
LR	0.94	0.94	0.94	0.94
LDA	0.96	0.97	0.97	0.97
DT	0.94	0.94	0.94	0.94

other three models. For hardness, the KNN classification model was selected to predict the initial (reddish pink) and end-point color (bluish violet).

The same procedure described above was followed to develop and test the models for FAC color change detection (straw color to clear). The summary of the results for FAC color

Table 14. Summary of various metrics for four different models tested for predicting straw color and clear solution in FAC titrations.

Metric				
Model	Accuracy	Precision	Recall	F1-score
KNN	0.95	1.0	1.0	1.0
LR	1.0	1.0	1.0	1.0
LDA	0.95	1.0	1.0	1.0
DT	0.95	1.0	1.0	1.0

prediction modeling was shown in Table 14. All the models had precision, recall and F1-score values of 1.0 but the logistic regression model had the highest accuracy of all (1.0) which makes it the choice for FAC titrations. In this case, the models have perfect scores for most of the metrics. This is likely due to the smaller sample size used to test the models and that a strong distinction exists between the spectral sensor channel readings for straw color and clear solution.

Chemicals, Reagents and Standards

All the reagents and standards were prepared using reagent grade water with a resistivity of at least 18.2 M Ω -cm and total organic carbon (TOC) of 10 μ g/L or less produced by a Barnstead E-Pure water purification system (ThermoFischer Scientific, Waltham, MA, USA). The calmagite indicator was indicator grade. All other chemicals used were reagent grade or ACS certified grade. All chemicals were purchased from Fischer scientific, USA unless mentioned specifically. Calmagite and sodium carbonate were purchased from Acros Organics. Tartaric acid was procured from Mallinckrodt, Italy and phosphoric acid was procured from EM chemicals, USA.

The hardness stock standard at 1000 mg/L as CaCO₃ was prepared by adding an appropriate amount of calcium carbonate (dried at 120 °C for 2 hrs) into a 500 mL beaker containing 250 mL reagent water. A 50% dilution by volume of concentrated hydrochloric acid (HCl) solution was added slowly until all the calcium carbonate is dissolved. The resulting solution was heated to expel all the CO₂ and pH was adjusted to approximately 5 with a 50% dilution by volume of concentrated ammonia solution (NH₃)⁵⁷. The solution was diluted to 500 mL using reagent water in a volumetric flask. The alkalinity stock standard at 1000 mg/L as CaCO₃ was prepared separately by diluting appropriate an amount of sodium carbonate (dried at 120°C for 2hrs) to 500 mL reagent water in a volumetric flask. The

working standards for alkalinity and hardness were prepared by diluting the stock solutions appropriately. A 0.02 N HCl solution was prepared by volumetrically diluting concentrated acid with reagent water and standardized with a sodium carbonate solution. 0.01 M ethylenediamine tetraacetic acid (EDTA) solution was prepared by dissolving an appropriate amount of EDTA disodium salt dihydrate into reagent water and standardized with a standard calcium ion solution. Calmagite indicator solution (0.1% W/V) was prepared by diluting 0.1 g of solid calmagite to 100.0 mL with reagent water in a volumetric flask. An ammonia buffer (pH 10.3) for the EDTA titration was prepared by dissolving 1.179 g EDTA disodium salt dihydrate and 0.780 g magnesium sulfate heptahydrate in 100 mL reagent water. Then 16.9 g ammonium chloride (NH_4Cl) and 143 mL of concentrated ammonium hydroxide (NH_4OH) was added to the solution above and diluted to 250 mL in a volumetric flask⁸⁰.

A 0.1 M potassium hydroxide (KOH) was prepared by diluting appropriate amounts of solid KOH pellets with the mass used corrected for purity (purity 85.5%) in reagent water to 1000 mL in a volumetric flask. The KOH solution was standardized with a 0.1 M potassium hydrogen phthalate (KHP) solution. A 0.1 M HCl solution was prepared by diluting concentrated acid volumetrically to 1000 mL and standardized with 0.1 M sodium carbonate solution. Solutions of 0.1 M tartaric acid, 0.1 M maleic acid, 0.1 phosphoric acid, 0.1 M phthalic acid, and 0.1 M oxalic acid dihydrate were prepared separately by diluting appropriate amounts each of the solid acids into 100.0 mL of reagent water.

Procedure for Total Alkalinity Using the EZ-AutoTitrator

For the automated alkalinity titration of drinking water, a 15 mL of water sample was transferred to a 30 mL beaker using a volumetric pipet. The sample was titrated to a pH value of 4.3 using standardized 0.02 N Hydrochloric acid (HCl) and measured potentiometrically. The endpoint volume was determined by linear interpolation. The linear interpolation approach is a simple method of estimating a value between given set of two data points. An

example of linear interpolation is shown in Figure 16 , where the volume of acid required to titrate water sample to pH 4.3 (V_x) was calculated using Equation (18). In this equation, pH1 and pH2 are pH values that bracket pH 4.3 and V1 and V2 are the added acid volumes at pH1 and pH2 respectively. V_x is the volume at pH 4.3 estimated by linear Interpolation.

$$V_x = V_1 + (pH_1 - 4.3) \times \frac{V_2 - V_1}{pH_1 - pH_2} \quad (18)$$

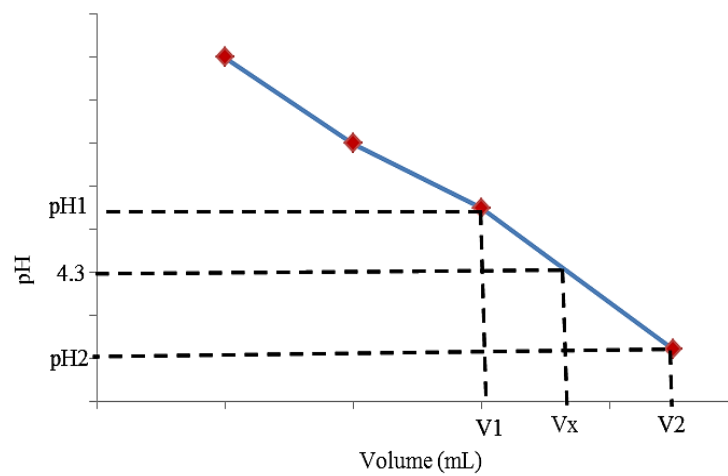


Figure 16. An example titration curve showing fast few points and linear interpolation to calculate the exact acid volume. pH1 and pH2 are pH values that bracket pH 4.3 and V1 and V2 are added acid volumes at pH1 and pH2 respectively. V_x is the volume at pH 4.3 estimated by linear Interpolation.

The alkalinity of the sample is calculated⁵⁶ as shown in Equation (19), where V_x is the volume of standardized acid used in mL to titrate the sample calculated using Equation (18) and N is the normality of the standardized acid. 50,000 is a conversion factor with units of mg/mol to convert equivalents per liter of carbonate ion to mg/L CaCO_3 .

$$\text{Alkalinity, } \frac{\text{mg}}{\text{L}} \text{CaCO}_3 = \frac{V_x \times N \times 50,000}{\text{sample volume}} \quad (19)$$

Procedure for Total Hardness Using the EZ-AutoTitrator

For the automated titration of total hardness, a 15 mL of water sample was transferred with a volumetric pipet into a 30 mL beaker. Once in the beaker, three drops of calmagite indicator and three drops of ammonia buffer (pH 10.3) were added. The sample was then titrated with standardized EDTA solution until sample color changed to bluish-violet as determined by the KNN color prediction model. The volume of the EDTA solution corresponding to the minimum in the first derivative curve was the endpoint volume of the titration. The Hardness of the sample is calculated⁵⁷ as shown in Equation (20)

$$\text{Hardness, } \frac{\text{mg}}{\text{L}} \text{ CaCO}_3 = \frac{V_y \times M \times 100,000}{\text{sample volume}} \quad (20)$$

Where V_y is the volume of standardized EDTA used to titrate the sample in mL calculated from first derivative curve and M is the molarity of the standardized acid. A conversion factor of 100,000 with units of mg/mol converts the sum of moles per liter of calcium and magnesium to mg/L CaCO_3 .

Procedure for FAC Using the EZ-AutoTitrator

The automated procedure for FAC analysis with the EZ-AutoTitrator starts with transfer of a 3 mL aliquot of the NaOCl solution by volumetric pipet into the 30 mL beaker and addition of ~15 mL of reagent water. Then, 1 g of excess potassium iodide (KI) and 5 mL of 0.2 M sulfuric acid was added to the diluted sample. The prepared sample was titrated with standardized sodium thiosulfate ($\text{Na}_2\text{S}_2\text{O}_3$) solution. The volume of $\text{Na}_2\text{S}_2\text{O}_3$ solution corresponding to the maximum in the first derivative curve was the endpoint volume of the titration. The FAC in the sample is calculated⁷⁶ as shown in Equation (21)

$$\text{FAC, } \frac{\text{mg}}{\text{L}} \text{Cl}_2 = \frac{V_y \times M \times 70900}{2 \times \text{sample volume}} \quad (21)$$

Where V_y is the volume of standardized $\text{Na}_2\text{S}_2\text{O}_3$ used to titrate the sample in mL calculated from first derivate curve and M is the molarity of the standardized $\text{Na}_2\text{S}_2\text{O}_3$. The conversion factor of 70900 mg/mol converts moles per liter of Cl_2 to mg/L Cl_2 .

Validation of EZ-AutoTitrator Analyses

Validation of the EZ-AutoTitrator titrimetric analysis was conducted with inter-day, intra-day, intra-instrumental, and inter-instrumental accuracy and precision. The accuracy and precision of each set of titrations were estimated by titrating standard alkalinity (50.8 mg/L of CaCO_3) and hardness (50.1 mg/L of CaCO_3) solutions seven times for each study to evaluate the performance of the EZ-AutoTitrator. Moreover, accuracy and precision of the autotitrator was calculated across a range of concentrations of hardness and alkalinity to evaluate the effect of sample concentration on the titration results.

The accuracy is calculated as mean percent recovery as shown in Equation (22). The precision is calculated as percent relative standard deviation of seven replicates using Equation (23).

$$\text{Accuracy} = \frac{\text{Mean Calculated Concentration}}{\text{Actual Concentration}} \times 100 \% \quad (22)$$

$$\text{Precision} = \frac{\text{Standard deviation}}{\text{Mean Calculated Concentration}} \times 100 \% \quad (23)$$

Real World testing of EZ-AutoTitrator

The EZ-AutoTitrator was tested at Lebanon TN, water treatment plant (WTP) and Woodruff-Roebuck, SC WTP. The alkalinity and hardness in finished and raw water were

measured by the EZ-AutoTitrator and compared with the manual titrations for over 4 months at Lebanon water treatment plant. At the Woodruff-Roebeck WTP, The EZ-AutoTitrator was compared with manual titrations for two days in finished, Floc-3 (water after flocculation) and raw water (the source water). A 100 mL and 50 mL sample volume were used for manual alkalinity and hardness titrations, respectively. For the EZ-AutoTitrator, a 15 mL of sample for both alkalinity and hardness titrations were analyzed. The manual alkalinity titration was based on bromocresol green indicator to detect the equivalence point in contrast to potentiometric detection in EZ-AutoTitrator. Bland-Altman Analysis^{81,82} and analytical bias^{83,84} was used to quantitatively compare the results from two methods.

Results and Discussion

Validation Results for the Automated Alkalinity Titrations

The laboratory prepared standard alkalinity solution was tested to evaluate inter-instrumental, intra-instrumental, intra-day and inter-day accuracy and precision of the EZ-AutoTitrator. A one-way ANOVA test was performed to compare the means within a test group. If the p-value is greater than significance level (0.05) then null hypothesis cannot be rejected⁶⁰. In other words, the group means are not statistically different and indicated as “NO” in Table 15. The EZ-AutoTitrator was compared to a Radiometer VIT 90 (Radiometer, Copenhagen, Denmark), a commercially available automated titrator for the inter-instrumental test (Table 5). The recoveries from both the instruments were lower than 100% but within a percentage of each other and the means agreed statistically. The low mean % recovery with both instruments indicates there might have been an error in preparation of the test solution as the remaining analyses with the EZ-AutoTitrator did not exhibit the low recovery. An alkalinity analysis with two EZ-AutoTitrators was compared for the intra-instrumental study. The means are found to be statistically similar indicating a good precision for the electronics and assembly of autotitrator. An inter-day comparison study was done by

conducting an analysis over three consecutive days using a single EZ-AutoTitrator. The accuracy ranged from 99.9 to 102.7% with maximum percent relative standard deviation of 3.3% with the means of the analysis statistically similar (agreed). Over the course the multiple day analysis, the EZ-Titrator performed consistently. Finally, alkalinity was measured three different times in a day for intra-day study and accuracy ranges from 99.9 to 100.6% with maximum relative standard deviation of 2.6%. Interestingly, the p-value is slightly less than 0.05 indicating statistical difference in means. On visual observation,

Table 15. Validation results of EZ-AutoTitrator method for Alkalinity.

Test(n=7)		True value (mg/L)	Calculated value (mg/L)	Accuracy	Precision	Means Statistically Different? (P < 0.05)
Inter-instrumental	EZ-Auto Titrator	50.8	46.9	92.3%	2.7%	NO
	VIT-90	50.8	47.4	93.3%	1.9%	
Intra-instrumental	EZ-Auto Titrator-1	50.8	52.5	103.3%	2.0%	NO
	EZ-Auto Titrator-2	50.8	51.5	101.4%	2.5%	
Inter-day	Day-1	50.8	50.8	99.9%	2.6%	NO
	Day-2	50.8	51.1	100.6%	2.4%	
	Day-3	50.8	52.2	102.7%	3.3%	
Intra-day	Iteration-1	50.8	51.1	100.6%	2.4%	YES
	Iteration-2	50.8	52.5	103.4%	2.3%	
	Iteration-3	50.8	50.8	99.9%	2.6%	

iteration-2 has slightly higher mean (52.5 ± 1.2 mg/L) than the other two iterations. Though the means are statistically different, difference between the lowest (50.8 mg/L) and highest (52.5 mg/L) mean is 1.7 mg/L which may not have significant effect on treatment dosing. Overall, excluding mean calculated alkalinity from the inter-instrumental analysis, the EZ-AutoTitrator has average recovery of $101.6 \pm 2.5\%$ (51.6 ± 1.3 mg/L CaCO_3).

A range of alkalinity concentrations starting from 10 mg/L to 300 mg/L were tested and each concentration was analyzed five times using an EZ-AutoTitrator. Except 10 mg/L, all other concentrations have accuracy close to 100% ranging from 98.7 to 102.4% with precision ranging from 0.5 to 5.3% as shown in Table 16. The 10 mg/L has a percent recovery of 147.6 and when 30 mL of sample was used instead of 15 mL the recovery was dropped to 125.4%. At lower concentrations (< 10 mg/L), an increase in sample volume or decrease in titrant concentration might be required to achieve better accuracy.

Table 16. Summary of results of Alkalinity from EZ-AutoTitrator at different concentrations.

Alkalinity Concentration (mg/L)							
True Alkalinity	10.0	50.1	100.3	150.4	200.5	250.6	300.8
Mean (n=5)	14.7	51.3	100.6	153.3	201.2	248.8	296.8
Accuracy	147.6%	102.4%	100.4%	101.9%	100.4%	99.3%	98.7%
Precision	1.6%	0.9%	5.3%	2.3%	0.5%	1.4%	1.0%

Table 17 presents the summary of results from the alkalinity comparison study between the manual and EZ-AutoTitrator. In this comparison, endpoint is determined potentiometrically for both the methods. The analyst for the manual titrations had coursework at the undergraduate level in chemistry, was familiar with potentiometric titrations, and the titration was the analyst's primary task. This comparison represents a better case scenario for

a comparison between manual titrations and the EZ-AutoTitrator. The EZ-AutoTitrator demonstrated better accuracy but slightly higher standard deviation than manual titrations. The t-test suggests that two means are statistically different which can be attributed to better dosing and endpoint detection by the autotitrator compared to the manual titrations. Ultimately, the EZ-AutoTitrator was a simpler approach from the perspective of the analyst while providing more accurate analyses with less labor required. At a WTP, the operators will

Table 17. Comparison of alkalinity results from EZ-AutoTitrator and manual titrations.

	Manual Titration	EZ-AutoTitrator
True concentration (mg/L)	50.6	50.6
Mean (n=20)	46.7	48.7
Accuracy	92.3%	96.4%
Precision	1.2%	1.9%
t-test	Failed: means are statistically different	

have less time for performing the manual titration with potentially less training. The EZ-AutoTitrator addresses these issues.

Comparison of the EZ-Autotitrator and Manual Titration Methods for Determination of Alkalinity at Lebanon TN, WTP

A series of alkalinity titration comparisons between the EZ-AutoTitrator and manual titration were conducted for a period of 4 months at the Lebanon, TN WTP. An operator at the plant performed finished and raw water titrimetric analysis for alkalinity on a daily basis at 7 am using both the EZ-AutoTitrator and manual titrations. A graduated cylinder was used to measure sample volume for both the manual titration and the EZ-AutoTitrator. Alkalinity comparisons at the Lebanon WTP from August 15, 2017 to January 11, 2018 are presented in Figure 18. The results of raw (Figure 18A) and finished water (Figure 18B) were not

continuous due to technical issues with the prototype of EZ-AutoTitrator. The Bland-Altman analysis is presented in Figure 17.

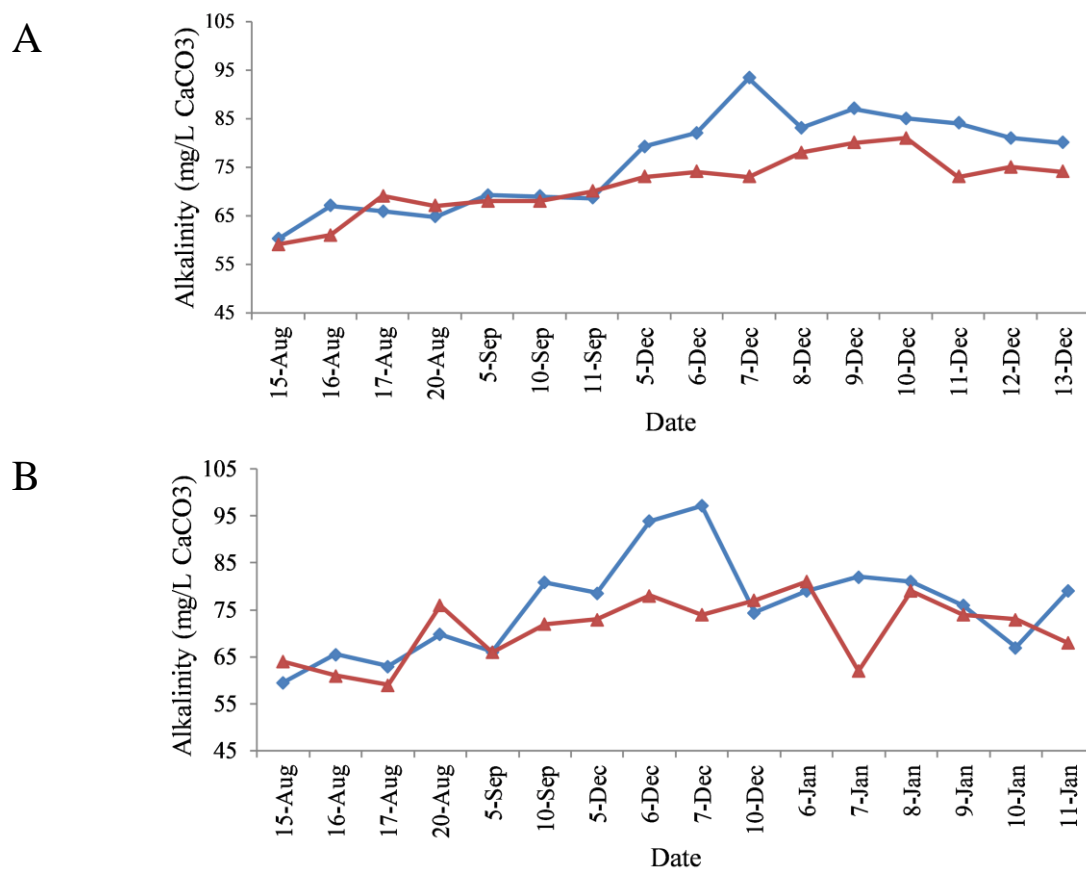


Figure 18. Alkalinity measured in (A) raw and (B) finished water by the EZ-AutoTitrator and manual titrations at Lebanon TN water treatment plant. In the red line with triangle markers is the alkalinity measured manually whereas the blue line with square markers shows the measurements from EZ-AutoTitrator.

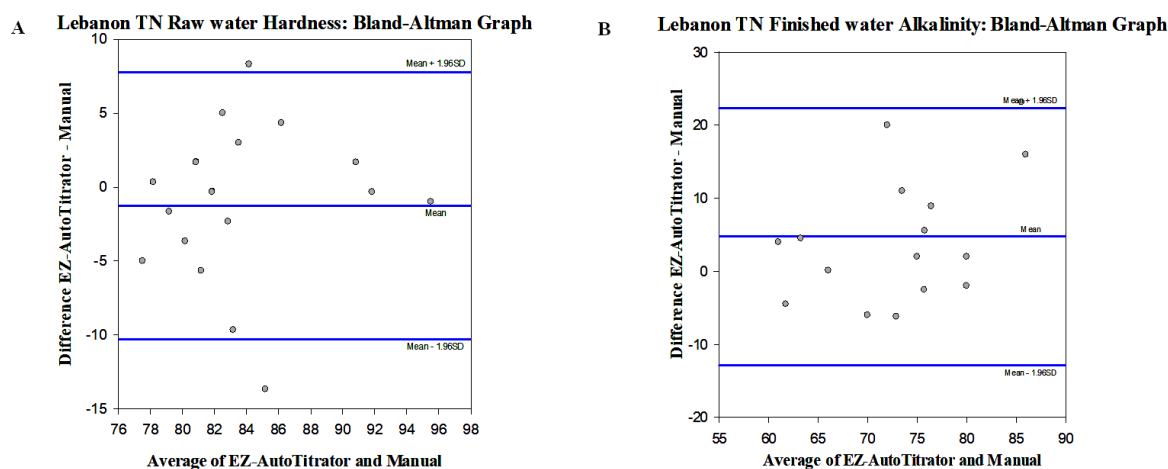


Figure 17. Bland-Altman plots for alkalinity comparisons in (A) raw and (B) finished water at Lebanon TN, WTP.

The average measured alkalinity ranges from 75 to 96 mg/L and 62 to 85 mg/L in raw and finished water, respectively. The average bias is calculated as the “experimental value – the true value.” Here the experimental value is the EZ-AutoTitrator and the “true” value is the manual titration. The analytical bias between two methods in raw water was found to be 4.7 ± 5.7 mg/L CaCO₃ whereas finished water has a bias of 4.7 ± 9.0 mg/L CaCO₃. The Bland-Altman plots for raw and finished water are shown in Figure 17A and B respectively. Neither the raw nor finished water show a proportional bias between two methods, *i.e.* there is no trend in bias as a function of average concentration. The raw water has narrow limits of agreement when compared to finished water as shown in Table 18. Overall, both samples had wider limits of agreement because the manual titrations were performed by a WTP operator and used color change to detect the endpoint.

Table 18. Summary of alkalinity testing in raw and finished water at Lebanon, TN WTP.

	Raw water	Finished water
n	16	16
Average Bias (mg/L)	4.7 ± 5.7	4.7 ± 9.0
Bias Range (mg/L)	-3.1 – 20.4	-6.2 – 23.1
Limits of Agreement (mg/L)	-6.5 – 16.0	-12.9 – 22.3

Comparison of the EZ-AutoTitrator and Manual titration Methods for Determination of Alkalinity at Woodruff-Roebuck SC, WTP

The alkalinity titration was compared again between the EZ-AutoTitrator and manual titration in raw (Figure 19A), floc-3 (water after flocculation) (Figure 19B), and finished water (Figure 19C) for two days. Measurements were performed every two to three hours between 8 am and 5 pm each day. The average measured alkalinity ranges from 15 to 21 mg/L for all the three samples. The average bias for three samples ranges from 2.2 to 4.8 mg/L CaCO_3 with highest bias being in raw water (4.8 ± 1.0 mg/L CaCO_3), followed by finished water (3.8 ± 1.9 mg/L CaCO_3), and lowest being in floc-3 water (2.2 ± 1.7 mg/L CaCO_3). All the three samples had smaller range of agreements (Table 19) when compared to Lebanon results. The reason for this is likely due to sample transfer was done using volumetric pipets rather than a graduated cylinder and the manual titrations were performed by the author (an experienced analyst). Additionally, sample size was smaller when compared to Lebanon testing. The bland-Altman plots for raw (Figure 20A), floc-3 (Figure 20B) and finished water (Figure 20C) had no proportional bias as well as bias evenly scattered around the mean bias. The Woodruff-Roebuck plant testing evaluates the performance of EZ-AutoTitrator at lower alkalinity range whereas testing at Lebanon plant evaluates the performance at mid to high range alkalinity.

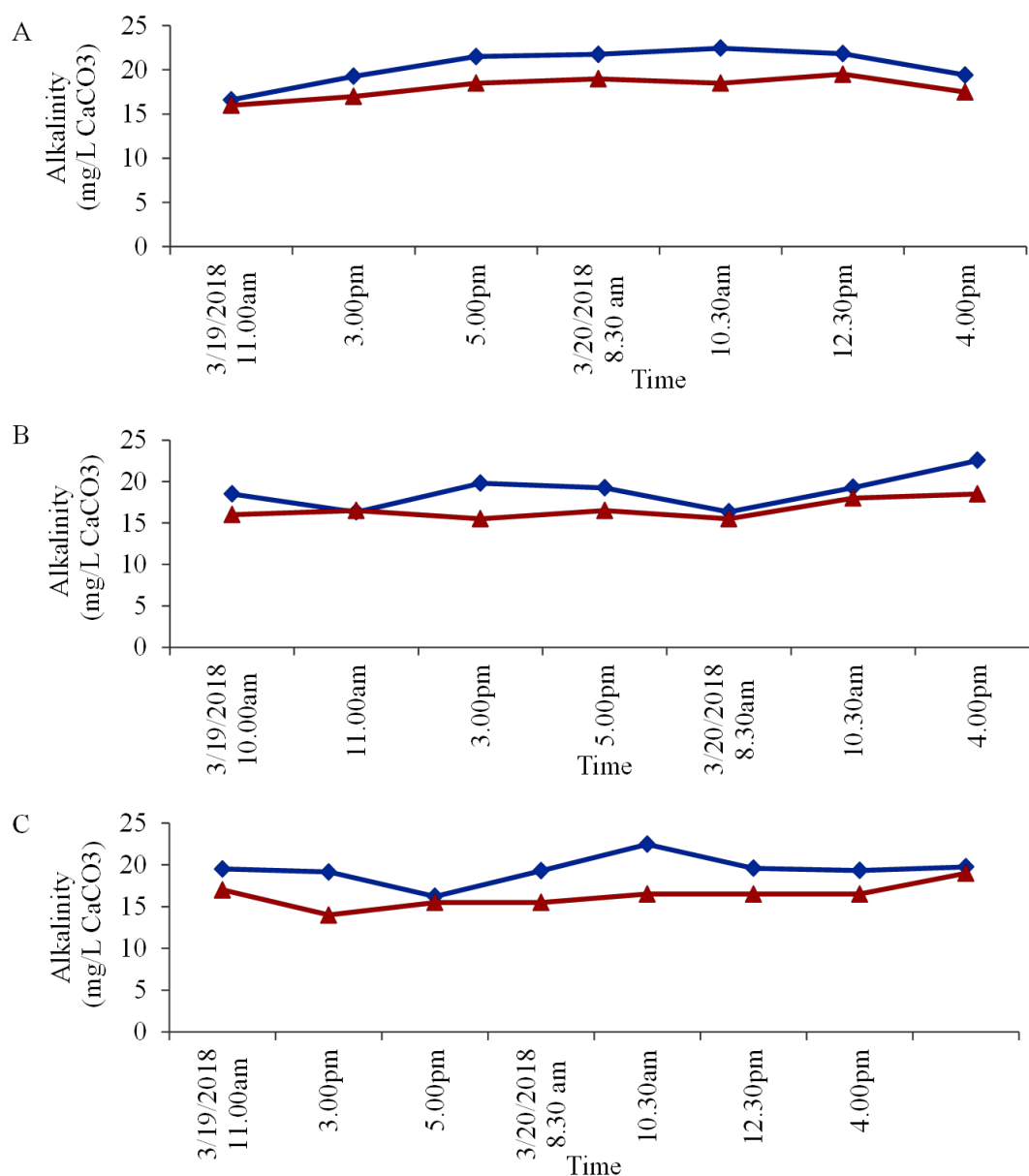


Figure 19. Alkalinity measured in raw (A), flocc-3 (B) and finished water (C) by EZ-AutoTitrator and manual titrations at woodruff SC, water treatment plant. In the red line with triangle markers is the alkalinity measured manually whereas the blue line with square markers shows the measurements from EZ-AutoTitrator.

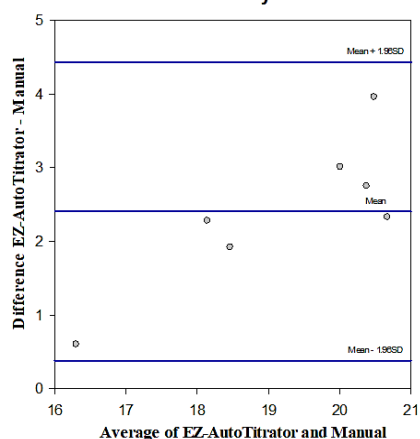
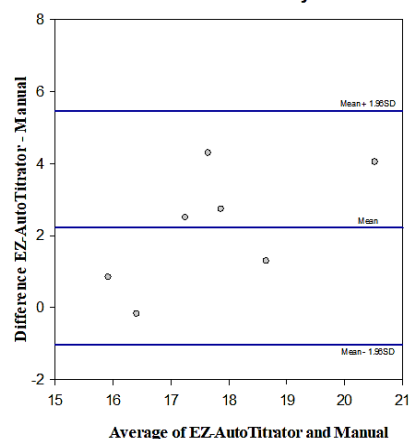
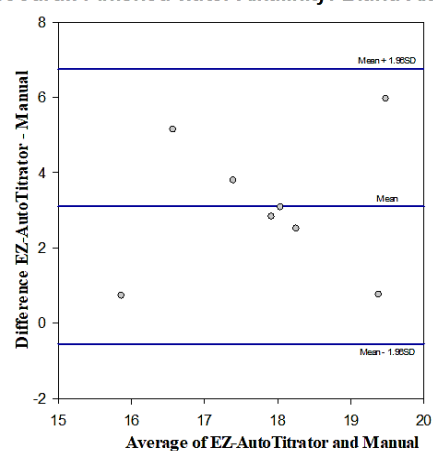
A Woodruff Raw water Alkalinity: Bland-Altman Graph**B Woodruff After Flocculation Alkalinity: Bland-Altman Graph****C Woodruff Finished water Alkalinity: Bland-Altman Graph**

Figure 20. Bland-Altman plots for comparison of alkalinity from EZ-AutoTitrator and manual titrations at Woodruff, SC water treatment plant in raw (A), floc-3 (B) and finished water (C).

Table 19. Summary of alkalinity testing in raw, floc-3 and finished water at woodruff, SC WTP.

	Raw water	Floc-3	Finished water
n	7	7	7
Average Bias (mg/L)	4.5 ± 1.0	2.2 ± 1.7	3.8 ± 1.9
Bias Range (mg/L)	0.6 – 4.0	-0.2 – 4.3	0.73 – 5.6
Limits of Agreement (mg/L)	0.3 – 4.4	-1.0 – 5.5	-0.5 – 6.7

Validation of the Hardness Titrimetric Analysis

The hardness titrimetric analysis was evaluated by comparing accuracy and precision in terms of intra-instrumental, inter-day, intra-day. The results of these validation studies are detailed in Table 20. For the intra-instrumental evaluation, a 50.1 mg/L hardness standard solution was compared using two different EZ-AutoTitrators. The mean hardness from the two titrators is exactly same (49.3 mg/L) indicating good precision of electronics particularly the AS7262 spectral sensor and the machine learning model used to detect the endpoint color.

Table 20. Validation results of EZ-AutoTitrator method for Hardness.

Test(n=7)		True value (mg/L)	Calculated value (mg/L)	Accuracy	Precision	Means Statistically Different? (P < 0.05)
Intra-instrumental	EZ-Auto Titrator-1	50.1	49.3	98.5%	0.0%	NO
	EZ-Auto Titrator-2	50.1	49.3	98.5%	0.0%	
Inter-day	Day-1	50.1	48.6	97.1%	3.1%	NO
	Day-2	50.1	49.3	98.5%	0.0%	
	Day-3	50.1	49.3	98.5%	0.0%	
Intra-day	Iteration-1	50.1	50.0	99.9%	3.0%	NO
	Iteration-2	50.1	49.3	98.5%	0.0%	
	Iteration-3	50.1	49.3	98.5%	0.0%	

The inter-day accuracy and precision was evaluated by comparing hardness over three days using same EZ-AutoTitrator. The ANOVA test shows that the means are not statistically different, and the average mean ranged from 48.6 to 49.3 mg/L. An intra-day evaluation of accuracy and precision was done by comparing the hardness analysis three different times within a single day. The means of three trials ranged from 49.3 to 50 mg/L and means are not statistically different. Most of the trials in validation tests shown in Table 20 and Table 21 have precision of 0.0% which is unexpected and counterintuitive for typical instrumental analysis. Normally, some variation is expected in the results due to random variations in the analytical signal. The uniformity of the precision values is due to the operation of the EZ-AutoTitrator. After the predose, the titrant is added in increments of 0.05 mL when titration is close to the endpoint. The 0.05 mL increment is equivalent to ~3 mg/L CaCO₃ of hardness. In addition, this also means that the random “noise” from the syringe pump and spectral sensor are less than 3 mg/L, indicating the hardness detection limit is likely lower. Ultimately, the EZ-AutoTitrator cannot distinguish a change in hardness below 3 mg/L and at a WTP this inability to distinguish below 3 mg/L is a negligible error in WTP operation. Overall, the EZ-AutoTitrator has average recovery of $98.5 \pm 0.8\%$ (49.3 ± 0.4 mg/L CaCO₃).

The Table 21 summarizes the accuracy and precision of hardness titrations over a range of concentrations starting from 10 to 200 mg/L. All the tested concentrations have good recoveries ranging from 93.4 to 104.4% except 10 mg/L where recovery is only 85%. At lower concentrations (around 10 mg/L), higher sample volumes (30 mL) might improve the accuracy of results

Table 21. Measured total hardness from EZ-AutoTitrator at different concentrations.

Total Hardness Concentration mg/L CaCO ₃					
True Hardness	10.0	20.0	50.1	100.1	200.2
Mean (n=5)	8.5	18.7	48.6	96.9	209.1
Accuracy	84.9%	93.4%	97.1%	96.8%	104.4%
Precision	0.0%	0.0%	3.1%	0.0%	0.0%

A t-test has been conducted to compare the EZ-AutoTitrator and manual hardness titration is shown in Table 22. Both the methods have mean % recoveries close to 100% but EZ-AutoTitrator is slightly better at 100.3% compared to the manual titrations at 102.6%. The t-test shows the means are statistically different. The reasons are that the manual titration relies upon a human analyst to reliably detect the endpoint after the calmagite indicator color transition has occurred. This typically means an analyst will deliver more titrant than necessary, resulting in a mean % recovery over 100 %. For the EZ-AutoTitrator, the high dosing accuracy in combination with detection of the endpoint by the AS7262 spectral sensor and a first derivative plot captures the transition between pinkish-red to bluish-violet at the correct point in the titration more accurately and reproducibly.

Table 22. Comparison of total hardness between the EZ-AutoTitrator and manual hardness titrations.

	Manual Titration	EZ-AutoTitrator
True Concentration (mg/L)	50.1	50.1
Mean (n=20)	51.4	50.2
Accuracy	102.6%	100.3%
Precision	2.0%	3.0%
t-test	Failed: means are statistically different	

Comparison of the EZ-AutoTitrator Method and Manual Titration for Hardness at the Lebanon TN, WTP

A comparison study was performed between the EZ-AutoTitrator and manual titrations for hardness at Lebanon, TN water treatment for a period of four months. Water hardness was measured by EZ-AutoTitrator and manual titrations by a WTP operator daily at 7 am for both finished and raw water. The hardness comparisons of the two methods are visually presented in Figure 21A and Figure 21B for raw and finished water, respectively. The average bias between the two methods was found to be -1.2 ± 4.6 mg/L CaCO_3 in raw and -0.6 ± 4.6 mg/L CaCO_3 in finished water. The Bland-Altman plot for raw water (Figure 22A) has bias scattered around the mean bias with no indication of a proportional bias.

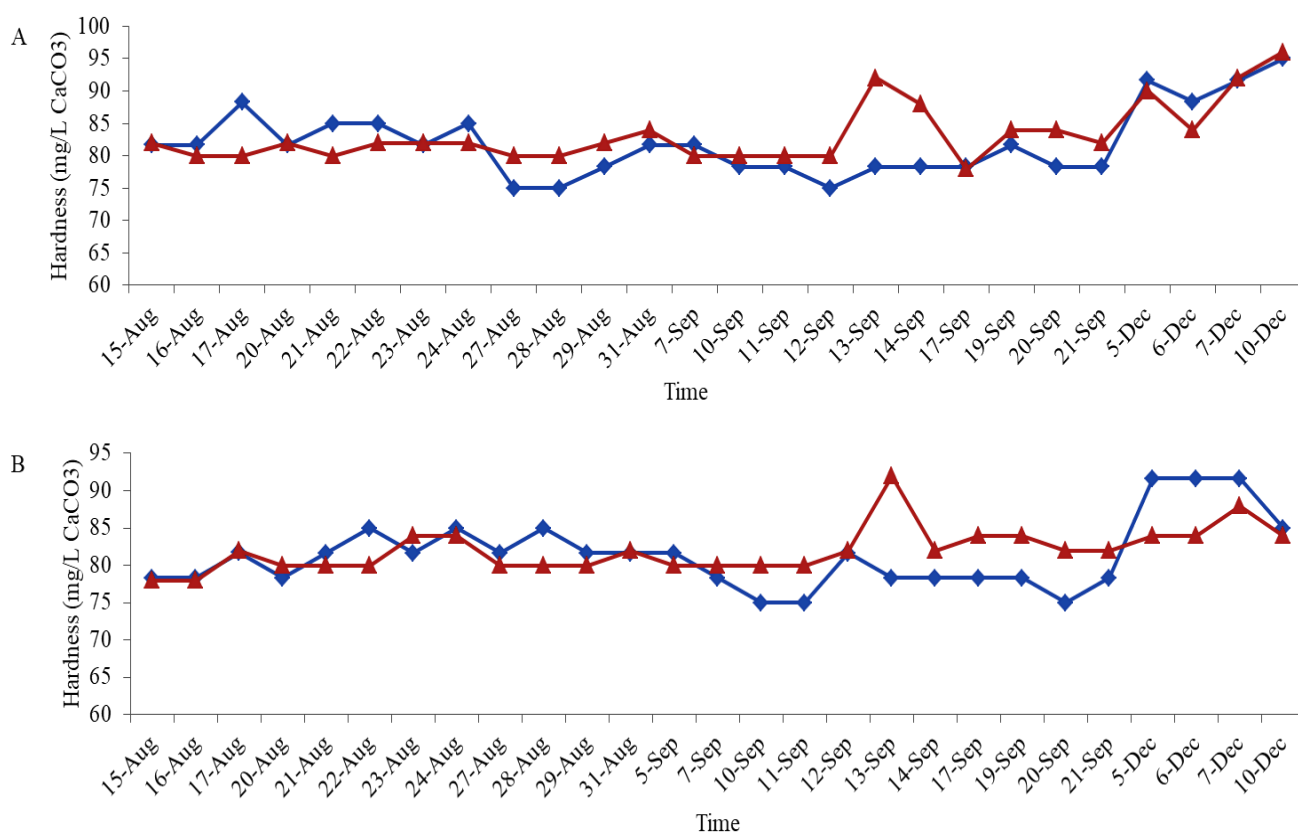


Figure 21. Total hardness measured in raw (A) and finished water (B) by EZ-AutoTitrator and manual titrations at Lebanon, TN water treatment plant. In the red line with triangle markers is the hardness measured manually whereas the blue line with square markers shows the measurements from EZ-AutoTitrator.

The finished water (Figure 22B) seems to have an apparent proportional error; however, the hardness range is narrow, 75 – 85 mg/L CaCO₃ thus it is difficult to conclude a proportional bias exists given that the range of hardness values for all the other samples was similar. The limits of agreement for both the samples were similar as shown in Table 23.

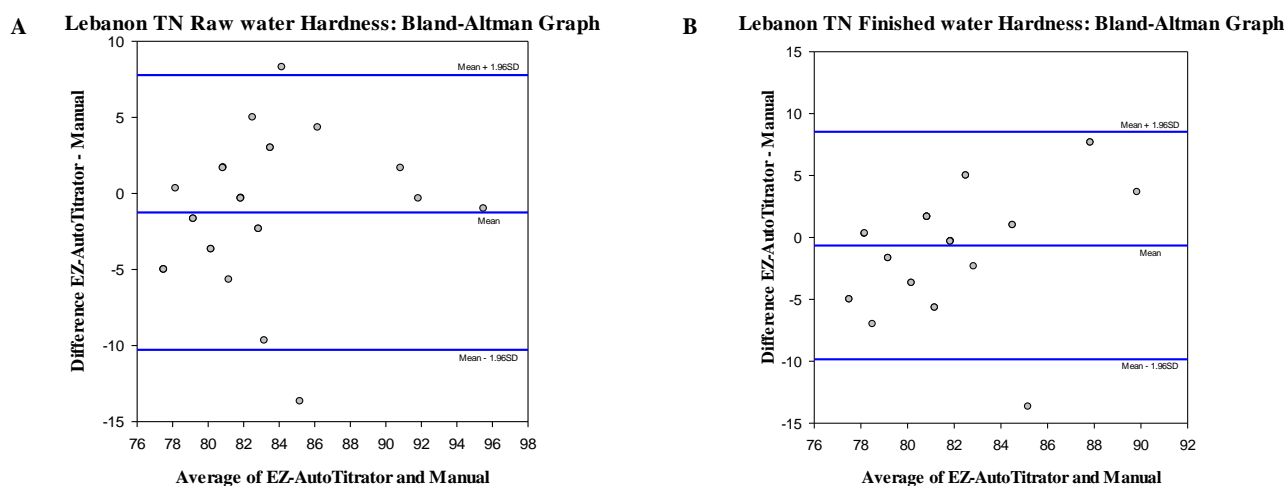


Figure 22. Bland-Altman plots for comparison of hardness from EZ-AutoTitrator and manual titrations at Lebanon, TN water treatment plant in raw (A) and finished water (B).

Table 23. Summary of hardness testing at Lebanon, TN WTP.

	Raw	Finished
n	27	27
Average Bias (mg/L)	-1.2 ± 4.6	-0.6 ± 4.7
Bias Range (mg/L)	-13.7 – 8.3	-13.6 – 7.6
Limits of Agreement (mg/L)	-10.3 – 7.7	-9.8 – 8.5

Comparison of the EZ-AutoTitrator and Manual Titration Methods for Determination of Total hardness at Woodruff SC, WTP

Total hardness measurements were compared between the EZ-AutoTitrator and manual titration in raw (Figure 22A), floc-3 (water after flocculation) (Figure 22B), and finished water (Figure 22C) for two days. Measurements were made every two to three hours between 8 am and 5 pm each day. The average measured hardness was found to be around 28 mg/L in finished water and floc-3. The lowest average hardness (18 mg/L) was measured in raw water. The average bias was found to be -2.9 ± 1.7 mg/L CaCO_3 , -2.6 ± 1.5 mg/L CaCO_3 and -1.9 ± 2.3 mg/L CaCO_3 in raw, floc-3 and finished water respectively. The Bland-Altman plots for raw, floc-3 and finished water were shown in Figure 24A, B and C respectively. All the three samples have smaller range of agreements (Table 24) than the Lebanon, TN results. The reason for this discrepancy could be due to careful measurement of sample (volumetric transfer) and titration by an experienced analyst. Additionally, sample size was smaller when compared to Lebanon testing could contribute to the discrepancy. The woodruff plant testing evaluates the performance of EZ-AutoTitrator at lower hardness range whereas testing at Lebanon plant evaluates the performance at high range of hardness.

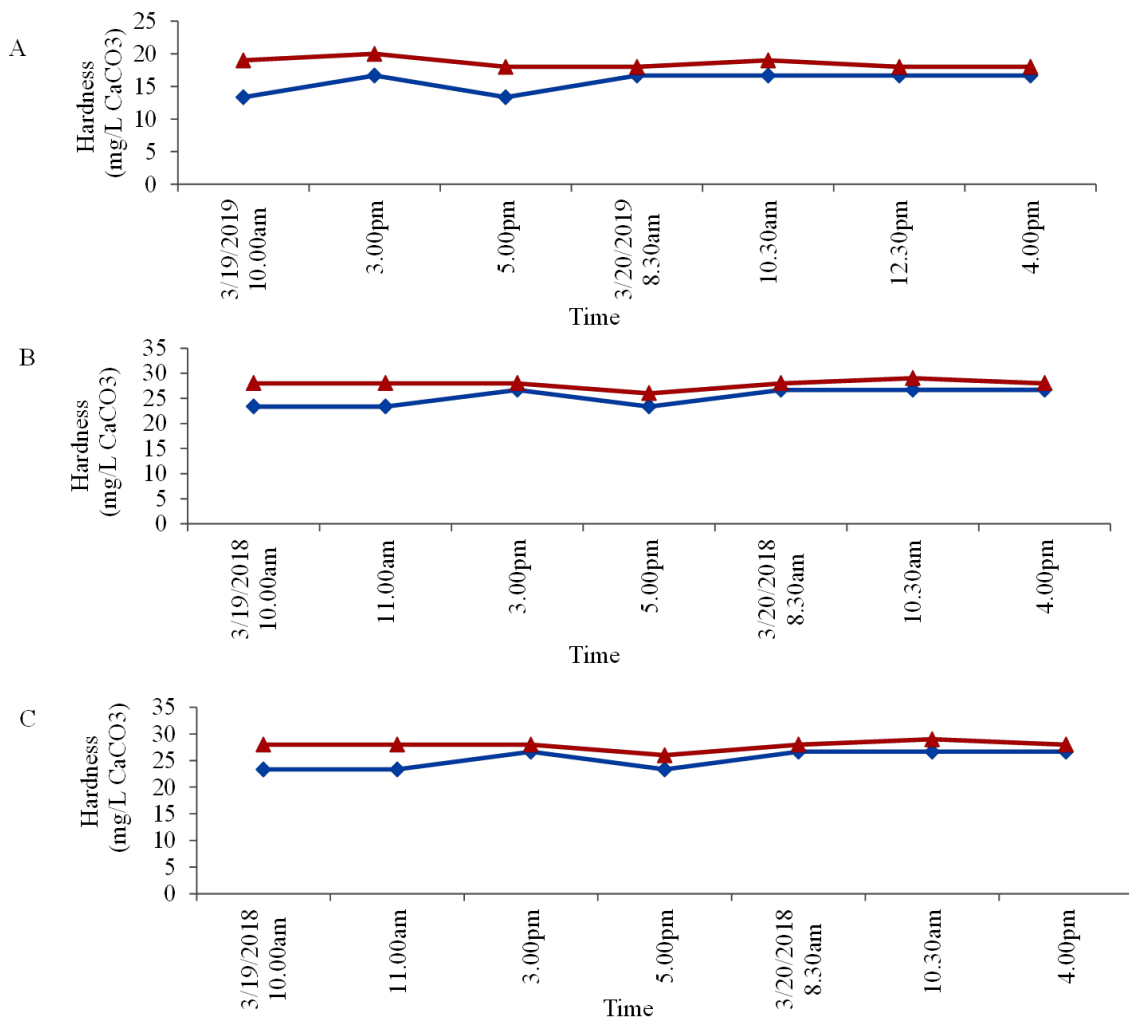


Figure 23. Total hardness measured in raw (A), flocc-3 (B) and finished water (C) using EZ-AutoTitrator and manual titrations at Woodruff, SC water treatment plant. In the red line with triangle markers is the hardness measured manually whereas the blue line with square markers shows the measurements from EZ-AutoTitrator.

Table 24. Summary of hardness testing at Woodruff, SC WTP.

	Raw	After Flocculation	Finished
n	7	7	7
Average Bias (mg/L)	-2.9 ± 1.7	-2.6 ± 1.5	-1.9 ± 2.3
Bias Range (mg/L)	$-5.6 - -1.3$	$-4.6 - -1.3$	$-4.7 - 2$
Limits of Agreement (mg/L)	$-6.3 - 0.6$	$-5.6 - 0.3$	$-6.4 - 2.6$

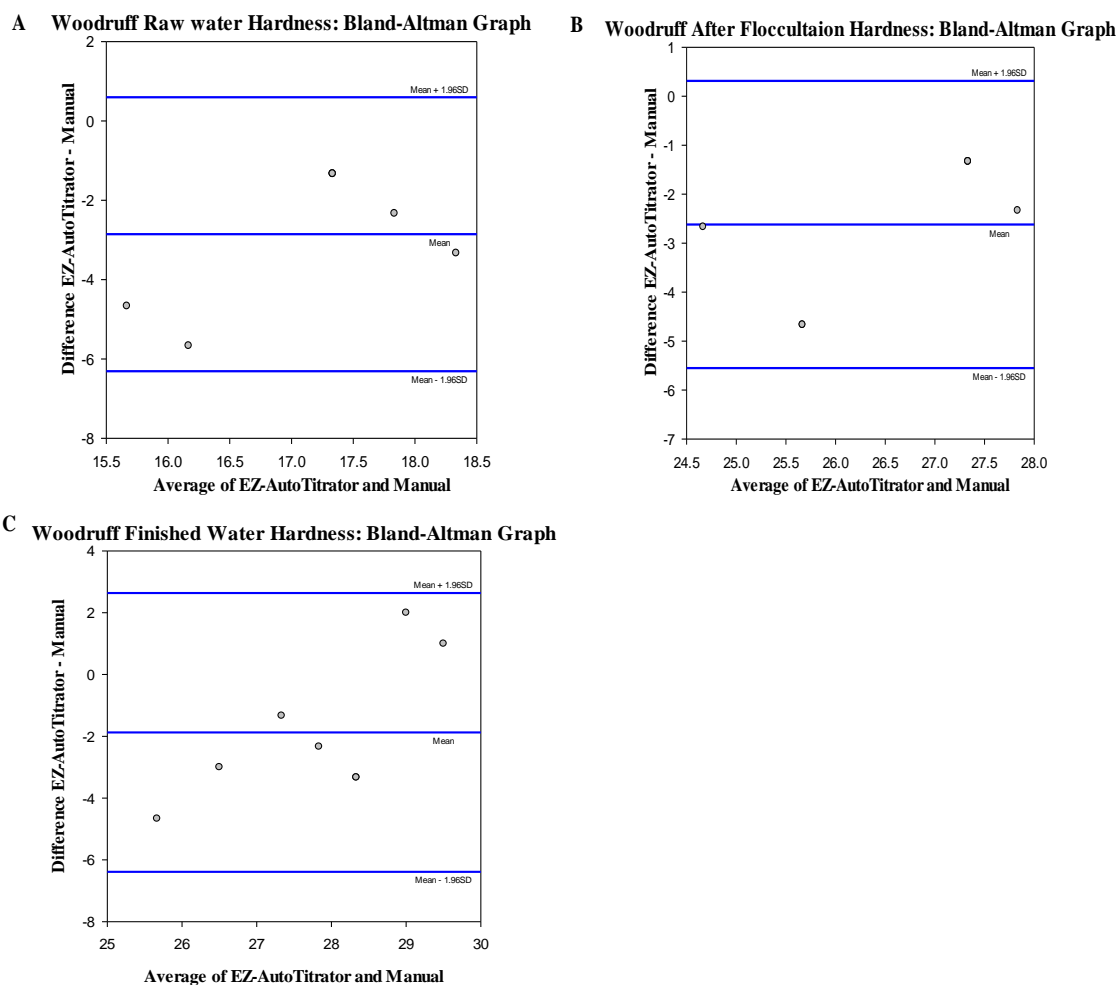


Figure 24. Bland-Altman plots for comparison of hardness from EZ-AutoTitrator and manual titrations at Woodruff, SC water treatment plant in raw (A), floc-3 (B), and finished water (C).

Results of Full Scale Titrations for Standardization of Strong Acids and Bases and pK_a

Determination of Unknown Acids

The EZ-AutoTitrator was used to perform full scale titrations to determine the endpoints for strong acid-base titrations. Results of strong acid-base titrations were compared between EZ-AutoTitrator, VIT-90, and manual titrations. Endpoints from three methods were determined potentiometrically. For these analyses, 1 mL of 0.0973 M KOH was transferred by volumetric pipet and diluted to 15 mL with reagent water. This solution was titrated potentiometrically with 0.0968 M HCl. The experimental concentration of KOH was determined using the first derivative curve⁸⁴. The mean concentrations of KOH (Table 25)

determined by EZ-AutoTitrator and Manual titrations were statistically equivalent with accuracy of 103.9 and 104.6% respectively. While the concentration of KOH determined by VIT-90 was not statistically equivalent to the other two methods and had an accuracy of 96.3%. The VIT-90 has highest precision (0.8%) followed by EZ-AutoTitrator (2.3%) and lowest being for manual titrations (4.4%).

Table 25. Results of acid-base titrations from EZ-AutoTitrator, VIT-90 and Manual Titrations.

n =7	Calculated KOH Concentration (M)	Accuracy & Precision	Are means statistically different? (p < 0.05)
EZ-AutoTitrator	$0.101 \pm 0.002_3$	$103.9 \pm 2.3\%$	
VIT-90	0.0937 ± 0.0007	$96.3 \pm 0.8\%$	YES
Manual	$0.101 \pm 0.004_5$	$104.6 \pm 4.4\%$	

Four weak polyprotic acids have been titrated separately with a standardized KOH solution to determine the molar mass of the acid. First the molarity of acid solution was determined using the endpoint volume and molarity of standardized KOH. The molar mass of the acid was determined from the calculated molarity of the acid and the mass of the acid used in the titration⁸⁴. The molar mass was determined using the first endpoint for all acids except for tartaric acid, where second endpoint was used because the first endpoint was not distinct.

Table 26. Molar mass of polyprotic acids determined using EZ-AutoTitrator.

ACID	Literature molar mass (g/mol)	Experimental molar mass (g/mol)	Absolute Error
tartaric acid	150.09	169.80	+19.71
maleic acid	116.07	120.88	+4.81
phthalic acid	166.13	170.99	+4.86
oxalic acid dihydrate	126.07	134.65	+8.58

Table 26 presents the results of molar masses determined using EZ-AutoTitrator. The absolute errors ranged from +19.71 to +4.81 g/mol. The higher absolute error for tartaric acid determination could be due to uncertainty in purity of tartaric acid standard and calculations were performed assuming 100% purity. The maleic and phthalic acids have calculated values close to literature values. Oxalic acid dihydrate has an error of + 8.58 g/mol. The accuracies can be improved further by using known high purity chemicals as well as further reducing the dosing volume to less than 0.050 mL when the titration approaches the endpoint.

The pK_a 's of phosphoric⁸⁵, maleic⁸⁶, and phthalic acid⁸⁷ was estimated using the half-equivalence method. The acids were titrated over the full range with standardized KOH to determine the endpoints. The pH at the half-equivalence point (halfway between origin and equivalence point) is equal to the pK_a of the acid. The estimated pK_a values, literature values and absolute errors were presented in Table 27. Though phosphoric acid was a triprotic acid, the third equivalence point was not distinct enough to estimate the third pK_a . So, only the first and second pK_a values have been presented. All the three acids have positive error for pK_{a1} ranging from +0.69 to +0.44 and pK_{a2} have negative error ranging from -1.23 to -0.52. The errors in the pK_a values could be attributed to temperature of the solution, ionic strength of the solution and higher dosing volumes near endpoint. In these titrations, a 0.050 mL minimum titrant delivery results in a standard deviation of ± 0.005 on the pK_a values.

Table 27. pK_a of weak polyprotic acids determined by EZ-AutoTitrator using half-equivalence method.

Acid	Literature	pK_{a1}		Literature	pK_{a2}	
		Experimental	Absolute Error		Experimental	Absolute Error
phosphoric	2.15	2.75	+0.60	7.09	5.83	-1.23
maleic	1.94	2.63	+0.69	6.22	5.75	-0.47
phthalic	2.76	3.20	+0.44	4.92	4.40	-0.52

Preliminary Spectrochemical Titrations of FAC in Sodium Hypochlorite Solutions

Several concentrations of NaOCl solutions ranging from 3,000 to 90,000 mg Cl₂/L were prepared by diluting a known concentration of NaOCl solution. The titration was conducted spectrochemically with the EZ-AutoTitrator and potentiometrically using the VIT-90 titrator. The t-test was used to compare the results between the two instruments at each concentration (Table 28). The accuracy of the EZ-AutoTitrator ranges from 96 to 112% across all concentrations of NaOCl solutions with an average of 101% and the precision ranges from 1% to 23%. At the concentration of 3,156 mg/L Cl₂, both EZ-AutoTitrator (23%) and VIT-90

Table 28. Comparison of FAC results from EZ-AutoTitrator and VIT-90. End-point detection of EZ-AutoTitrator is by color change while VIT-90 based on potentiometry.

True value (mg/L)	n=7	Calculated value (mg/L)	Accuracy & Precision	Means Statistically Different? ($t_{cal} > t_{critical}$)
3,156	EZ-AutoTitrator	3,529 ± 807	112 ± 23%	NO
	VIT-90	3,309 ± 421	105 ± 13%	
31,560	EZ-AutoTitrator	32,261 ± 2,225	102 ± 7%	YES
	VIT-90	34,402 ± 965	109 ± 3%	
47,034	EZ-AutoTitrator	46,275 ± 595	98 ± 1%	NO
	VIT-90	46,200 ± 1,267	98 ± 3%	
70,551	EZ-AutoTitrator	46,275 ± 2,547	96 ± 4%	NO
	VIT-90	46,200 ± 1,605	99 ± 2%	
89,365	EZ-AutoTitrator	87,793 ± 1,497	98 ± 2%	NO
	VIT-90	87,365 ± 2,227	98 ± 3%	

(13%) have higher percent relative standard deviations than the other concentrations tested. Except for 31560 mg/L concentration, the calculated t-value (t_{cal}) is less than t-critical value (t_{critical}) which indicates means are not statistically different and indicated with “NO” in Table 28. EZ-AutoTitrator produced equivalent results for FAC with that of VIT-90 for most concentrations. It is likely that at low FAC concentrations, the volume of titrant delivered is small and the resulting error from a 0.050 mL minimum delivery results in a standard deviation of approximately ± 160 mg/L. Using EZ-AutoTitrator, lower FAC concentrations (1 mg/L to 1000 mg/L) should be tested and method needs to be optimized. The EZ-AutoTitrator FAC method needs to be tested rigorously and validated as done for hardness and alkalinity methods.

Comparison of the Specifications of the EZ-AutoTitrator to a Commercially Available Autotitrator

In Table 29, a detailed comparison of the EZ-AutoTitrator specifications to a commercially-available autotitrator is presented. Many of the specifications for the various measurements are equivalent or nearly so. The most significant difference between the two automated titrators is the capability of spectrochemical titrations on the EZ-AutoTitrator. While the current selection of spectrochemical titration methods are limited, the 6-channel AS7262 spectral sensor provides the opportunity to add more indicator-based titrations that can be adapted from Standard Methods for Water and Wastewater. The versatility is provided by the spectral sensor is nearly limitless and a significant advantage over the commercial instrument.

Table 29. Detailed comparison of EZ-AutoTitrator with Hannah instruments titration system.

Specification	EZ-AutoTitrator	Hanna H1902C ⁸⁸
pH Range	0.001 to 14.000	-2.000 to 20.000
pH Resolution	0.001	0.001
pH Accuracy	±0.002 pH	±0.001 pH
pH Calibration	Up to 3-point calibration	Up to 5-point calibration
Ion selective electrode	No	YES
Temperature Range	-55 to 125°C	-5 to 105°C
Temperature Resolution	0.1 °C	0.1 °C
Temperature accuracy	± 0.1 °C	± 0.1 °C
Temperature compensation	Automatic or Manual	Automatic or Manual
Display	7.0" touch display	5.7" display (non-touch)
Buret or syringe size	Variable	Variable
Titrant delivery	stepper motor-based syringe pump	stepper motor-based piston pump
Dosing Accuracy	± 0.1% of full syringe volume	± 0.1% of full buret volume
Dynamic Dosing	YES	YES
Auto Buret/syringe detection	NO	YES
Data logging	YES	YES
Potentiometric titrations	YES	YES

Table 29. Continued.

Specification	EZ-AutoTitrator	Hanna H1902C ⁸⁸
Spectrochemical Titrations	YES	NO
Methods	Extendable	Extendable
End point determination	Equivalence point (1 st derivative) or Fixed pH	Equivalence point (1 st or 2 nd derivative) or Fixed pH
Autosampler compatible	NO	YES
Peripherals	connections for HDMI display, PC-keyboard, USB device input	connections for VGA display, PC-keyboard, parallel printer, USB device input, RS232, interface for autosampler
Operating Environment	10 to 40°C, up to 95% RH	10 to 40°C, up to 95% RH
Power supply	240 VAC	100 – 240 VAC
Dimensions	15 x 14 x 9 in	15.3 x 13.8 x 14.9 in
Cost	\$4,999	\$ 6400

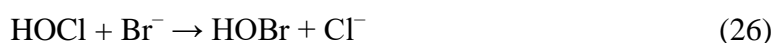
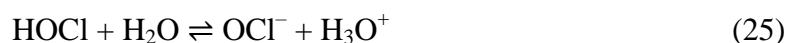
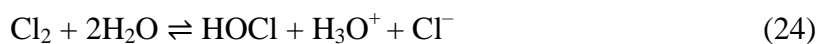
Conclusions

An automated titration system (EZ-AutoTitrator) has been developed using a Raspberry Pi single board computer and commercial-off-the-shelf components. A two channel EZ-AutoTitrator was constructed for under \$1,000, building off of the EZ-AutoPipet detailed in Chapter 2. Total hardness and Total alkalinity methods have been developed and rigorously tested demonstrating equivalent or better results to manual titrations and commercial automated titrator. EZ-AutoTitrator was successfully tested for alkalinity and hardness at Lebanon TN WTP for over three months in raw and drinking water. A second on-site test was conducted at the Woodruff-Roebuck SC WTP comparing the EZ-AutoTitrator to a manual titration for alkalinity and hardness for two days in raw, water after flocculation and finished water. Lebanon study evaluated the performance of the EZ-AutoTitrator at mid to higher alkalinity and hardness while Woodruff study evaluated the performance at lower concentrations. Preliminary studies indicate potential for using EZ-AutoTitrator to perform FAC determination in bleach. A lower dosing volume near the endpoint and better control over temperature and ionic strength of the solution may improve pK_a and molar mass results. The EZ-AutoTitrator was certified to use as standard method for measuring pH, temperature, hardness and alkalinity by LabtronX Inc. a company specialized in quality assurance.

CHAPTER 4
ON-LINE ADDITION OF INTERNAL STANDARD (2-BBA) FOR
CONTINUOUS CALIBRATION OF HALOACETIC ACID RAPID-RESPONSE
SYSTEM (HAA-RR)

Introduction

Disinfection is an important process to ensure that drinking water is free from harmful microorganisms. For over a century, chlorination by gaseous chlorine, sodium hypochlorite and calcium hypochlorite have been considered to be a safe and economical method to disinfect water⁶⁴. In this process, chlorine gas hydrolyzes to form hypochlorous acid, hydrogen ion and chloride ion⁸⁹ (Equation (24)). At the pH of drinking water, hypochlorous acid dissociates to form hypochlorite ion with a pK_a of ~ 7.53 (Equation (25)). In addition, the presence of bromide ion will result in the formation of hypobromous acid (Equation (26)) and hypobromite ion⁹⁰ (Equation (27)).



Hypochlorous and hypobromous acid react with natural organic matter in water to form halogenated disinfection by-products (DBPs)^{58,64}. There are two classes of halogenated DBPs regulated by the United States Environmental Protection Agency (USEPA), the trihalomethanes (THMs) and haloacetic acids (HAAs). The most common chlorinated and brominated HAA species includes monochloroacetic acid (MCAA), monobromoacetic acid (MBAA), dichloroacetic acid (DCAA), dibromoacetic acid (DBAA), bromochloroacetic acid

(BCAA), trichloroacetic acid (TCAA), bromodichloroacetic acid (BDCAA), dibromochloroacetic acid (DBCAA), tribromoacetic acid (TBAA). Some studies show THMs and HAAs can increase the risk of bladder and liver cancer⁹¹⁻⁹³. The five regulated HAA species are MCAA, DCAA, TCAA, MBAA and DBAA and are collectively called as HAA5. Currently, the USEPA has set the maximum contamination level (MCL) as 0.060 mg/L⁶³ for HAA5.

According to the Disinfectant and Disinfection By-Product rule, water treatment plants are mandated to monitor HAAs and comply with USEPA regulations in their drinking water distribution systems. The USEPA has developed standard methods for analyzing HAAs such as method 552.3⁹⁴ and 557⁹⁵. Both the methods have their own advantages and disadvantages. USEPA Method 552.3 (GC-ECD) is comparatively cost effective but involves a tedious, complex extraction and derivatization process, requiring well trained and skilled personnel. USEPA Method 557 (Ion chromatography-tandem mass spectrometry (IC-MS/MS)) method involves high cost for analysis due to necessary instrumentation and requires highly trained and experienced personnel to operate the mass spectrometer. A simple, low cost and easy to operate method involving post-column reaction ion chromatography⁹⁶⁻⁹⁹ (PCR-IC) has been developed by MAMML group to address the issues with USEPA methods for HAA analysis. This method involves separation of HAAs using an anion exchange chromatographic column and the selective reaction of the post-column reagents with HAA species. The separated HAAs react with nicotinamide (NCA) in presence of potassium hydroxide (KOH) as shown in Equation (28), to produce a fluorescence product detected by the fluorescence detector (EX: 365 nm, EM: 450 nm).



Overview of Haloacetic Acid Rapid Response (HAA-RR)

The patented PCR-IC system is commercialized as the HAA-RR¹⁰. The HAA-RR operates similarly to the PCR-IC system with key differences in the pumping of reagents and operating parameters such as a column cooler and a filter-based fluorescence detector. The HAA-RR first starts with an injection of 2 mL of sample onto the anion-exchange column as shown in Figure 25. A DionexTM, IonPacTM AG18 guard column (50mm x 4 mm) followed by IonPacTM AS18 separation column (250 mm x 4 mm) is maintained at 15°C using a Peltier column cooler. A gradient elution program with a mobile phase flow rate of 1 mL/min where the ratio of 200 mM KOH and degassed reagent water varies with time to achieve chromatographic separation of nine HAAs. A 1:1 post-column reagent mixture of 3.07 M NCA and 2.0 M KOH is delivered into the column effluent at the rate of 0.4 mL/min using a low-pressure gradient mixer coupled with a high pressure pump (GP1 in Figure 25).

The HAAs from the column effluent selectively react with the post column reagent mixture in a 40-meter, 0.75 mm ID knitted open tubular coil (KOTs) at 98°C to form a fluorescent product. The reaction mixture then flows through a 1 meter, 0.75 mm ID KOT placed inside the column cooler. The fluorescent products are detected by a filter-based LED fluorescence detector, previously described in detail¹⁰. In summary, the excitation source is a 365 nm LED and the excitation filter is a 365 ± 5 nm interference filter. The emission filter used is a 425 nm long-pass filter.

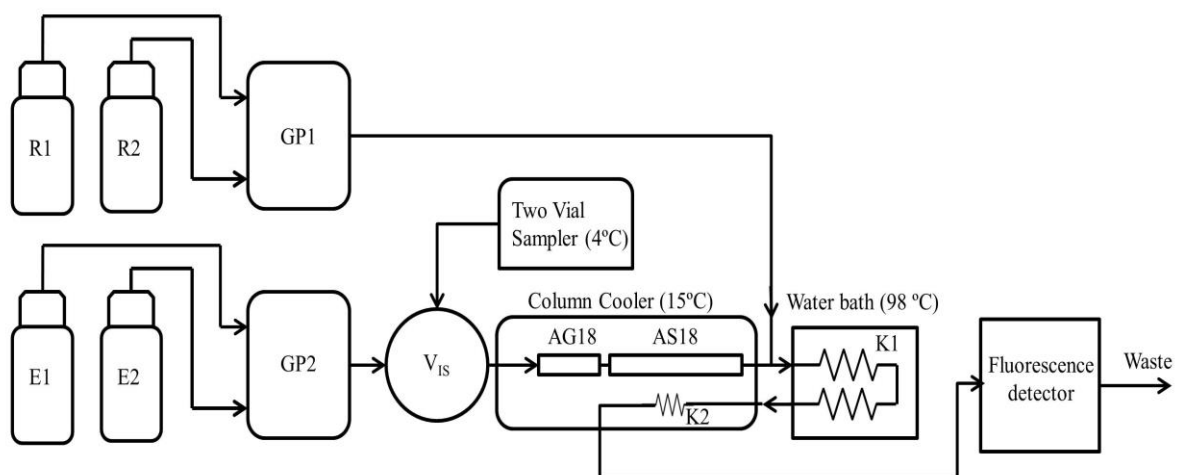


Figure 25. Block Diagram of HAA-RR. E1 and E2 are 200mM KOH and Reagent water eluent respectively. R1 and R2 are 2M KOH and 3.2M NCA post column reagents respectively. GP1 and GP2 are high pressure gradient pumps. V_{is} is the 6-port injection valve. K1 is 40 m KOT and K2 is 1 m KOT.

Overview of External Calibration for On-Line Monitoring of HAA9 Species

The HAA-RR is typically calibrated using an external calibration protocol. In the external calibration mode, at least five calibration standards ranging from 10 $\mu\text{g/L}$ to 80 $\mu\text{g/L}$ are analyzed and a plot of analytical signal (y-axis) vs. concentration (x-axis) is constructed for the individual HAA9 species. Then a check standard will be analyzed at least three times to evaluate the accuracy and precision of the method. The slope (m) and intercept (b) from the linear regression line is used to calculate the concentration (x) of HAAs in samples from the analytical signal⁸³ (y) as shown in Equation (29)

$$x = \frac{y - b}{m} \quad (29)$$

There are certain concerns running HAA-RR in external calibration mode namely:

Operation Cost: To complete an external calibration of the HAA-RR, it requires a minimum of 12 hours which uses a substantial amount of standards, eluents and post column reagents.

This ultimately increases the cost of operation and more over it increases the frequency of maintenance on the high-pressure pumps.

Accuracy: Accuracy of the results depends on preparation of the standards which will be a challenge to WTP operators who doesn't have formal experience in analytical chemistry.

Personnel-hours: Without an expensive auto-sampler, an operator has to dedicate his/her work hours performing the calibration. If HAA-RR was equipped with an auto-sampler, then the retail cost of instrument may rise by \$10,000 - \$15,000.

Process Time: As mentioned earlier, external calibration requires around 12 hours which takes away a day of monitoring in each week as well as valuable water treatment plant operator time.

Instrument Variability: External calibration will not account for any changes in the instrument such as, but not limited to, changes in reagent concentration, reagent flow rate, changes in detector sensitivity, and changes in LED light intensity.

Overview of Single Point Internal Standard Calibration for On-line Monitoring of HAA9 Species

An internal standard (IS) is a compound that has similar physical and chemical properties as the analyte and added in constant amount to blank, standard and samples⁸³. The single point internal calibration is based on the response factor (RF) which is analyte response per unit concentration. The ratio of analyte RF to internal standard RF is called as Relative Response Factor (RRF) as shown in Equation (30)

$$RRF = \frac{S_s/C_s}{S_i/C_i} \quad (30)$$

Where S_s is the analyte response from calibration standard, C_s is the concentration of analyte in calibration standard, S_i is the internal standard response and C_i is the concentration of internal standard. A sample analysis is performed by adding the same amount of internal standard to the sample as the calibration standard and unknown concentration (C_x) is then calculated as shown in Equation (31)

$$C_x = \frac{S_x/C_i}{RRF/S_i} \quad (31)$$

As opposed to absolute measurements in external calibration, the measurements in internal calibration are relative, thus compensating for random and systematic changes that affect analyte response⁸⁴. For instance, variations in reagent flow rates and concentrations, LED intensity of detector etc. can be minimized using internal standard calibration. The single point internal calibration can address all the issues with external calibration that are identified in the previous section.

Significance and Goals of Research

The previous research in 2009 used a syringe pump to deliver the internal standard. The internal standard flowing at 0.08 mL/min is mixed with sample or standard flowing at 0.89 mL/min via peristaltic pump⁹⁷. This method needs a syringe pump setup, proper programming and accurate timing to deliver the internal standard accurately and reproducibly. In addition, mixing the internal standard with the drinking water sample results in a dilution of the sample by ~10%. When measuring the HAAs at the 10 – 80 µg/L range, minimizing the sample dilution is also important.

The major goals of this research are:

1. To develop an on-line single point internal calibration method for HAA-RR without using a syringe pump.

2. To validate the robustness of the single point internal calibration method. Various parameters of HAA-RR such as LED intensity, reagent flow rate and reagent concentrations etc. that govern the HAA9 response will be studied.
3. To run HAA-RR system every six hours at least a week using internal calibration with minimal human interaction.

Experimental

Modified HAA-RR Sample Injection System for On-Line Internal Standard

Typically, the HAA-RR system uses a two-position, six-port injection valve with a peristaltic pump to load sample loop and inject the sample on to the column. Previous work used a syringe pump to mix internal standard into the drinking water prior to analysis. In this work, the modified internal standard calibration method was based on injecting sample and internal standard (IS) on to the column sequentially using a two-position, 10 port injection valve. A peristaltic pump was used to pull the sample or IS through their respective sample loops sequentially and a 3-way valve was used to select either sample or internal standard (Figure 26). Initially, the 10-port valve will be in position B and the 3-way valve in normally open mode. In this state, peristaltic pump pulls the sample or HAA9 standard through the 2 mL sample loop. After six minutes, the 10-port valve is actuated to position A which injects sample or HAA9 standard on to the column. Simultaneously, the 3-way valve is actuated in order to fill the 20 μ L IS loop while sample being injected on to column. After 5 minutes of sample injection, the 10-port valve will be actuated to position B which subsequently injects the internal standard on to the column and returns the valve to loading sample for the next analysis. For this study, 5,000 μ g/L of 2-BBA has been used as internal standard. Essentially, 20 μ L of 5,000 μ g/L injects equivalent amount to 2 mL of 50 μ g/L which is 100 ng of 2-BBA.

The IS IN and sample IN lines were connected to a two-vial sampler. The two-vial sampler is a simple aluminum block with two slots - one for holding a 60 mL round glass vial for internal standard and the other for 40 mL round glass vial for grab sample or standard, both using vial caps with PTFE septa. Each slot has a needle for sample flow and a needle for air venting. The aluminum block has been equipped with a Peltier cooler to facilitate necessary cooling (2°C) to prevent thermal degradation of internal standard.

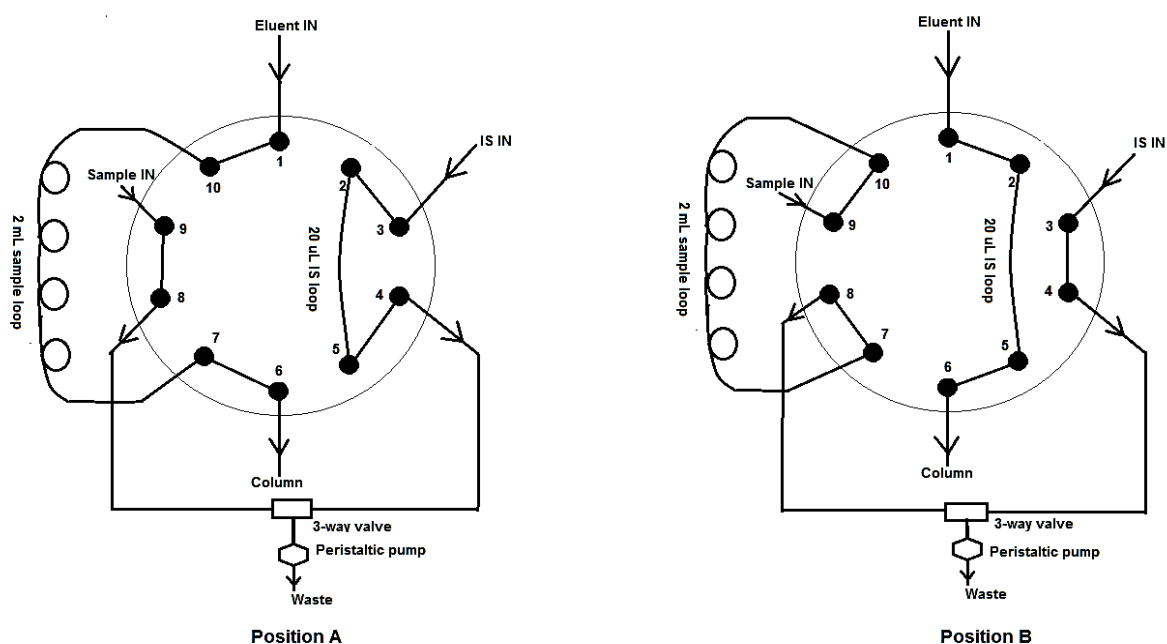


Figure 26. On-line Internal standard injection system. Position A injects the sample on to the column and allows loading of the IS (20 µL loop). Position B injects IS on to the column and allows loading of sample (2 mL loop).

When a vial has been inserted into the slot, both needles pierce through the septa allowing liquid to be drawn from the vial. For a typical analysis, 6 mL of sample is passed through the 2 mL sample loop and 1.5 mL of the 5,000 µg/L IS solution is passed through the 20 µL loop. This approach allows each 60 mL vial of IS to last for approximately 40 sample analyses, or approximately 10 days at a rate of four samples analyzed per day.

Chemicals, Reagents and Standards

All the reagents and standards were prepared using reagent grade water with a resistivity of at least 18.2 M Ω -cm and total organic carbon (TOC) of 10 μ g/L or less produced by a Barnstead E-Pure water purification system (ThermoFischer Scientific, Waltham, MA, USA). All the chemicals used were HPLC grade, Reagent grade, ACS certified grade or better except the ACS grade potassium hydroxide with 85% purity. A certified reference standard for HAA9 at a concentration of 2000 mg/L for each HAA species was obtained from Sigma-Aldrich USA. The 2-bromobutanoic acid (2-BBA), nicotinamide (NCA), and potassium hydroxide (KOH) and methyl tertiary butyl ether (MTBE) were procured from ThermoFischer Scientific. 0.1 g of pure 2-BBA was added to 10 mL volumetric flask and diluted with MTBE to obtain a stock concentration of 10,000 mg/L.

A 5,000 μ g/L of 2-BBA was prepared by volumetrically diluting the stock standard with reagent water. The required concentration of HAA9 for each standard was prepared by volumetrically diluting the reference standard with reagent water. The reagent water eluent was degassed by bubbling nitrogen gas for 45 mins. The 200 mM KOH eluent was prepared by diluting 25.78 g of KOH to 2.0 L with degassed reagent water. The 3.07 M NCA reagent was prepared by diluting 750 g NCA to 2.0 L with reagent water. The 2.0 M KOH was prepared by diluting 257.8 g KOH to 2.0 L with reagent water.

Results and Discussion

Stability of Internal Standard (2-BBA)

One of the goals of this research was to run the HAA-RR every six hours to analyze drinking water using single point internal calibration. To achieve this goal, 2-BBA (IS) must be stable in the reagent water for at least one week. The stability of a 5,000 $\mu\text{g/L}$ 2-BBA solution in reagent water has been studied for 10 days at a temperature of 2°C and room temperature. The Figure 27 shows the response of 2-BBA solution analyzed once every 24 hours for 10 days at 2°C. The red central line in Figure 27 is the average response of the first two analyses at 0 hours and 24 hours. The black dotted lines represent the 3% deviation of average response which was the typical standard deviation observed on the HAA-RR system for 2-BBA in previous analyses at this concentration. The response of 2-BBA was within the 3% deviation for 10 days proving the stability of IS solution. Figure 28 shows the response of 2-BBA solution at room temperature. The response starts to decline after 24 hours proving that internal standard needs to be maintained at 2 °C to prevent thermal degradation.

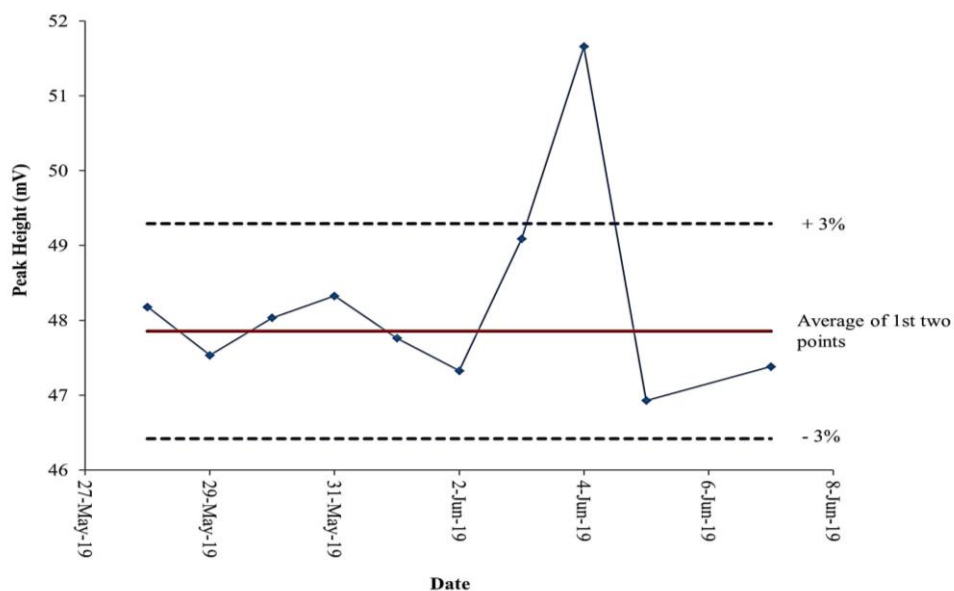


Figure 27. Stability of 2-BBA in reagent water at 2°C. The central line is the average of day 1 and day 2 responses. The upper and lower dotted lines represent the 3% deviation window

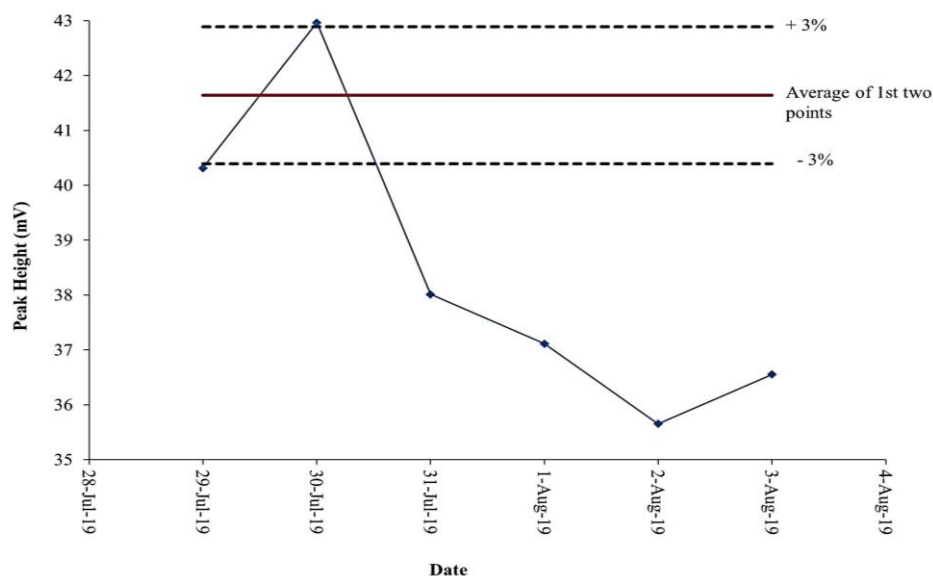


Figure 28. Stability of 2-BBA in reagent water at room temperature. Over the week, the response of 2-BBA decreased.

Preliminary Testing of the Modified Injection System

Prior to the detailed robustness studies, the modified internal standard injection approach was tested to ensure the approach worked as expected and was reproducible. First, reagent water blanks were injected in place of both sample and IS where the chromatograms shows no peaks except injection artifact (Figure 29). Next, the internal standard vial slot had

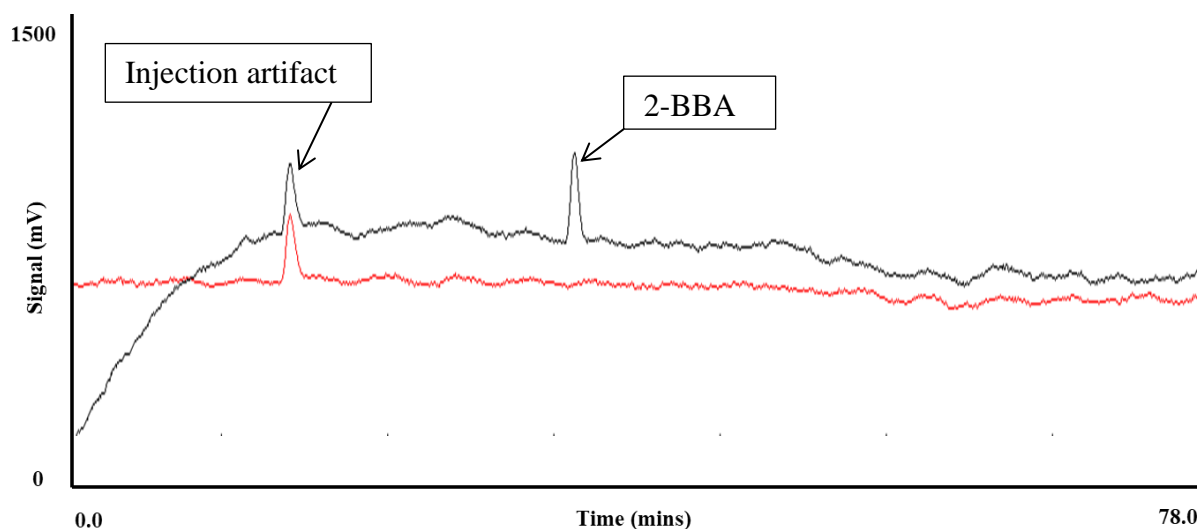


Figure 29. Comparison between blank chromatogram and chromatogram with only internal standard injection. The red line represents the blank run and the black line represents a run with internal standard (2-BBA) injection and injected reagent water as a sample.

a 5,000 $\mu\text{g/L}$ 2-BBA solution put in place that was injected sequentially along with reagent water blank. The chromatogram shows 2-BBA peak along with injection artifact. Finally, Figure 30 depicts a 50 $\mu\text{g/L}$ HAA9 standard injected sequentially with 2-BBA (red chromatogram) and a chromatogram with the internal standard only reagent water blank (black chromatogram).

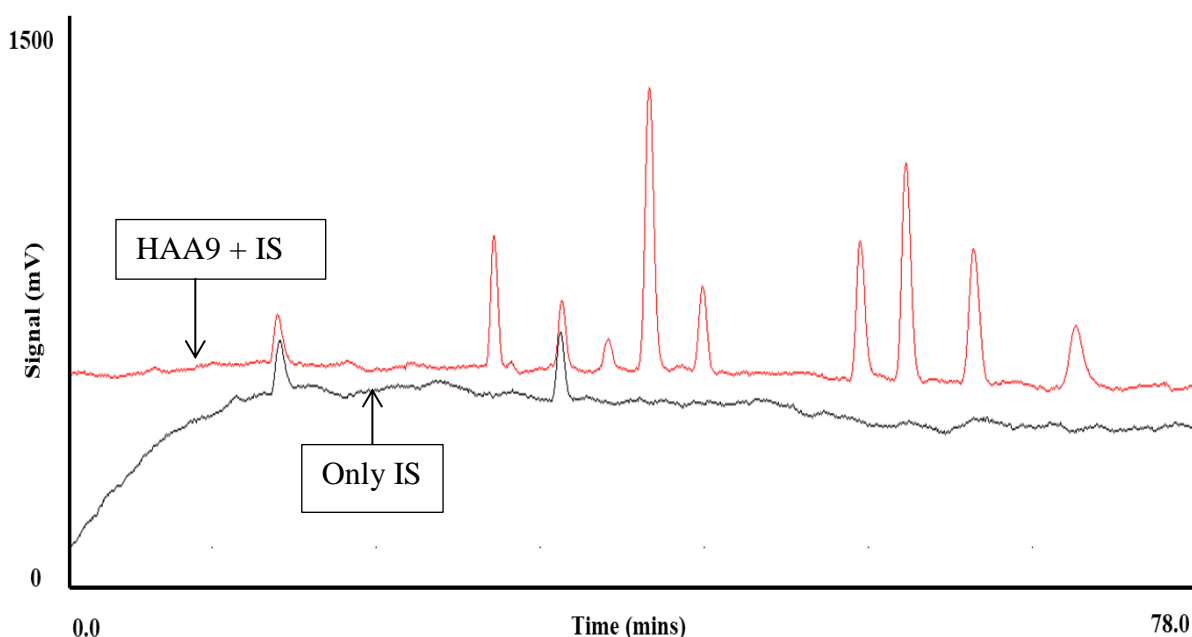


Figure 30. Comparison between chromatogram with both IS and standard HAA9 injection (Red chromatogram) and only IS injection (black chromatogram).

Robustness of HAA-RR using Single Point Internal Standard Calibration

Robustness is defined as “*being the capacity of an analytical procedure to produce unbiased results when small changes in the experimental conditions are made voluntarily*”¹⁰⁰.

In the following studies, the robustness of the on-line, single point internal standard calibration will be evaluated and compared against an external calibration curve. The parameters studied include LED intensity, NCA and KOH concentration, reagent mix flow rate which are all expected to have the most impact on the HAA9 analytical signal. For these robustness studies, the HAA-RR system was calibrated using a four-point external calibration with calibration standards ranging from 11 $\mu\text{g/L}$ to 44 $\mu\text{g/L}$. The relative response factors for

individual HAA species for single point internal calibration were calculated (Equation (30)) by analyzing a 44 µg/L HAA9 standard and 5,000 µg/L 2-BBA. For each of the comparisons, a check standard of 33 µg/L HAA9 was analyzed in triplicate at the HAA-RR standard operating conditions and then each parameter was altered systematically followed by triplicate analysis of the 33 µg/L check standard. The results of the triplicate analyses were used for the robustness comparisons of the HAA-RR between external calibration and internal standard calibration.

LED Intensity Robustness Study

The fluorescence emission analytical signal will be greatly influenced by the excitation light intensity of the LED⁸³. The LED intensity of the fluorescence detector can be controlled by varying the control voltage of the LED driver module. Over the course of operation on the 3 – 6 months' timescale, the intensity of the LED emitter will decrease over time, even at the same control voltage. In this study, a decrease of the LED intensity over time was simulated by decreasing the LED control voltage and determining the concentration of a check standard. Initially, the HAA-RR system was calibrated using external calibration at 9.09 V. The percent recovery of HAA9 check standard was compared between external and single point internal calibration at three different LED intensities. Figure 31 shows the results for MCAA only; however, all the HAA9 species had similar results. As the LED intensity decreases, the calculated concentration of check standard from external calibration decreases while the calculated concentration from single point internal calibration method remains nearly constant. The detailed results for all the HAA9 species were summarized in Table 30. In Table 30, the results are tabulated with the parameter value at the top of each column. The results of the triplicate analysis of the experimental check standard concentration, the percent recovery, and the percent change compared to the initial value are

grouped by external calibration (Ext.) and single point internal standardization (SIS) for each HAA9 species.

This same grouping and presentation of data is used for the remaining parameters of the robustness studies. Overall, external calibration produces on an average of 10.83 $\mu\text{g/L}$ change in concentration per unit change in the LED control voltage with lowest being for

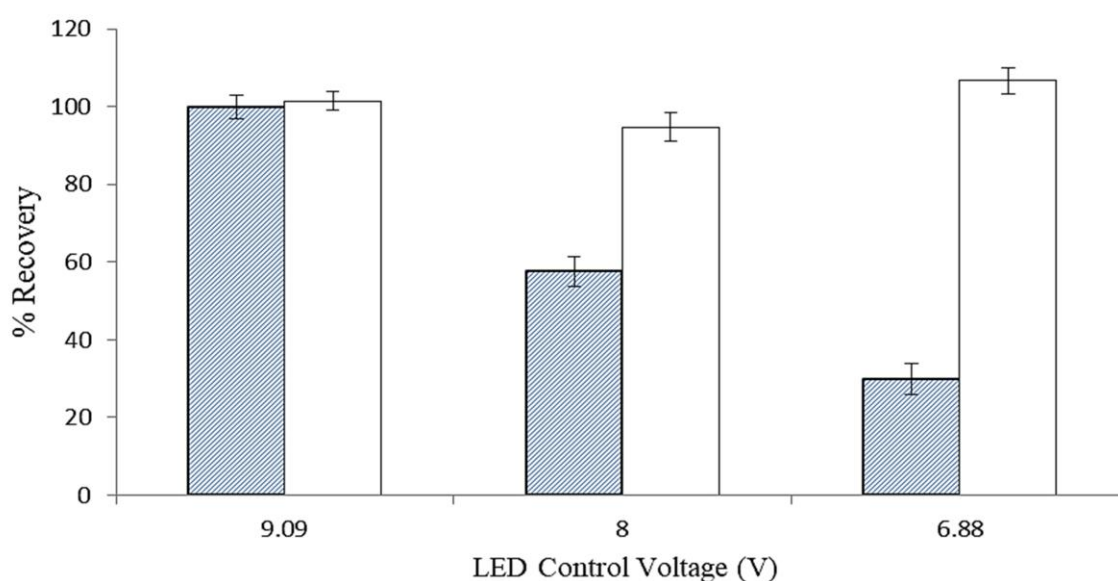


Figure 31. The % Recovery of MCAA was calculated using external calibration and single point internal standard calibration at three different source LED intensities. The blue, striped bars represent concentration from external calibration and white bars represent the concentration from single point internal standard calibration. The error bars show the % RSD from three replicates.

MBAA (9.21 $\mu\text{g/L}$) and highest being for TCAA (11.81 $\mu\text{g/L}$). While the internal standard calibration produces less than 1 $\mu\text{g/L}$ change in concentration per unit change in control voltage. These results demonstrate the value of on-line, single point standardization for the HAA-RR system. That is, when the instrument parameters are changing, the single point internal standardization ensures that the HAA-RR system reports HAA9 concentrations that are unbiased.

Table 30. Summary of HAA-RR results using external and single point internal calibration at three different LED intensities.

LED control voltage (V)			9.09	8	6.88
MCAA		Experimental (μg/L)	32.9 ± 1	19 ± 0.73	9.9 ± 0.39
	Ext.	% Recovery	99.8 ± 3%	57.7 ± 3.9%	29.9 ± 3.9%
		% Change	0.0%	-42.2%	-69.9%
		Experimental (μg/L)	33.5 ± 0.8	31.3 ± 1.14	35.2 ± 1.18
	SIS	% Recovery	101.5 ± 2.4%	94.7 ± 3.6%	106.7 ± 3.4%
		% Change	0.0%	-6.6%	1.7%
MBAA		Experimental (μg/L)	28.9 ± 7.5	16.9 ± 2.4	8.5 ± 1.0
	Ext.	% Recovery	87.5 ± 25.9%	51.2 ± 14%	25.8 ± 11.4%
		% Change	0.0%	-41.5%	-70.6%
		Experimental (μg/L)	30.1 ± 7.2	30.02 ± 3.8	37.03 ± 3.4
	SIS	% Recovery	91.2 ± 23.9%	90.97 ± 12.5%	112.2 ± 9.2%
		% Change	0.0%	-0.3%	22.9%
DCAA		Experimental (μg/L)	34.6 ± 2.1	19.5 ± 4.6	8.6 ± 1.4
	Ext.	% Recovery	105 ± 6.0%	59.1 ± 23.5%	26.2 ± 16.0%
		% Change	0.0%	-43.6%	-75.1%
		Experimental (μg/L)	33.3 ± 2.2	30.8 ± 7.3	30.6 ± 3
	SIS	% Recovery	100.9 ± 6.6%	93.37 ± 23.5%	92.8 ± 9.8%
		% Change	0.0%	-7.5%	-8.1%

Table 30. Continued.

LED control voltage (V)		9.09	8	6.88	
BCAA		Experimental (µg/L)	32.9 ± 0.4	20.2 ± 0.2	9.1 ± 0.03
	Ext.	% Recovery	99.7 ± 1.4%	61.1 ± 1.1%	27.5 ± 0.3%
		% Change	0.0%	-38.6%	-72.3%
	SIS	Experimental (µg/L)	33.6 ± 0.2	33.8 ± 0.6	34.5 ± 2.61
		% Recovery	101.7 ± 0.4%	102.54 ± 1.7%	104.6 ± 7.6%
		% Change	0.0%	0.6%	2.7%
DBAA		Experimental (µg/L)	34.5 ± 0.4	21 ± 2.0	8.4 ± 0.6
	Ext.	% Recovery	104.5 ± 1%	63.8 ± 9.5%	25.4 ± 6.7%
		% Change	0.0%	-44.9%	-75.7%
	SIS	Experimental (µg/L)	35.1 ± 0.3	35.8 ± 3.6	34.2 ± 4.7
		% Recovery	106.3 ± 0.8%	108.5 ± 9.9%	103.6 ± 13.9%
		% Change	0.0%	2.0%	-2.6%
TCAA		Experimental (µg/L)	33.9 ± 0.2	20.5 ± 0.2	8.5 ± 0.7
	Ext.	% Recovery	102.8 ± 0.6%	62.1 ± 1.2%	25.8 ± 8.3%
		% Change	0.0%	-39.5%	-74.9%
	SIS	Experimental (µg/L)	35.4 ± 0.3	36.2 ± 0.7	37.3 ± 3.3
		% Recovery	107.2 ± 0.8%	109.7 ± 1.8%	113.1 ± 8.8%
		% Change	0.0%	2.5%	5.4%

Table 30. Continued.

LED control voltage (V)			9.09	8	6.88
BDCAA		Experimental (μg/L)	33.3 ± 0.7	21 ± 0.5	9.2 ± 0.1
	Ext.	%Recovery	101 ± 2.2%	63.5 ± 2.5%	27.8 ± 1.1%
		% Change	0.0%	-36.9%	-72.4%
	SIS	Experimental (μg/L)	34.2 ± 0.4	35.5 ± 0.9	35 ± 2.8
		%Recovery	103.7 ± 1.1%	107.4 ± 2.5%	106.1 ± 8.0%
		% Change	0.0%	3.8%	2.3%
DBCAA		Experimental (μg/L)	32.9 ± 0.4	20.2 ± 0.2	9.1 ± 0.03
	Ext.	%Recovery	99.7 ± 1.4%	61.1 ± 1.1%	27.5 ± 0.3%
		% Change	0.0%	-38.6%	-72.3%
	SIS	Experimental (μg/L)	33.6 ± 0.2	33.8 ± 0.6	34.5 ± 2.6
		%Recovery	101.7 ± 0.4%	102.5 ± 1.7%	104.6 ± 7.6%
		% Change	0.0%	0.6%	2.7%
TBAA		Experimental (μg/L)	32.9 ± 1.0	19.4 ± 0.7	10 ± 0.6
	Ext.	%Recovery	99.7 ± 3%	58.9 ± 3.8%	30.4 ± 6.2%
		% Change	0.0%	-41.0%	-69.6%
	SIS	Experimental (μg/L)	34.7 ± 1.0	33.3 ± 1.3	37.8 ± 1.6
		%Recovery	105.3 ± 3.0%	101 ± 3.8%	114.5 ± 4.1%
		% Change	0.0%	-4.0%	8.9%

Nicotinamide Robustness Study

The rate of formation of the NCA and HAA9 fluorescence products in the post column reaction is dependent on the NCA concentration. High concentrations of NCA in aqueous solution (*e.g.* 3.07 M) have been shown to produce the most analytical signal compared to lower concentrations (*e.g.* 2.75 M)⁹⁶. For this study, the HAA-RR system was calibrated using external calibration using the standard operating concentration of 3.07 M NCA. The percent recovery of HAA9 check standard was compared between external and single point internal calibration at three different NCA concentrations (3.07, 2.9, 2.75 M). Figure 32 shows the results for MCAA and each of the HAA9 species follow a similar trend; decreasing NCA concentration results in decreasing external calibration reported concentration. However, the calculated concentration from single point internal calibration remains almost constant. The comparison results for all the HAA9 species are summarized in Table 31.

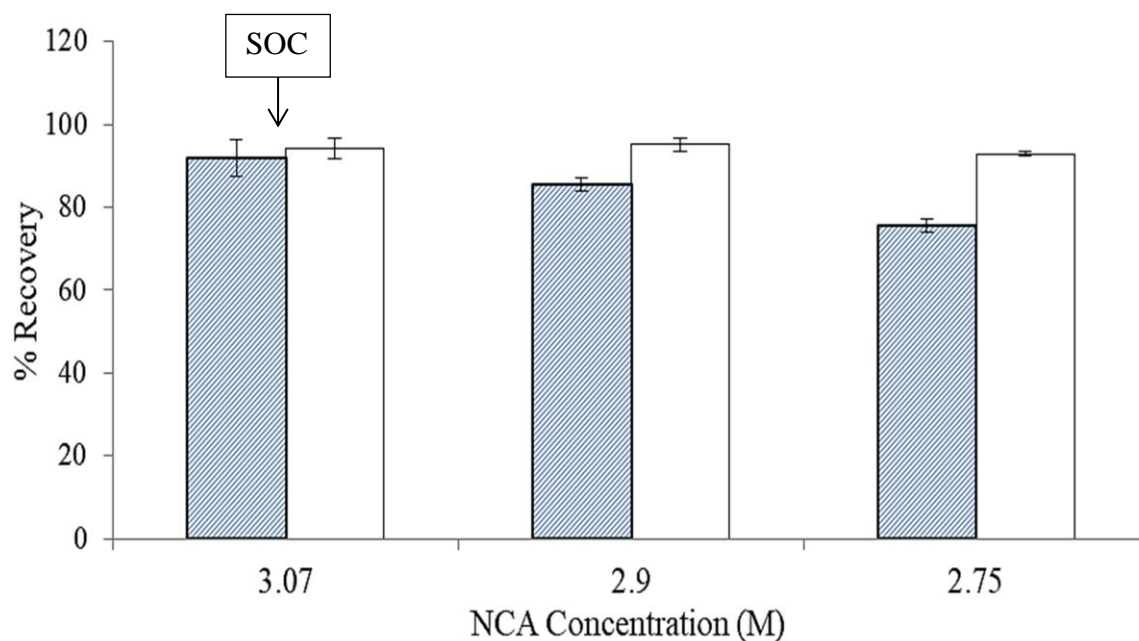


Figure 32. The % Recovery of MCAA calculated using external calibration (blue, striped bars) and single point internal standard calibration (white bars) at three different NCA concentration. The error bars shows the % RSD from three replicates. SOC represents the standard operating concentration of NCA.

Table 31. Summary of HAA-RR results using external and single point internal calibration at three different NCA concentrations.

NCA concentration (M)			3.07	2.9	2.75
MCAA	Ext.	Experimental (µg/L)	30.4 ± 1.3	28.2 ± 0.4	25 ± 0.4
		%Recovery	92 ± 4.4%	85.5 ± 1.5%	75.7 ± 1.6%
		% Change	0.0%	-7.2%	-17.8%
	SIS	Experimental (µg/L)	31.1 ± 0.8	31.4 ± 0.5	30.7 ± 0.2
		%Recovery	94.2 ± 2.6%	95.1 ± 1.5%	92.9 ± 0.6%
		% Change	0.0%	1.0%	-1.3%
MBAA	Ext.	Experimental (µg/L)	29.1 ± 5.0	28.2 ± 4.4	25.2 ± 3.0
		%Recovery	88.2 ± 17.2%	85.5 ± 15.7%	76.4 ± 12%
		% Change	0.0%	-3.1%	-13.4%
	SIS	Experimental (µg/L)	38.6 ± 5.7	40.9 ± 6.4	40.7 ± 4.1
		%Recovery	117.1 ± 14.6%	123.98 ± 15.7%	123.3 ± 10.0%
		% Change	0.0%	6.0%	5.4%
DCAA	Ext.	Experimental (µg/L)	30.1 ± 1.3	27.7 ± 2.6	24.4 ± 0.8
		%Recovery	91.2 ± 4.3%	83.9 ± 9.3%	74.1 ± 3.5%
		% Change	0.0%	-8.0%	-18.9%
	SIS	Experimental (µg/L)	27.2 ± 1.8	27.2 ± 2.5	26.6 ± 0.55
		%Recovery	82.5 ± 6.7%	82.38 ± 9%	80.7 ± 2.1%
		% Change	0.0%	0.0%	-2.2%

Table 31. Continued.

NCA concentration (M)			3.07	2.9	2.75
BCAA		Experimental (µg/L)	31.4 ± 0.5	28.7 ± 0.4	25.7 ± 0.4
	Ext.	%Recovery	95.2 ± 1.6%	86.9 ± 1.4%	77.9 ± 1.6%
		% Change	0.0%	-8.6%	-18.2%
		Experimental (µg/L)	31.1 ± 1.7	30.8 ± 0.6	30.6 ± 0.5
	SIS	%Recovery	94.1 ± 5.4%	93.26 ± 2.0%	92.7 ± 1.5%
		% Change	0.0%	-1.0%	-1.6%
DBAA		Experimental (µg/L)	32.6 ± 1.4	28.6 ± 0.9	26.8 ± 0.9
	Ext.	%Recovery	98.9 ± 4.2%	86.7 ± 3.1%	81.1 ± 3.5%
		% Change	0.0%	-12.3%	-17.8%
		Experimental (µg/L)	32.6 ± 2.3	31.2 ± 0.8	32.4 ± 1.0
	SIS	%Recovery	98.9 ± 7.2%	94.4 ± 2.7%	98.2 ± 3.1%
		% Change	0.0%	-4.3%	-0.6%
TCAA		Experimental (µg/L)	32.3 ± 0.6	28.6 ± 0.4	25.6 ± 0.8
	Ext.	%Recovery	97.8 ± 1.7%	86.5 ± 1.6%	77.7 ± 3.2%
		% Change	0.0%	-11.5%	-20.7%
		Experimental (µg/L)	30.6 ± 0.8	29.6 ± 0.4	29.6 ± 1.3
	SIS	%Recovery	92.6 ± 2.7%	89.6 ± 1.2%	89.7 ± 4.2%
		% Change	0.0%	-3.3%	-3.3%

Table 31. Continued.

NCA concentration (M)			3.07	2.9	2.75
BDCAA		Experimental (µg/L)	32.4 ± 0.6	29 ± 0.4	25.9 ± 0.1
	Ext.	%Recovery	98.3 ± 1.8%	87.9 ± 1.4%	78.3 ± 0.5%
		% Change	0.0%	-10.5%	-20.1%
		Experimental (µg/L)	32 ± 1.7	31.1 ± 0.7	30.7 ± 0.5
	SIS	%Recovery	96.9 ± 5.4%	94.2 ± 2.3%	93.1 ± 1.6%
		% Change	0.0%	-2.8%	-4.1%
DBCAA		Experimental (µg/L)	32.4 ± 1.0	29.7 ± 0.6	26.4 ± 0.5
	Ext.	%Recovery	98.3 ± 3.2%	89.9 ± 2.2%	80.1 ± 1.7%
		% Change	0.0%	-8.3%	-18.5%
		Experimental (µg/L)	31 ± 1.7	30.8 ± 0.8	30.4 ± 0.1
	SIS	%Recovery	94 ± 5.4%	93.3 ± 2.5%	92 ± 0.4%
		% Change	0.0%	-0.6%	-1.9%
TBAA		Experimental (µg/L)	31.8 ± 1.2	28.9 ± 0.8	26.5 ± 0.7
	Ext.	%Recovery	96.2 ± 3.9%	87.7 ± 2.6%	80.4 ± 2.6%
		% Change	0	-9.1%	-16.7%
		Experimental (µg/L)	30.1 ± 0.1	29.8 ± 0.9	30.3 ± 0.9
	SIS	%Recovery	91.3 ± 0.4%	90.4 ± 3%	91.9 ± 3.1%
		% Change	0.0%	-1.0%	0.7%

Overall, external calibration produces on an average of 17.38 $\mu\text{g/L}$ change in concentration per unit change in the NCA concentration with lowest being for MBAA (12.08 $\mu\text{g/L}$) and highest being for TCAA (20.81 $\mu\text{g/L}$). While the internal calibration produces a less than 1 $\mu\text{g/L}$ change in concentration per unit change in NCA concentration suggesting the robustness of the single point internal calibration.

KOH Reagent Robustness Study

The rate of formation of fluorescence products in the post column reaction also depends on KOH concentration. The HAA-RR system was calibrated using external calibration using the standard operating concentration of 2 M KOH. The percent recovery of HAA9 check standard was compared between external and internal calibration at four different KOH concentrations (2.1, 2.0, 1.9, 1.5 M). The Figure 33 shows the results of MCAA and the detailed results for all HAA9 species results are presented in Table 32. Unlike nicotinamide, the decreasing KOH concentration has smaller effects on the HAA response.

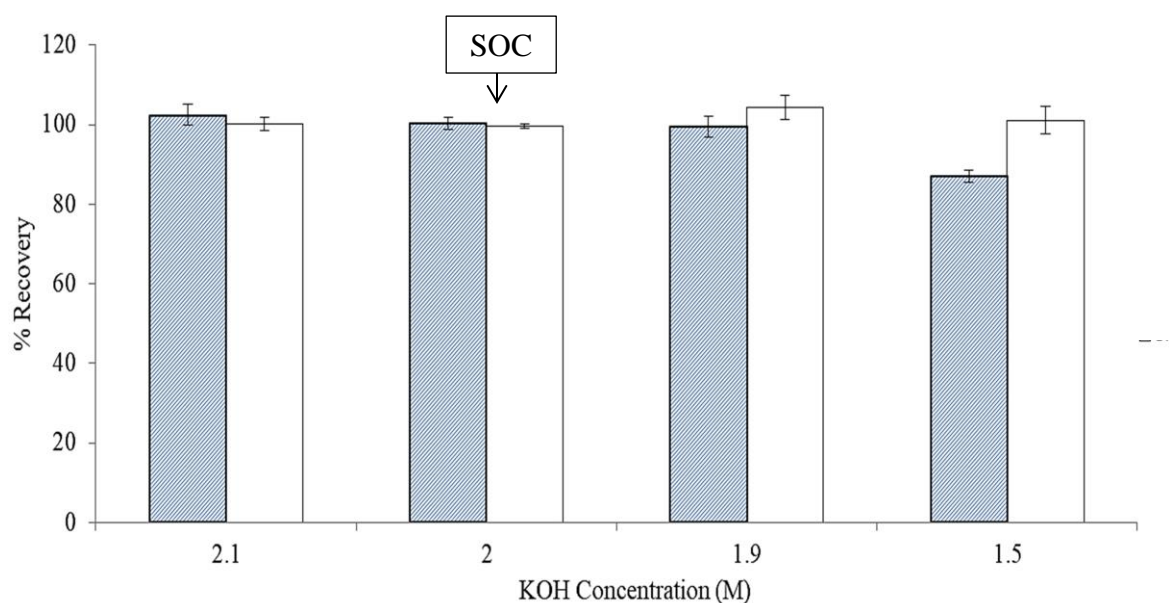


Figure 33. The % Recovery of MCAA was calculated using external calibration and single point internal standard calibration at four different KOH concentration. The striped bars represent concentration from external calibration and clear bars represent the concentration from single point internal standard calibration. The error bars shows the % RSD from three replicates. SOC represents standard operating concentration for KOH.

A \pm 5% change in the KOH concentration had no marked effect on the reported check standard concentration from both the calibration methods. Interestingly, even a 25 % (1.5 M) decrease in KOH concentration produced less than 2 $\mu\text{g/L}$ decrease in check standard concentration from external calibration for majority of HAA species.

While the internal calibration predicted 15 - 25 % higher concentration with 1.5 M KOH as opposed to compensating for the systematic changes in the instrument. Since internal calibration depends on the relative response between the analyte and internal standard, this indicates that a decreased in KOH concentration, and thus ionic strength, resulted in a fluorescence enhancement compared to standard operating conditions for either the HAA9 species or 2-BBA.

Table 32. Summary of HAA-RR results using external and single point internal calibration at four different KOH concentrations.

KOH concentration (M)			2.1	2	1.9	1.5
MCAA	Ext	Experimental (µg/L)	32.8 ± 0.9	33.1 ± 0.5	33.8 ± 0.9	28.7 ± 0.4
		%Recovery	99.4 ± 2.7%	100.2 ± 1.5%	102.4 ± 2.6%	87 ± 1.5%
		% Change	0.0%	-15.9%	-6.0%	2.0%
	SIS	Experimental (µg/L)	34.4 ± 1.1	32.9 ± 0.2	33.1 ± 0.6	33.3 ± 1.1
		%Recovery	104.3 ± 3.1%	99.6 ± 0.5%	100.2 ± 1.7%	101 ± 3.4%
		% Change	0.0%	10.7%	-4.8%	-2.0%
MBAA	Ext	Experimental (µg/L)	40.4 ± 4.7	36.9 ± 2.3	35.2 ± 1.9	31.7 ± 8.5
		%Recovery	122.4 ± 11.6%	111.7 ± 6.3%	106.6 ± 5.3%	96.2 ± 26.8%
		% Change	0.0%	-21.2%	-14.7%	-11.3%
	SIS	Experimental (µg/L)	44.09 ± 3.8	38.3 ± 2.0	36.05 ± 2.8	38.17 ± 9.0
		%Recovery	133.6 ± 8.7%	116 ± 5.2%	109.26 ± 7.7%	115.7 ± 23.5%
		% Change	0.0%	5.7%	-12.6%	-14.6%
DCAA	Ext	Experimental (µg/L)	33 ± 0.9	36.7 ± 2.0	31.8 ± 2.7	34.7 ± 1.9
		%Recovery	100 ± 2.8%	111.1 ± 5.5%	96.5 ± 8.5%	105.1 ± 5.4%
		% Change	0.0%	-8.4%	-1.6%	-4.9%
	SIS	Experimental (µg/L)	37.2 ± 1.7	39.2 ± 2.2	33.4 ± 2.8	43 ± 2.1
		%Recovery	112.8 ± 4.6%	118.7 ± 5.5%	101.34 ± 8.2%	130.2 ± 4.9%
		% Change	0.0%	22.4%	-0.3%	-8.3%

Table 32. Continued.

KOH concentration (M)		2.1	2.0	1.9	1.5	
BCAA	Ext	Experimental (µg/L)	33.8 ± 0.3	34.1 ± 0.5	34.5 ± 0.3	33.3 ± 0.2
		%Recovery	102.6 ± 0.9%	103.3 ± 1.5%	104.5 ± 1.0%	100.8 ± 0.7%
		% Change	0.0%	-15.9%	-6.0%	2.0%
	SIS	Experimental (µg/L)	35.5 ± 1.0	33.9 ± 1.0	33.7 ± 0.1	38.8 ± 1.0
		%Recovery	107.6 ± 2.8%	102.7 ± 2.8%	102.2 ± 0.3%	117.5 ± 2.4%
		% Change	0.0%	10.7%	-4.8%	-2.0%
DBAA	Ext	Experimental (µg/L)	35.3 ± 0.9	35.7 ± 1.1	36.9 ± 2.4	34.9 ± 1.7
		%Recovery	106.8 ± 2.6%	108.2 ± 3.0%	111.9 ± 6.6%	105.6 ± 5.0%
		% Change	0.0%	-4.5%	-1.0%	5.8%
	SIS	Experimental (µg/L)	37 ± 0.4	35.5 ± 1.4	36.1 ± 1.2	40.2 ± 1.8
		%Recovery	112.2 ± 1.0%	107.7 ± 3.9%	109.4 ± 3.4%	122 ± 4.6%
		% Change	0.0%	27.2%	0.0%	1.7%
TCAA	Ext	Experimental (µg/L)	36.2 ± 0.7	35.6 ± 1.2	35.6 ± 1.2	38 ± 0.4
		%Recovery	109.8 ± 2.0%	108 ± 3.3%	107.8 ± 3.3%	115.1 ± 1.0%
		% Change	0.0%	-3.6%	0.0%	1.9%
	SIS	Experimental (µg/L)	36 ± 0.6	33.5 ± 0.7	32.9 ± 1.0	41.4 ± 1.0
		%Recovery	109 ± 1.6%	101.6 ± 2.2%	99.8 ± 3.0%	125.4 ± 2.5%
		% Change	0.0%	17.1%	4.6%	-2.3%

Table 32. Continued.

KOH concentration (M)		2.1	2	1.9	1.5	
BDCAA	Ext	Experimental (µg/L)	35.9 ± 0.6	35.3 ± 0.6	35.2 ± 0.8	37.3 ± 0.2
		%Recovery	108.7 ± 1.7%	107 ± 1.6%	106.5 ± 2.3%	113.2 ± 0.7%
		% Change	0.0%	-7.2%	-1.6%	1.0%
	SIS	Experimental (µg/L)	36.4 ± 0.6	33.9 ± 0.6	33.2 ± 1.0	41.6 ± 0.5
		%Recovery	110.2 ± 1.8%	102.6 ± 1.8%	100.6 ± 3.1%	126.2 ± 1.2%
		% Change	0.0%	23.9%	-0.3%	-2.6%
DBCAA	Ext	Experimental (µg/L)	35.4 ± 0.1	36.1 ± 0.7	36.7 ± 0.4	35.7 ± 0.9
		%Recovery	107.2 ± 0.3%	109.2 ± 2.0%	111.1 ± 1.2%	108.3 ± 2.7%
		% Change	0.0%	-8.1%	0.6%	1.6%
	SIS	Experimental (µg/L)	35.3 ± 1.1	34.1 ± 1.2	34.1 ± 1.0	39.2 ± 0.8
		%Recovery	107.1 ± 3.2%	103.3 ± 3.5%	103.4 ± 2.9%	118.9 ± 1.9%
		% Change	0.0%	22.1%	2.0%	-2.2%
TBAA	Ext	Experimental (µg/L)	34.7 ± 1.6	35.2 ± 1.1	37.5 ± 0.4	34.3 ± 1.0
		%Recovery	105.1 ± 4.8%	106.6 ± 3.1%	113.8 ± 1.0%	104.1 ± 3.0%
		% Change	0.0%	-12.9%	-5.0%	-1.6%
	SIS	Experimental (µg/L)	34.1 ± 2.8	32.7 ± 1.6	34.4 ± 0.9	37.1 ± 0.7
		%Recovery	103.4 ± 8.1%	99.2 ± 4.9%	104.2 ± 2.6%	112.3 ± 1.9%
		% Change	0.0%	15.3%	-4.0%	-5.4%

Post Column Reagent Mixture Flow Rate

The flow rate of the post-column reagent mixture has two effects on the analytical signal of the HAA9 species. The first is an expected direct change of the analytical signal (increase or decrease) due a change in the reagent flow rates (increase or decrease). The second is a shift in the retention time of the HAA9 and 2-BBA species due to the change in reagent flow rate. An increase in flow rate will shorten the elution times from the reaction system and a decrease in flow rate will lengthen the elution times. The results on the effect of the reagent flow rate are presented here.

Effect of Flow Rate on Analytical Signal

The HAA-RR system was calibrated using external calibration and response factors for internal calibration were calculated at 0.4 mL/min. The percent recovery of HAA9 check standard was compared between external and internal calibration at four different flow rates (0.40, 0.42, 0.38, and 0.30 mL/min). Figure 34 shows the results for MCAA and representative of all the HAA species. As the flow rate changes, the recoveries of check standard calculated from external calibration changes. Overall, with $\pm 5\%$ change (0.42 and 0.38 mL/min) the external calibration resulted in concentration changes of less than 2 $\mu\text{g/L}$ for all HAA species and concentrations from internal standard remained same.

At 0.3 mL/min flow rate, check standard recoveries decreased markedly with external calibration ranging from 3.6% for TCAA to 21.2% for MBAA. The opposite proved true for internal standardization at 0.3 mL/min. The recoveries for check standard increased, ranging from 5.9% for MBAA to 27.2% for DBAA with internal calibration. In similar results as the NCA concentration study, this reagent flow rate study shows that internal standard calibration corrects only for small changes in the reagent mixture flow rate and not been able compensate for large changes in the flow rate. The results of reagent flow rate study have been detailed for all HAA9 species in Table 33.

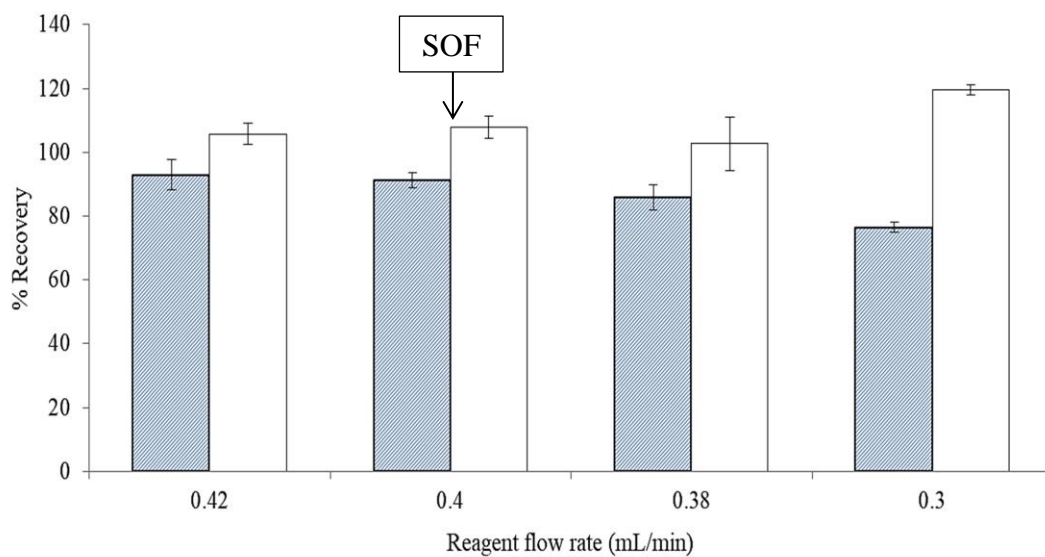


Figure 34. The % Recovery of MCAA calculated using external calibration and single point internal standard calibration at four different reagent mixture flow rate. The HAA-RR was calibrated by External calibration at 0.4 mL/min. The striped bars represent concentration from external calibration and clear bars represent the concentration from single point internal standard calibration. The error bars shows the % RSD from three replicates. SOF represents standard operation flow rate.

Table 33. Summary of HAA-RR results from external and internal calibration at four different reagent flow rates.

Reagent flow rate (mL/min)		0.42	0.40	0.38	0.30	
MCAA	Ext	Experimental (µg/L)	30.7 ± 1.5	30.1 ± 0.7	28.3 ± 1.1	25.3 ± 0.4
		%Recovery	93 ± 4.8%	91.3 ± 2.4%	85.9 ± 3.9%	76.5 ± 1.7%
		% Change	2.0%	0.0%	-6.0%	-15.9%
	SIS	Experimental (µg/L)	34.9 ± 1.1	35.6 ± 1.2	33.9 ± 2.8	39.4 ± 0.6
		%Recovery	105.7 ± 3.2%	107.8 ± 3.5%	102.6 ± 8.3%	119.5 ± 1.6%
		% Change	-2.0%	0.0%	-4.8%	10.7%
MBAA	Ext	Experimental (µg/L)	25.9 ± 4.0	29.2 ± 5.9	24.9 ± 7.0	23 ± 1.8
		%Recovery	78.3 ± 15.3%	88.6 ± 20.3%	75.5 ± 28.0%	69.8 ± 7.7%
		% Change	-11.3%	0.0%	-14.7%	-21.2%
	SIS	Experimental (µg/L)	36.8 ± 5.2	43.0 ± 8.8	37.7 ± 11.6	45.5 ± 3.0
		%Recovery	111.4 ± 14.2%	130.4 ± 20.4%	114.1 ± 30.9%	138.0 ± 6.7%
		% Change	-14.6%	0.0%	-12.6%	5.7%
DCAA	Ext	Experimental (µg/L)	29.4 ± 1.1	30.9 ± 2.5	30.4 ± 1.0	28.3 ± 3.1
		%Recovery	89.2 ± 3.6%	93.6 ± 8%	92.2 ± 3.4%	85.9 ± 10.9%
		% Change	-4.9%	0.0%	-1.6%	-8.4%
	SIS	Experimental (µg/L)	36.5 ± 0.8	39.8 ± 3.6	39.7 ± 2.3	48.7 ± 6.7
		%Recovery	110.5 ± 2.3%	120.6 ± 9.1%	120.2 ± 5.8%	147.5 ± 13.8%
		% Change	-8.3%	0.0%	-0.3%	22.4%

Table 33. Continued.

Reagent flow rate (mL/min)		0.42	0.40	0.38	0.30	
BCAA	Ext	Experimental (µg/L)	30.7 ± 1.5	30.1 ± 0.7	28.3 ± 1.1	25.3 ± 0.4
		%Recovery	93 ± 4.8%	91.3 ± 2.4%	85.9 ± 3.9%	76.5 ± 1.7%
		% Change	2.0%	0.0%	-6.0%	-15.9%
	SIS	Experimental (µg/L)	34.9 ± 1.1	35.6 ± 1.2	33.9 ± 2.8	39.4 ± 0.6
		%Recovery	105.7 ± 3.2%	107.8 ± 3.5%	102.64 ± 8.3%	119.5 ± 1.6%
		% Change	-2.0%	0.0%	-4.8%	10.7%
DBAA	Ext	Experimental (µg/L)	30.8 ± 0.3	29.1 ± 1.8	28.8 ± 1.2	27.8 ± 1.0
		%Recovery	93.4 ± 0.9%	88.2 ± 6.2%	87.1 ± 4.2%	84.3 ± 3.5%
		% Change	5.8%	0.0%	-1.0%	-4.5%
	SIS	Experimental (µg/L)	35.1 ± 0.6	34.5 ± 1.9	34.5 ± 2.9	43.9 ± 0.8
		%Recovery	106.4 ± 1.8%	104.4 ± 5.4%	104.6 ± 8.5%	132.9 ± 1.9%
		% Change	1.7%	0.0%	0.0%	27.2%
TCAA	Ext	Experimental (µg/L)	31.5 ± 1.0	30.9 ± 1.9	30.9 ± 1.8	29.8 ± 1.5
		%Recovery	95.3 ± 3.1%	93.6 ± 6.1%	93.7 ± 5.7%	90.3 ± 5.2%
		% Change	1.9%	0.0%	0.0%	-3.6%
	SIS	Experimental (µg/L)	34.2 ± 1.4	35 ± 2.2	36.6 ± 1.0	41 ± 5.4
		%Recovery	103.6 ± 4.1%	106.1 ± 6.2%	111 ± 2.8%	124.3 ± 13.2%
		% Change	-2.3%	0.0%	4.6%	17.1%

Table 33. Continued.

Reagent flow rate (mL/min)		0.42	0.40	0.38	0.3	
BDCAA	Ext	Experimental (µg/L)	31 ± 0.6	30.7 ± 0.9	30.2 ± 0.6	28.5 ± 0.4
		%Recovery	93.9 ± 2.0%	92.9 ± 3.0%	91.4 ± 1.9%	86.4 ± 1.4%
		% Change	1.0%	0.0%	-1.6%	-7.2%
	SIS	Experimental (µg/L)	34.3 ± 0.4	35.2 ± 0.4	35.1 ± 1.8	43.6 ± 1.6
		%Recovery	103.9 ± 1.2%	106.7 ± 1.2%	106.3 ± 5.2%	132.1 ± 3.7%
		% Change	-2.6%	0.0%	-0.3%	23.9%
DBCAA	Ext	Experimental (µg/L)	31.4 ± 1.2	30.9 ± 0.6	31.1 ± 0.6	28.4 ± 0.6
		%Recovery	95.1 ± 4.0%	93.6 ± 2.0%	94.3 ± 1.9%	86.1 ± 2.2%
		% Change	1.6%	0.0%	0.6%	-8.1%
	SIS	Experimental (µg/L)	35 ± 0.8	35.8 ± 1.4	36.5 ± 1.5	43.7 ± 2.2
		%Recovery	106 ± 2.4%	108.4 ± 3.8%	110.6 ± 4.2%	132.6 ± 5.0%
		% Change	-2.2%	0.0%	2.0%	22.1%
TBAA	Ext	Experimental (µg/L)	31.4 ± 1.4	31.9 ± 1.9	30.3 ± 1.3	27.8 ± 1.3
		%Recovery	95.2 ± 4.5%	96.7 ± 6.1%	91.9 ± 4.4%	84.3 ± 4.8%
		% Change	-1.6%	0.0%	-5.0%	-12.9%
	SIS	Experimental (µg/L)	33.3 ± 1.6	35.2 ± 3.0	33.8 ± 2.3	40.6 ± 2.3
		%Recovery	100.9 ± 4.8%	106.6 ± 8.4%	102.4 ± 7.1%	123.2 ± 5.7%
		% Change	-5.4%	0.0%	-4.0%	15.3%

Effect of Reagent Flow Rate on Retention Times

The absolute retention times of the compounds are primarily affected by a number of parameters such as the flow rate of ion chromatography eluent, reagent mixture flow rate, concentrations of common anions in the matrix, and column age. Retention shifts are often undesirable making identification of the desired compound more difficult particularly in case of samples with closely eluting matrix components or matrix components that affects the retention times of analyte. With the use of internal standardization, the relative retention time (RRT) can be used to correct for retention shifts and reduce the errors in identification of a compound. RRT is the ratio of retention time of a compound (RT_x) to retention time of a reference (RT_s) as in Equation (32).

$$RRT = \frac{RT_x}{RT_s} \quad (32)$$

In this work, the internal standard peak is used as a reference to correct for the systematic retention shifts. The relative retention time calculations for this analysis were used from the changes in retention times determined in the reagent mixture flow rate study. Table 34 shows the retention times and relative retention times of the HAA9 species. The retention times of the HAA9 species increase as the flow rate of reagent mix decreases. However, the relative retention times remain markedly constant which aids in HAA9 identification, particularly the monohalogenated and dihalogenated species.

Table 34. Summary of retention and relative retention times of HAA9 with changing reagent flow rates.

Flow rate (mL/min)		0.42	0.4	0.38	0.3
MCAA	RT (mins)	33.45	33.71	33.95	34.74
	RRT	0.91	0.91	0.91	0.91
MBAA	RT (mins)	34.45	34.72	34.94	35.73
	RRT	0.93	0.93	0.93	0.93
DCAA	RT (mins)	40.07	40.39	40.58	41.33
	RRT	1.08	1.08	1.09	1.08
BCAA	RT (mins)	42.50	42.81	43.00	43.73
	RRT	1.15	1.15	1.15	1.14
DBAA	RT (mins)	45.87	46.14	46.34	47.11
	RRT	1.24	1.24	1.24	1.23
TCAA	RT (mins)	55.62	55.83	56.03	56.91
	RRT	1.50	1.50	1.51	1.49
BDCAA	RT (mins)	58.48	58.71	58.90	59.76
	RRT	1.58	1.57	1.58	1.56
DBCAA	RT (mins)	62.83	63.05	63.24	64.10
	RRT	1.69	1.69	1.70	1.68
TBAA	RT (mins)	69.46	69.66	69.90	70.67
	RRT	1.87	1.87	1.88	1.85

Single Point Internal Standard Calibration Performance at Different Concentrations of HAA9

The relative response factor between the HAA9 species and internal standard was examined at concentrations that are expected to be observed at a typical drinking water plant. Several different concentrations of HAA9 standards were analyzed using HAA-RR. Each concentration level was analyzed four times and then the experimental recoveries of HAA

species from a four-point external calibration and single point internal calibration were compared. Table 35 shows the recoveries of individual HAA species at different concentrations calculated using both external and internal standard calibration. MBAA and DCAA have the highest recoveries (> 130%) with internal standard calibration at concentrations below 20 µg/L which is at or below the MDL for the HAA-RR. External calibration performed better than internal calibration at lower concentrations for MBAA and

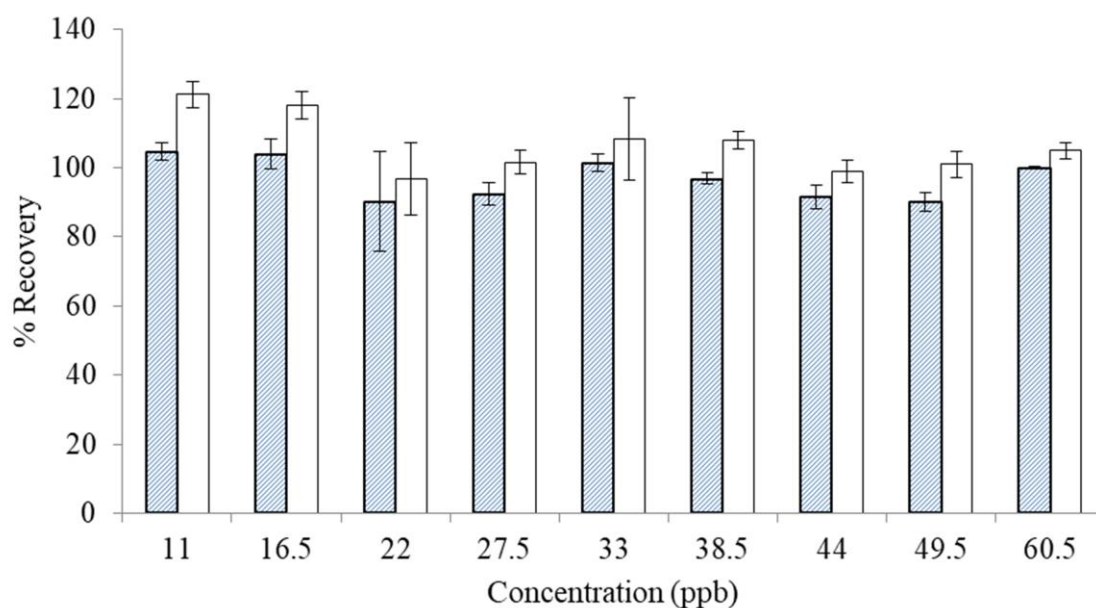


Figure 35. Bar graph shows the % Recoveries of MCAA at various concentrations. The striped Bars shows the concentration from external and clear bars shows concentrations from internal standard calculations. The concentrations were calculated using peak heights and error bars shows the % RSD from quadruplicate analyses.

DCAA. Overall, the internal standard calibration always predicted higher numbers than the external calibration. Figure 35 shows the percent recoveries of MCAA from both external and internal calibration at various concentrations ranging from 11 µg/L to 60.5 µg/L. All the other HAA species follow similar trend as that of MCAA, as the concentration of the check standard was further from the MDL, the percent recovery of the check standard trended towards 100%.

Table 35. The % Recoveries calculated for individual HAA species using single point internal standard (SIS) and External calibration (Ext.).

Concentration ($\mu\text{g/L}$)		11	16.5	22	27.5	33	38.5	44	49.5	60.5
MCAA	Ext.	105 ± 3	104 ± 4	90 ± 14	92 ± 3	101 ± 3	97 ± 2	92 ± 4	90 ± 3	100 ± 0.3
	SIS	121 ± 4	118 ± 4	97 ± 11	102 ± 3	108 ± 12	108 ± 3	99 ± 3	101 ± 4	105 ± 2
MBAA	Ext.	92 ± 22	84 ± 11	86 ± 31	92 ± 12	96 ± 6	90 ± 6	81 ± 12	79 ± 16	99 ± 6
	SIS	134 ± 14	113 ± 8	106 ± 29	110 ± 12	111 ± 6	105 ± 12	92 ± 7	94 ± 14	105 ± 5
DCAA	Ext.	135 ± 15	117 ± 17	123 ± 24	100 ± 17	116 ± 4	99 ± 7	91 ± 5	98 ± 2	100 ± 4
	SIS	170 ± 12	142 ± 14	139 ± 19	114 ± 15	129 ± 9	115 ± 8	100 ± 2	113 ± 5	104 ± 3
BCAA	Ext.	95 ± 1	94 ± 2	99 ± 5	88 ± 2	98 ± 1	94 ± 2	87 ± 2	93 ± 1	99 ± 1
	SIS	126 ± 3	119 ± 2	108 ± 4	105 ± 3	106 ± 10	105 ± 3	101 ± 3	104 ± 4	110 ± 2
DBAA	Ext.	94 ± 10	93 ± 7	102 ± 7	86 ± 5	99 ± 2	92 ± 6	86 ± 7	92 ± 2	96 ± 1
	SIS	128 ± 7	118 ± 5	115 ± 5	101 ± 4	108 ± 11	103 ± 6	95 ± 5	103 ± 5	102 ± 1
BDCAA	Ext.	79 ± 6	83 ± 2	91 ± 6	84 ± 2	98 ± 3	93 ± 2	84 ± 1	91 ± 1	101 ± 1
	SIS	129 ± 4	120 ± 1	107 ± 5	109 ± 2	108 ± 8	107 ± 1	102 ± 3	104 ± 4	116 ± 2
DBCAA	Ext.	71 ± 6	83 ± 4	94 ± 13	83 ± 4	98 ± 4	96 ± 4	89 ± 1	92 ± 3	103 ± 1
	SIS	121 ± 5	120 ± 3	111 ± 13	106 ± 4	109 ± 14	110 ± 2	105 ± 4	104 ± 3	115 ± 3
TBAA	Ext.	90 ± 12	95 ± 10	95 ± 16	87 ± 5	99 ± 5	93 ± 8	89 ± 3	88 ± 4	98 ± 3
	SIS	131 ± 10	126 ± 8	108 ± 12	106 ± 3	108 ± 11	105 ± 7	102 ± 5	99 ± 3	107 ± 4

Spiked Recovery Studies in Memphis Tap Water

A final evaluation with check standards was conducted in a real-world drinking water matrix. Typically, the tap water in the City of Memphis has very low HAA9 concentrations because the aquifer used as the source has low TOC concentrations. In this study, tap water was spiked with HAA9 standard to evaluate the performance of internal standard calibration in real water samples. The spike recovery for individual HAA species was calculated as shown in Equation (33).

$$\text{Spiked recovery} = \frac{C_t - C_u}{C_s} \times 100 \quad (33)$$

Where C_t is the experimental concentration of a HAA in spiked sample and C_u is the concentration of a HAA in unspiked sample. C_s is the nominal spiked concentration.

The Memphis tap water sample without spiking was analyzed to determine the C_u of each HAA. Then HAA9 standard was spiked with at a low-level of 11 $\mu\text{g/L}$ and a mid-level of 33 $\mu\text{g/L}$ HAA9 standard and each spiked sample has been analyzed several times. The spiked recoveries of 33 $\mu\text{g/L}$ spike sample from external calibration ranges from 84 (DBAA) to 96% (MBAA) and for internal calibration ranges from 102 (TBAA) to 119% (MBAA). The spiked recoveries of 11 $\mu\text{g/L}$ using internal calibration ranges from 131 (MCAA) to 174% (DCAA) and external calibration ranges from 71 (BDCAA) to 130% (DCAA) as shown with the detailed results presented in Table 36.

Table 36. Spiked recoveries from external and single point internal calibration in Memphis tap water.

HAA	Concentration ($\mu\text{g/L}$)	11	33
MCAA	Ext	99 ± 5	90 ± 3
	SIS	131 ± 5	105 ± 3
MBAA	Ext	103 ± 15	96 ± 11
	SIS	162 ± 10	119 ± 8
DCAA	Ext	130 ± 23	85 ± 35
	SIS	174 ± 17	103 ± 31
BCAA	Ext	97 ± 5	89 ± 2
	SIS	145 ± 6	108 ± 3
DBAA	Ext	95 ± 11	84 ± 3
	SIS	149 ± 9	110 ± 4
BDCAA	Ext	71 ± 7	85 ± 4
	SIS	131 ± 5	112 ± 3
DBCAA	Ext	76 ± 8	86 ± 3
	SIS	145 ± 7	109 ± 4
TBAA	Ext	79 ± 20	85 ± 7
	SIS	138 ± 15	102 ± 6

Comparison of MDL, Accuracy and Precision from current research to previous research

The MDL, Accuracy and Precision results from the present work were compared to previously published research in 2011 and 2019. The PCR-IC 2011 method used a syringe pump for addition of internal standard whereas current work used a ten-port injection valve for on-line internal standard addition. The HAA-RR system uses LED Fluorescence detector and PCR-IC method used commercially available Xenon arc lamp Fluorescence detector.

Table 37 presents the detailed comparison of results between three methods. The USEPA MDLs for all HAA9 species in the current work were below 5 µg/L except DCAA (8.0 µg/L) and MBAA (19.8 µg/L). When compared to previous work, the MDLs for all HAA9 species from the current method were similar to previous results except for MBAA. The PCR-IC method has almost six-fold lower MDL values for MBAA when compared to 2019 HAA-RR method and current method. The accuracy, estimated as mean % recovery, from current work for all HAA9 species ranges from 90.5 to 119 % with highest being MCAA and lowest being DBAA. The 2019 work has accuracies ranged from 74 % (DCAA) to 119 % (MCAA). The 2011 published work reported the accuracies ranging from 80 % to 112 % with the lowest being TCAA and the highest being DBAA. Overall, the accuracies for all HAA9 species were comparable between the three methods. The precision for all HAA9 species from present work were below 10 % with an exception of MBAA (35.4%), DCAA (14.9%) and DBAA (11.6%) which also exhibited the highest MDL values.

The precision values reported in 2019 were comparable to present work except for MBAA where %RSD increased by 39% for the current method. The precisions reported in 2011 were higher compared to current results for all HAA9 species except for MBAA and DBAA. The principal reason for higher %RSDs in 2011 results could be due to the internal standard addition via a syringe pump. The concentrations of HAA standard and internal standard injected on to the column were greatly affected by the incoming flow rates which leads to a source of variability in the results. When the three approaches are compared for on-line internal standardization, 2011 approach, 2019 approach, and the current approach, the use of a second injection loop on a 10-port injection valve provides a more reproducible method. The current approach does not involve manual addition of internal standard like the 2019 approach (leading to high %RSD) nor does it require dilution of the sample as in the 2011 approach.

Table 37. Detailed comparison of USEPA MDL, Accuracy and Precision from present work to previous work from 2011⁹⁸ and 2019¹⁰. PCR-IC 2011 work uses syringe pump for on-line internal standard addition whereas in present work a ten port two position injection valve was used for on-line internal standard addition.

	USEPA MDL (µg/L)			Accuracy (mean % Recovery)			Precision (% RSD)		
	PCR-IC 2011	HAA-RR 2019	HAA-RR-IS 2020	PCR-IC 2011	HAA-RR 2019	HAA-RR-IS 2020	PCR-IC 2011	HAA-RR 2019	HAA-RR-IS 2020
MCAA	2.7	4.5	2.9	102	101	97.7	11.3	7.7	6.2
MBAA	3.1	17.5	19.8	92.2	119	119	14.8	25.4	35.4
DCAA	7.8	7.2	8.0	98.1	74	103	34.6	16.8	14.9
BCAA	2.5	2.6	1.8	95.7	96	93	11.2	4.6	4.1
DBAA	1.8	3.1	5.0	112	95	90.5	7.0	5.7	11.6
TCAA	3.9	5.0	2.6	79.6	104	92.2	21.1	8.3	6.1
BDCAA	3.2	2.9	1.2	88.8	104	93.5	15.8	4.7	2.7
DBCAA	3.1	2.8	3.2	95.4	89	92.4	14.3	5.4	7.5
TBAA	3.3	4.2	4.2	83.3	94	93.2	17.5	7.7	9.7

Conclusions

The on-line, single-point internal standard method has been developed successfully using a ten-port two position injection valve. This method allows the water treatment plant operators to run the HAA-RR three to four times a day with continuous calibration on each analysis. The MDLs, accuracy and precision values are comparable to those of previous reports. A detailed robustness for both external calibration and single point internal calibration of the parameters that would have the most impact on analytical signal was presented for the first time. The internal calibration has been proved to be effective in correcting for fluctuations in HAA-RR response with fluctuations in LED intensity of fluorescence detector and nicotinamide concentrations. The minor fluctuations in reagent flow and KOH concentrations have been effectively compensated however internal calibration has not been able compensate for major changes in reagent flow and KOH concentrations. The relative retention times calculated with reference to internal standard remained constant which assists in identifying the compounds as result of retention shifts due to column aging and reagent flow rate.

CHAPTER 5

CONCLUSIONS AND RECOMMENDATIONS FOR FUTURE RESEARCH

The main goal of this research was development of low-cost analytical instrumentation such as the EZ-AutoPipet and EZ-AutoTitrator using Raspberry Pi, off the shelf sensors, and 3D printing technology. The other objective of this research was to develop on-line addition of internal standard for single point internal calibration method for haloacetic acid rapid response (HAA-RR) system and evaluate the robustness of the system.

Microliter Volume Liquid Delivery System - EZ-AutoPipet

A low-cost liquid delivery system (EZ-AutoPipet) was successfully developed under \$1000. The single channel system, dual channel system, and thermoelectric cooled system variants of EZ-AutoPipet has been developed. This thermoelectric cooled system will be helpful in remote places where a refrigerator is not accessible to store the solutions or reagents containing thermolabile compounds. The EZ-AutoPipet has been rigorously tested to



Figure 36. The Picture of EZ-AutoPipet.

evaluate the accuracy and precision of liquid delivery at various volumes. Various validation studies proved accuracy and precision of liquid delivery. The EZ-AutoPipet produced excellent accuracy and precision of liquid delivery regardless of analyst experience. The

lower limits of liquid delivery for 5 mL, 1 mL, and 0.1 mL syringes were 0.1 mL, 0.05 mL and 0.002 mL respectively. The EZ-AutoPipet has shown great potential to be used as digital buret. Finally, the EZ-AutoPipet has been adapted to develop the EZ-AutoTitration system.

Future Work

The delivery rate for the current system is relatively slow and large volume deliveries take additional time. There are two ways to improve the speed of liquid delivery: one by replacing current stepper driver with more efficient one such as TIC stepper drivers from Pololu. The second route is to optimize the stepper motor operational voltage, current, thread pitch of lead screw, gear ratio and acceleration profile to have maximum rotations per minute (RPM). Some work needs to be done to reduce the overall size and make it aesthetically appealing. The system could be adapted to perform simultaneous multiple deliveries of a liquid into well plates for immunoassays. Furthermore, dual channel system can be improved to make the solvent and solute delivery simultaneously to make the solutions. The developed syringe pump technology can be applied to deliver reagents in various future systems such as *TotalTHM-NOW*, LEAD-RR etc.

The Automated Titration System – EZ-AutoTitrator

The EZ-AutoTitrator has been successfully developed to perform potentiometric, spectrochemical titrations and monitoring of pH and temperature. This semi-automated system was developed using a Raspberry Pi and commercial-off-the-shelf components. The build cost was under \$1000 for a dual channel system. The total alkalinity and total hardness methods have been rigorously tested in the lab as well as at two different water treatment plants. A machine learning protocol for color change prediction has been developed which can be modified effortlessly to develop new spectrochemical titration methods.



Figure 37. The Picture of EZ-AutoTitrator.

Future Work

The speed of titrations can be improved by increasing the delivery rate. The suggestions mentioned in future work section for EZ-AutoPipet apply here as well. The titrant concentration and sample volume need to be optimized to improve accuracy of alkalinity and hardness titrations for concentrations below 10 mg/L CaCO_3 . The preliminary free available chlorine titration results in bleach are promising and this needs to be tested rigorously just as the alkalinity and hardness methods. The FAC method could be optimized further to perform lower concentration analysis of FAC in bleach and water. The current system is only able to detect a single endpoint in full pH scale titration. When multiple endpoints exist in a titration curve, EZ-AutoTitrator recognizes only the endpoint with highest slope value. This problem can be addressed by assigning threshold slope values for automatic detection or an adjustable line can be programmed so that user can move the adjustable line to different points on the derivative curve to identify the endpoints. The spectrochemical detector has a much broader potential to perform many of the titrations in Standard Methods for Water and Wastewater. One example is turbidimetric titrations for the determination of sulphate concentration by titrating with a barium chloride solution.

Currently, spectrochemical cell design only allows a maximum of 25 mL of sample for spectrochemical titration. The spectrochemical cell design should be modified such that variable sample volumes can be titrated. Overall, the current design needs to be modified in a way that it is more aesthetically appealing to bring commercial viability.

On-line Single Point Internal Calibration – HAA-RR

The issues related to external calibration has been addressed by single point internal calibration through this work. A ten-port injection valve has been used to inject the internal standard and haloacetic acids (HAA) sequentially. This configuration allowed on-line, continuous calibration of the HAA-RR system. This work has led to a complete automation of the HAA-RR system and eliminated the errors associated with the manual preparation of sample with the internal standard. Robustness studies showed that changes in the instrument response has been compensated due to changes in the system parameters such as LED intensity, reagent concentrations and flow rates. The present version of HAA-RR can analyze four samples a day up to a week without any human involvement.

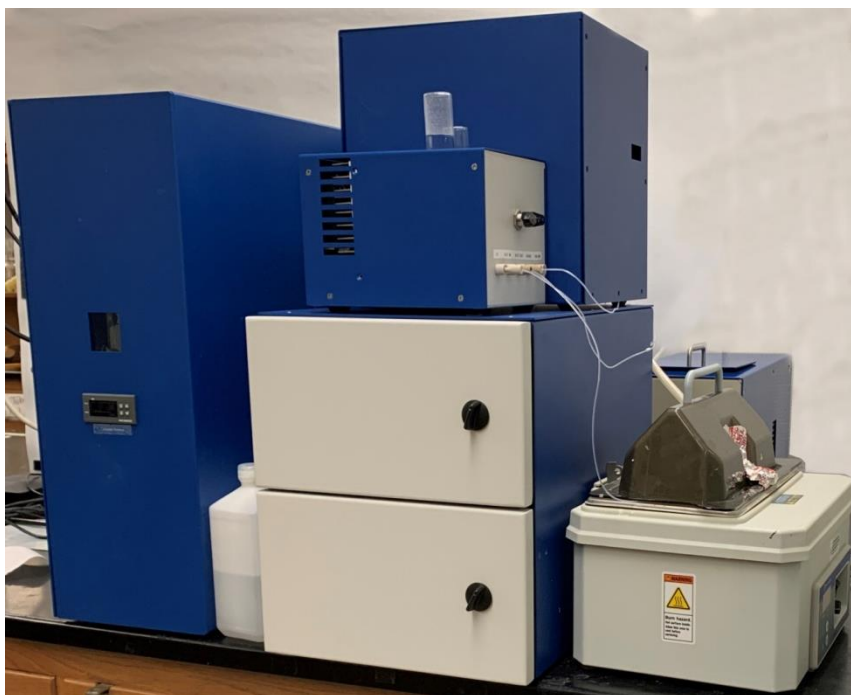


Figure 38. The Picture of HAA-RR system.

Future Work

The HAA-RR system with the current setup has been tested rigorously in the laboratory using standard solutions but not in real world setup. The system should be tested at a water treatment plant to evaluate the performance in real world conditions and also this gives a chance to resolve any issues encountered. All the testing was performed using a single instrument. So, two or more HAA-RR systems should be modified to perform single point internal calibration method and tested to increase the confidence in the method.

The on-line continuous single point internal calibration can be applied to several other techniques. For example, the capillary membrane sampling flow injection analyzer (CMS-FIA) for simultaneous analysis of THM and HAAs in drinking water would benefit from this method⁵⁸. The CMS-FIA analyzer uses the same nicotinamide reaction chemistry and fluorescence detection for Total THMs and Total HAAs analysis. Commercialization of the CMS-FIA as the *TotalTHM-NOW* is currently on-going and funded by a National Institute of Environmental Health Sciences Small Business Innovation Research Phase I grant (award ID: R43ES031465-01).

References

- (1) Gordon E. Moore. *Progress In Digital Integrated Electronics*; 1975.
- (2) Moore, G. E. *Cramming More Components onto Integrated Circuits*; 1965; Vol. 38.
<https://doi.org/10.1109/JPROC.1998.658762>.
- (3) J.J. Abrams. *Star Trek (2009)* ; 2009.
- (4) Raspberry Pi sold over 12.5 million boards in five years - The Verge
<https://www.theverge.com/circuitbreaker/2017/3/17/14962170/raspberry-pi-sales-12-5-million-five-years-beats-commodore-64> (accessed Mar 25, 2020).
- (5) Raspberry Pi becomes best selling British computer | Technology | The Guardian
<https://www.theguardian.com/technology/2015/feb/18/raspberry-pi-becomes-best-selling-british-computer> (accessed Mar 25, 2020).
- (6) Bougot-Robin, K.; Paget, J.; Atkins, S. C.; Edel, J. B. Optimization and Design of an Absorbance Spectrometer Controlled Using a Raspberry Pi to Improve Analytical Skills. *J. Chem. Educ.* **2016**, 93 (7), 1232–1240.
<https://doi.org/10.1021/acs.jchemed.5b01006>.
- (7) Foster, S. W.; Alirangues, M. J.; Naese, J. A.; Constans, E.; Grinias, J. P. A Low-Cost, Open-Source Digital Stripchart Recorder for Chromatographic Detectors Using a Raspberry Pi. *J. Chromatogr. A* **2019**, 1603, 396–400.
<https://doi.org/10.1016/j.chroma.2019.03.070>.
- (8) Boehle, K. E.; Doan, E.; Henry, S.; Beveridge, J. R.; Pallickara, S. L.; Henry, C. S. Single Board Computing System for Automated Colorimetric Analysis on Low-Cost Analytical Devices. *Anal. Methods* **2018**, 10 (44), 5282–5290.
<https://doi.org/10.1039/c8ay01874j>.
- (9) Vijayakumar, N.; Ramya, R. The Real Time Monitoring of Water Quality in IoT Environment. In *ICIIECS 2015 - 2015 IEEE International Conference on Innovations in Information, Embedded and Communication Systems*; Institute of Electrical and Electronics Engineers Inc., 2015. <https://doi.org/10.1109/ICIIECS.2015.7193080>.
- (10) Snow, R. *DEVELOPMENT AND APPLICATION OF 3D PRINTED DETECTORS FOR ENVIRONMENTAL ANALYSIS*; 2019.
- (11) Srinath, K. R. Python-The Fastest Growing Programming Language. *Int. Res. J. Eng. Technol.* **2017**.
- (12) Dietterich, T.; Bishop, C.; Heckerman, D.; Jordan, M.; Kearns, M. *Introduction to Machine Learning Second Edition Adaptive Computation and Machine Learning*.
- (13) How Netflix's Recommendations System Works
<https://help.netflix.com/en/node/100639> (accessed Mar 26, 2020).
- (14) Alsmadi, I.; Alhami, I. Clustering and Classification of Email Contents. *J. King Saud Univ. - Comput. Inf. Sci.* **2015**, 27 (1), 46–57.

<https://doi.org/10.1016/j.jksuci.2014.03.014>.

- (15) Garreta, R.; Moncecchi, G. *Learning Scikit-Learn: Machine Learning in Python*; Packt Publishing Ltd: Birmingham, 2013.
- (16) Shai Shalev-Shwartz; Shai Ben-David. *Understanding Machine Learning: From Theory to Algorithms*; Cambridge Press: Newyork, 2014.
- (17) Brunner, T. R.; Wilkins, C. L.; Williams, R. C.; McCombie, P. J. Pattern Recognition Analysis of Carbon-13 Free Induction Decay Data. *Anal. Chem.* **1975**, *47* (4), 662–665. <https://doi.org/10.1021/ac60354a030>.
- (18) Zupan, J. Combined Retrieval System for Infrared, Mass, and Carbon-13 Nuclear Magnetic Resonance Spectra. *Anal. Chem.* **1977**, *49* (14), 2141–2146. <https://doi.org/10.1021/ac50022a012>.
- (19) Abe, H.; Jure, P. C. Automated Chemical Structure Analysis of Organic Molecules with a Molecular Structure Generator and Pattern Recognition Techniques. *Anal. Chem.* **1975**, *47* (11), 1829–1835. <https://doi.org/10.1021/ac60361a007>.
- (20) Ziemer, J. N.; Peronel, S. P.; Caprioli, R. M.; Seifert, W. E. Computerized Pattern Recognition Applied to Gas Chromatography/Mass Spectrometry Identification of Pentafluoropropionyl Dipeptide Methyl Esters. *Anal. Chem.* **1979**, *51* (11), 1732–1738. <https://doi.org/10.1021/ac50047a034>.
- (21) Rotter, H.; Varmuza, K. Computer-Aided Interpretation of Steroid Mass Spectra by Pattern Recognition Methods. Part III. Computation of Binary Classifiers by Linear Regression. *Anal. Chim. Acta* **1978**, *103* (1), 61–71. [https://doi.org/10.1016/S0003-2670\(01\)83807-1](https://doi.org/10.1016/S0003-2670(01)83807-1).
- (22) Klawun, C.; Wilkins, C. L. Optimization of Functional Group Prediction from Infrared Spectra Using Neural Networks. *J. Chem. Inf. Comput. Sci.* **1996**, *36* (1), 69–81. <https://doi.org/10.1021/ci950102m>.
- (23) Kowalski, B. R.; Jurs, P. C.; Isenhour, T. L.; Reilley, C. N.; Isenhour, T. L.; Jurs, P. C. Computerized Learning Machines Applied to Chemical Problems Interpretation of Infrared Spectrometry Data. *Anal. Chem.* **1969**, *41* (14), 1945–1949. <https://doi.org/10.1021/ac50159a026>.
- (24) Ghosh, K.; Stuke, A.; Todorović, M.; Jørgensen, P. B.; Schmidt, M. N.; Vehtari, A.; Rinke, P. Deep Learning Spectroscopy: Neural Networks for Molecular Excitation Spectra. *Adv. Sci.* **2019**, *6* (9), 1801367. <https://doi.org/10.1002/advs.201801367>.
- (25) Bryant, C. H.; Adam, A. E.; Taylor, D. R.; Rowe, R. C. Toward an Expert System for Enantioseparation: Induction of Rules Using Machine Learning. *Chemom. Intell. Lab. Syst.* **1996**, *34* (1), 21–40. [https://doi.org/10.1016/0169-7439\(96\)00016-0](https://doi.org/10.1016/0169-7439(96)00016-0).
- (26) Bryant, R. Knowledge Discovery in Databases: Application to Chromatography Title Knowledge Discovery in Databases: Application to Chromatography. **1998**. [https://doi.org/10.1016/S0165-9936\(97\)00094-0](https://doi.org/10.1016/S0165-9936(97)00094-0).
- (27) I, T. P.; Smith, R.; Guhan, S.; Taksen, K.; Vavra, M.; Myers, D.; Hearn, M. T. W.

- Intelligent Automation of High-Performance Liquid Chromatography Method Development by Means of a Real-Time Knowledge-Based Approach. *J. Chromatogr. A* **2002**, 972 (1), 27–43. [https://doi.org/10.1016/S0021-9673\(02\)01075-0](https://doi.org/10.1016/S0021-9673(02)01075-0).
- (28) Sharma, A. Y.; Sahni, R.; Herald, S. *Review of Artificial Intelligence Driven Chemistry*; 2019; Vol. 7.
 - (29) Zhavoronkov, A. Artificial Intelligence for Drug Discovery, Biomarker Development, and Generation of Novel Chemistry. *Molecular Pharmaceutics*. American Chemical Society October 1, 2018, pp 4311–4313. <https://doi.org/10.1021/acs.molpharmaceut.8b00930>.
 - (30) Gross, B.; Lockwood, S. Y.; Spence, D. M. Recent Advances in Analytical Chemistry by 3D Printing. *Analytical Chemistry*. American Chemical Society 2017, pp 57–70. <https://doi.org/10.1021/acs.analchem.6b04344>.
 - (31) He, Y.; Wu, Y.; Fu, J.; Gao, Q.; Qiu, J. Developments of 3D Printing Microfluidics and Applications in Chemistry and Biology: A Review. *Electroanalysis* **2016**, 28 (8), 1658–1678. <https://doi.org/10.1002/elan.201600043>.
 - (32) Gross, B. C.; Erkal, J. L.; Lockwood, S. Y.; Chen, C.; Spence, D. M. Evaluation of 3D Printing and Its Potential Impact on Biotechnology and the Chemical Sciences. *Anal. Chem.* **2014**, 86 (7), 3240–3253. <https://doi.org/10.1021/ac403397r>.
 - (33) Calderilla, C.; Maya, F.; Cerdà, V.; Leal, L. O. 3D Printed Device for the Automated Preconcentration and Determination of Chromium (VI). *Talanta* **2018**, 184, 15–22. <https://doi.org/10.1016/j.talanta.2018.02.065>.
 - (34) Su, C. K.; Peng, P. J.; Sun, Y. C. Fully 3D-Printed Preconcentrator for Selective Extraction of Trace Elements in Seawater. *Anal. Chem.* **2015**, 87 (13), 6945–6950. <https://doi.org/10.1021/acs.analchem.5b01599>.
 - (35) Fee, C.; Nawada, S.; Dimartino, S. 3D Printed Porous Media Columns with Fine Control of Column Packing Morphology. *J. Chromatogr. A* **2014**, 1333, 18–24. <https://doi.org/10.1016/j.chroma.2014.01.043>.
 - (36) Sandron, S.; Heery, B.; Gupta, V.; Collins, D. A.; Nesterenko, E. P.; Nesterenko, P. N.; Talebi, M.; Beirne, S.; Thompson, F.; Wallace, G. G.; et al. 3D Printed Metal Columns for Capillary Liquid Chromatography. *Analyst* **2014**, 139 (24), 6343–6347. <https://doi.org/10.1039/c4an01476f>.
 - (37) Prikryl, J.; Foret, F. Fluorescence Detector for Capillary Separations Fabricated by 3D Printing. *Anal. Chem.* **2014**, 86 (24), 11951–11956. <https://doi.org/10.1021/ac503678n>.
 - (38) Duval, C. Francois Descroizilles, the Inventor of Volumetric Analysis. *J. Chem. Educ.* **1951**, 28 (10), 508. <https://doi.org/10.1021/ed028p508>.
 - (39) Crosland, M. P. *Gay-Lussac : Scientist and Bourgeois*; Cambridge University Press, 2002.
 - (40) Klingenberg, M. When a Common Problem Meets an Ingenious Mind. *EMBO Reports*. European Molecular Biology Organization September 2005, pp 797–800.

<https://doi.org/10.1038/sj.embor.7400520>.

- (41) *GUIDE TO PIPETTING Third Edition*.
- (42) US4671123A - Methods and apparatus for pipetting and/or titrating liquids using a hand held self-contained automated pipette - Google Patents
<https://patents.google.com/patent/US4671123A/en> (accessed Feb 8, 2020).
- (43) Sutter, P. W.; Sutter, E. A. Dispensing and Surface-Induced Crystallization of Zeptolitre Liquid Metal-Alloy Drops. *Nat. Mater.* **2007**, 6 (5), 363–366.
<https://doi.org/10.1038/nmat1894>.
- (44) Epstein, D. M.; Tebbett, I. R.; Boyd, S. E. *Eliminating Sources of Pipetting Error in the Forensic Laboratory*; 2003; Vol. 5.
- (45) Kong, F.; Yuan, L.; Zheng, Y. F.; Chen, W. Automatic Liquid Handling for Life Science. *J. Lab. Autom.* **2012**, 17 (3), 169–185.
<https://doi.org/10.1177/2211068211435302>.
- (46) Lichty, M. G.; Janowitz, I. L.; Rempel, D. M. Ergonomic Evaluation of Ten Single-Channel Pipettes. *Work* **2011**, 39 (2), 177–185. <https://doi.org/10.3233/WOR-2011-1164>.
- (47) Björkstén, M. G.; Almby, B.; Jansson, E. S. Hand and Shoulder Ailments among Laboratory Technicians Using Modern Plunger-Operated Pipettes. *Appl. Ergon.* **1994**, 25 (2), 88–94. [https://doi.org/10.1016/0003-6870\(94\)90069-8](https://doi.org/10.1016/0003-6870(94)90069-8).
- (48) Raspberry Pi hardware - Raspberry Pi Documentation
<https://www.raspberrypi.org/documentation/hardware/raspberrypi/README.md> (accessed Feb 8, 2020).
- (49) GPIO - Raspberry Pi Documentation
<https://www.raspberrypi.org/documentation/usage/gpio/> (accessed Feb 8, 2020).
- (50) Rashed, M. G.; Ahsan, R. *Python in Computational Science: Applications and Possibilities*; 2012; Vol. 46.
- (51) RPi.GPIO · PyPI <https://pypi.org/project/RPi.GPIO/> (accessed Dec 6, 2019).
- (52) Grayson, J. E. *Python and Tkinter Programming*; Manning, 2000.
- (53) Wong, K. V.; Hernandez, A. A Review of Additive Manufacturing. *ISRN Mech. Eng.* **2012**, 2012, 1–10. <https://doi.org/10.5402/2012/208760>.
- (54) How Stepper Motors Work <https://www.orientalmotor.com/stepper-motors/technology/stepper-motor-overview.html> (accessed Feb 8, 2020).
- (55) What is a stepper motor? - Principles, types and crontollers
https://www.omega.co.uk/prodinfo/stepper_motors.html# (accessed Feb 8, 2020).
- (56) Lenore S. Clesceri, Arnold E. Greenberg, A. D. E. 2320 Alkalinity. In *Standard Methods For The Examination of Water and Waste water*; APHA/WEF/AWWA,

- 1992; pp 2-25-2–28.
- (57) Lenore S. Clesceri, Arnold E. Greenberg, A. D. E. 2340 Hardness. In *Standard Methods For the Examination of Water and Wastewater*; APHA/WEF/AWWA: Washington, DC, 1992; pp 2-35-2–38.
 - (58) Geme, G.; Brown, M. A.; Simone, P.; Emmert, G. L. Measuring the Concentrations of Drinking Water Disinfection By-Products Using Capillary Membrane Sampling-Flow Injection Analysis. *Water Res.* **2005**, 39 (16), 3827–3836.
<https://doi.org/10.1016/j.watres.2005.07.015>.
 - (59) Emmert, G. L.; Geme, G.; Brown, M. A.; Simone, P. S. A Single Automated Instrument for Monitoring Total Trihalomethane and Total Haloacetic Acid Concentrations in near Real-Time. *Anal. Chim. Acta* **2009**, 656 (1–2), 1–7.
<https://doi.org/10.1016/j.aca.2009.10.002>.
 - (60) Kim, H.-Y. Analysis of Variance (ANOVA) Comparing Means of More than Two Groups. *Restor. Dent. Endod.* **2014**, 39 (1), 74.
<https://doi.org/10.5395/rde.2014.39.1.74>.
 - (61) David S.Hage, J. D. C. *Analytical Chemistry and Quantitative Analysis*; PEARSON, 2011.
 - (62) Denver Instruments - Analytical balance Data sheet
<http://www.denverinstrument.com/denverusa/media/pdf/OpManSummitRevA.pdf>
(accessed Dec 6, 2019).
 - (63) National Primary Drinking Water Regulations | Ground Water and Drinking Water | US EPA <https://www.epa.gov/ground-water-and-drinking-water/national-primary-drinking-water-regulations#Byproducts> (accessed Mar 21, 2020).
 - (64) Emmert, G. L.; Brown, M. A.; Simone, P. S.; Geme, G.; & Cao, G. *Methods for Real-Time Measurement of THMs and HAAs in Distribution Systems--Part 2.*; AWWA Research Foundation: Denver, CO, 2007.
 - (65) Brown, A. W.; Simone, P. S.; York, J. C.; Emmert, G. L. A Device for Fully Automated On-Site Process Monitoring and Control of Trihalomethane Concentrations in Drinking Water. *Anal. Chim. Acta* **2015**, 853 (1), 351–359.
<https://doi.org/10.1016/j.aca.2014.10.052>.
 - (66) Stanley, R. Automation in Analytical Chemistry—from Rule of Thumb to Fully Automated Methods. Some Philosophies and Social Consequences. *J. Automat. Chem.* **1984**, 6 (1), 6–13. <https://doi.org/10.1155/S1463924684000031>.
 - (67) Olsen, K. The First 110 Years of Laboratory Automation: Technologies, Applications, and the Creative Scientist. *J. Lab. Autom.* **2012**, 17 (6), 469–480.
<https://doi.org/10.1177/2211068212455631>.
 - (68) Mark A. Hetherington, Min Chen, R. S. R. *A Novel PC-Based Gravimetric Autotitrator with a Multi-Solution Delivery System*.
 - (69) Trick, J. K.; Stuart, M.; Reeder, S. Contaminated Groundwater Sampling and Quality

- Control of Water Analyses. In *Environmental Geochemistry: Site Characterization, Data Analysis and Case Histories: Second Edition*; Elsevier, 2018; pp 25–45. <https://doi.org/10.1016/B978-0-444-63763-5.00004-5>.
- (70) Gebbie, P. *AN OPERATOR'S GUIDE TO WATER TREATMENT COAGULANTS*; 2006.
 - (71) Iriarte-Velasco, U.; Álvarez-Uriarte, J. I.; González-Velasco, J. R. Enhanced Coagulation under Changing Alkalinity-Hardness Conditions and Its Implications on Trihalomethane Precursors Removal and Relationship with UV Absorbance. *Sep. Purif. Technol.* **2007**, 55 (3), 368–380. <https://doi.org/10.1016/j.seppur.2006.12.022>.
 - (72) Crittenden, J. C. (John C.; Montgomery Watson Harza (Firm). *MWH's Water Treatment : Principles and Design.*; John Wiley & Sons, 2012.
 - (73) Hardness of Water https://www.usgs.gov/special-topic/water-science-school/science/hardness-water?qt-science_center_objects=0#qt-science_center_objects (accessed Dec 6, 2019).
 - (74) Birch, E. J. H. Hardness in Water—A Demonstration. *J. Chem. Educ.* **1949**, 26 (4), 196. <https://doi.org/10.1021/ed026p196>.
 - (75) Duane J PowellRobert B. BebowBrent J. Hardman. *United States Patent US007 175824B2*; 2005.
 - (76) Lenore S. Clesceri, Arnold E. Greenberg, A. D. E. 4500-C1 C. Iodometric Method I. In *Standard Methods For the Examination of Water and Wastewater*; APHA/WEF/AWWA: Washington, DC, 1992; pp 4-38-4.39.
 - (77) Therrien, R.; Doyle, S. Role of Training Data Variability on Classifier Performance and Generalizability. In *Medical Imaging 2018: Digital Pathology*; Gurcan, M. N., Tomaszewski, J. E., Eds.; SPIE, 2018; Vol. 10581, p 5. <https://doi.org/10.1117/12.2293919>.
 - (78) Hossin, M.; Sulaiman. A REVIEW ON EVALUATION METRICS FOR DATA CLASSIFICATION EVALUATIONS. *Int. J. Data Min. Knowl. Manag. Process* **2015**, 5 (2). <https://doi.org/10.5121/ijdkp.2015.5201>.
 - (79) *Amazon Machine Learning Developer Guide*; 2020.
 - (80) Adams, V. D. *Water & Wastewater Examination Manual*; Lewis Publishers: Chelsea, Michigan, 1990.
 - (81) Bland, J. M.; Altman, D. G. Measuring Agreement in Method Comparison Studies. *Stat. Methods Med. Res.* **1999**, 8 (2), 135–160. <https://doi.org/10.1177/096228029900800204>.
 - (82) Altman, D. G.; Bland, J. M. *Measurement in Medicine: The Analysis of Method Comparison Studies* †; 1983; Vol. 32.
 - (83) Skoog, D.A., F.J. Holler, and S. R. C. *Principles of Instrumental Analysis*, 6th ed.; Thomson Brooks/Cole: California, 2006.

- (84) Harris, D. . *Quantitative Chemical Analysis*, 7th ed.; W.H. Freeman & Company: Newyork, 2007.
- (85) Phosphoric acid | H₃PO₄ - PubChem
<https://pubchem.ncbi.nlm.nih.gov/compound/1004> (accessed Feb 12, 2020).
- (86) Maleic acid | C₄H₄O₄ - PubChem
<https://pubchem.ncbi.nlm.nih.gov/compound/444266#section=2D-Structure> (accessed Feb 12, 2020).
- (87) Phthalic acid | H₂C₈H₄O₄ - PubChem
<https://pubchem.ncbi.nlm.nih.gov/compound/Phthalic-acid> (accessed Feb 12, 2020).
- (88) Automatic Potentiometric (pH/mV/ISE) Titration System - HI902C
<https://www.hannainst.com/hi902c-automatic-titration-system.html> (accessed Feb 15, 2020).
- (89) Connick, R. E.; Chia, Y. T. The Hydrolysis of Chlorine and Its Variation with Temperature. *J. Am. Chem. Soc.* **1959**, *81* (6), 1280–1284.
<https://doi.org/10.1021/ja01515a004>.
- (90) Gordon, G.; Cooper, W. J.; Rice, R. G.; Pacey, G. E. Methods of Measuring Disinfectant Residuals. *J. Am. Water Works Assoc.* **1988**, *80* (9), 94–108.
<https://doi.org/10.1002/j.1551-8833.1988.tb03104.x>.
- (91) Richardson, S. D.; Plewa, M. J.; Wagner, E. D.; Schoeny, R.; DeMarini, D. M. Occurrence, Genotoxicity, and Carcinogenicity of Regulated and Emerging Disinfection by-Products in Drinking Water: A Review and Roadmap for Research. *Mutation Research - Reviews in Mutation Research*. November 2007, pp 178–242.
<https://doi.org/10.1016/j.mrrev.2007.09.001>.
- (92) Coffin, J. C.; Ge, R.; Yang, S.; Kramer, P. M.; Tao, L.; Pereira, M. A. Effect of Trihalomethanes on Cell Proliferation and DNA Methylation in Female B6C3F1 Mouse Liver. *Toxicol. Sci.* **2000**, *58* (2), 243–252.
<https://doi.org/10.1093/toxsci/58.2.243>.
- (93) Villanueva, C. M.; Cantor, K. P.; Grimalt, J. O.; Malats, N.; Silverman, D.; Tardon, A.; Garcia-Closas, R.; Serra, C.; Carrato, A.; Castaño-Vinyals, G.; et al. Bladder Cancer and Exposure to Water Disinfection By-Products through Ingestion, Bathing, Showering, and Swimming in Pools. *Am. J. Epidemiol.* **2007**, *165* (2), 148–156.
<https://doi.org/10.1093/aje/kwj364>.
- (94) United States Environmental Protection Agency. Method 552.3 Determination of Haloacetic Acids and Dalapon in Drinking Water by Liquid-Liquid Microextraction, Derivatization, and Gas Chromatography with Electron Capture Detection. **2003**.
- (95) United States Environmental Protection Agency. Method 557: Determination of Haloacetic Acide, Bromate, and Dalapon in Drinking Water by Ion Chromatography Electrospray Ionization Tandem Mass Spectrometry. **2009**.
- (96) Simone, P. S.; Anderson, G. T.; Emmert, G. L. On-Line Monitoring of Mg/L Levels of Haloacetic Acids Using Ion Chromatography with Post-Column Nicotinamide

- Reaction and Fluorescence Detection. *Anal. Chim. Acta* **2006**, 570 (2), 259–266. <https://doi.org/10.1016/j.aca.2006.04.014>.
- (97) Simone, P. S.; Ranaivo, P. L.; Geme, G.; Brown, M. A.; Emmert, G. L. On-Line Monitoring of Nine Haloacetic Acid Species at the Mg L-1 Level Using Post-Column Reaction-Ion Chromatography with Nicotinamide Fluorescence. *Anal. Chim. Acta* **2009**, 654 (2), 133–140. <https://doi.org/10.1016/j.aca.2009.09.021>.
- (98) Ranaivo, P. L.; Henson, C. M.; Simone, P. S.; Emmert, G. L. Analysis of Haloacetic Acids in Drinking Water Using Post-Column Reaction-Ion Chromatography with on-Line Internal Standardization. *Anal. Methods* **2011**, 3 (12), 2873–2880. <https://doi.org/10.1039/c1ay05398a>.
- (99) Henson, C. M.; Emmert, G. L.; Simone, P. S. A Fully-Automated Analyzer for Determining Haloacetic Acid Concentrations in Drinking Water. *Chemosphere* **2014**, 117 (1), 586–595. <https://doi.org/10.1016/j.chemosphere.2014.09.018>.
- (100) Ferreira, S. L. C.; Caires, A. O.; Borges, T. da S.; Lima, A. M. D. S.; Silva, L. O. B.; dos Santos, W. N. L. Robustness Evaluation in Analytical Methods Optimized Using Experimental Designs. *Microchemical Journal*. Elsevier Inc. March 1, 2017, pp 163–169. <https://doi.org/10.1016/j.microc.2016.12.004>.
- (101) AMIS-30543 - Micro-Stepping Motor Driver <http://onsemi.com> (accessed Feb 8, 2020).

Appendix

The EZ-AutoPipet and EZ-AutoTitrator were developed using commercially available components. Both these devices share same electrical schematic except EZ-AutoTitrator has additional sensors to measure pH, light intensity at six wavelengths and temperature. The AMIS-30543 stepper driver communicates via SPI interface and the two drivers share same master input slave output (MISO), master Output slave input (MOSI) and Clock pins. A different chip select pin (CS) was used to select the driver for communication. The EZO pH board, AS7262, and ADS115 all connected to same I2C bus. The temperature sensor (DS18B20) communicates via one-wire interface. A 12 V 2.1 (LS25-12, TDK-Lambda, USA) power supply was used to drive the stepper motors and 3-way valves. A 5 V 3A (RS15-5, MEANWELL, Taiwan) power supply was used to power the Raspberry Pi and touch display. N-Channel MOSFET (IRF540N) was used to actuate the 3-way valves.

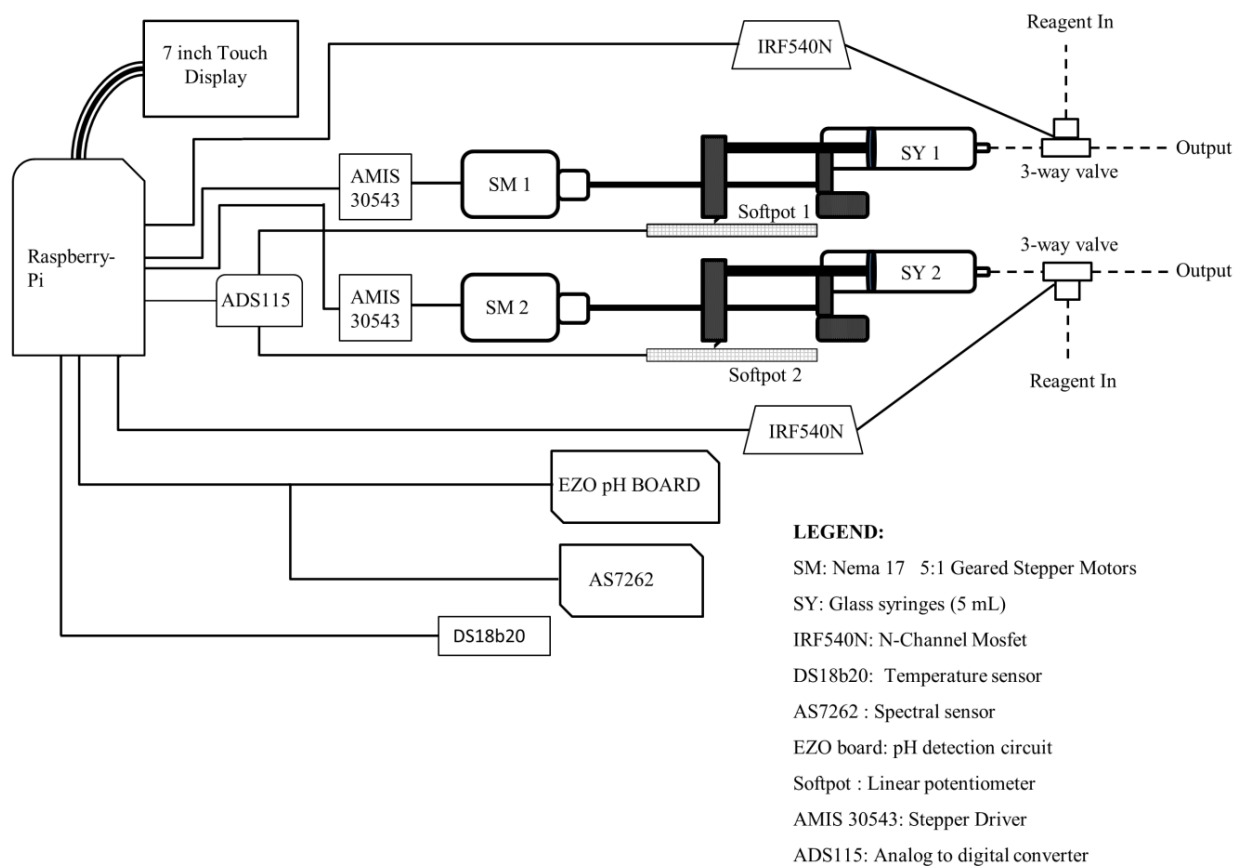


Figure 39. The schematic of EZ-AutoTitrator.

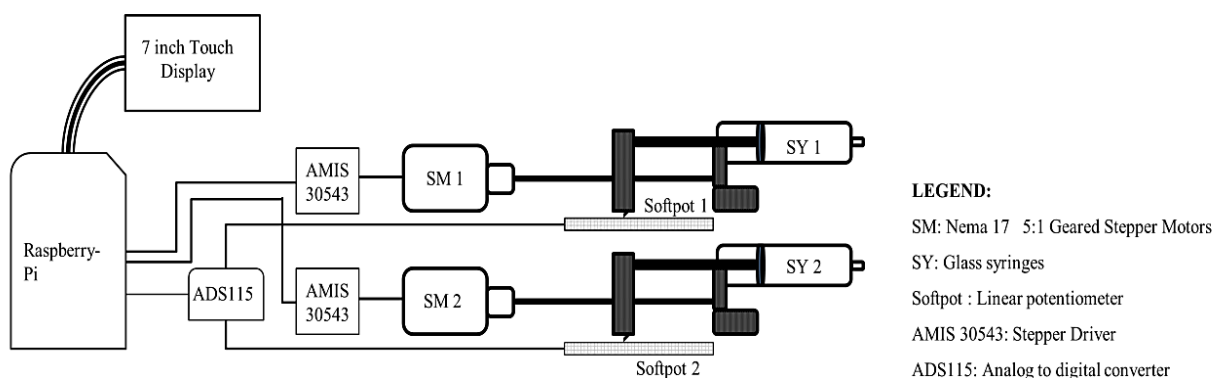


Figure 40. The schematic of EZ-AutoPipet.

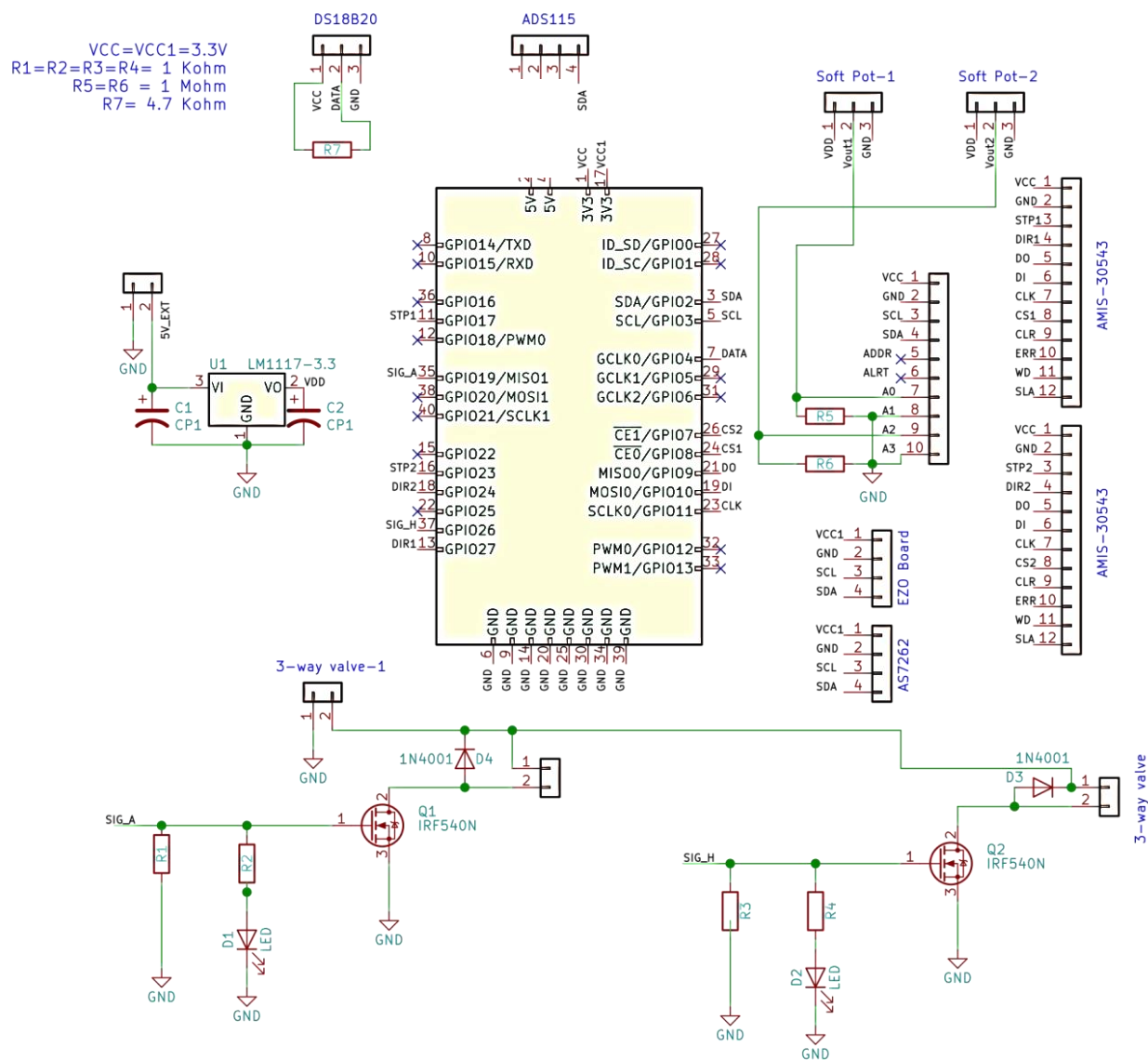


Figure 41. The electrical schematic of EZ-AutoTitrator/EZ-AutoPipet.